NATIONAL ADVISORY COMMITTEE FOR AERONAUTICS

TECHNICAL NOTE 4369

SLIP-FLOW HEAT TRANSFER FROM CYLINDERS IN SUBSONIC AIRSTREAMS

By Lionel V. Baldwin

Lewis Flight Propulsion Laboratory
Cleveland, Ohio

Washington
September 1958

TABLE OF CONTENTS

5111

CS-1

NATIONAL ADVISORY COMMITTEE FOR AERONAUTICS

TECHNICAL NOTE 4369

SLIP-FLOW HEAT TRANSFER FROM CYLINDERS IN SUBSONIC AIRSTREAMS

By Lionel V. Baldwin

SUMMARY

Over 1000 measured convective heat-transfer coefficients for normal cylinders in subsonic slip flow have been correlated by using Nusselt number as a function of Reynolds and Knudsen (or Mach) numbers. The experimental range corresponds to the following dimensionless groups: Mach number M, 0.05 to 0.80; Reynolds number Re, 1 to 75; Knudsen number Kn, 0.009 to 0.077. Air temperatures between 0° and 280° F and cylinder temperatures between 34° and 620° F were used. At $Kn = 0.009$, the Nusselt number (Nu) correlation extrapolated smoothly into continuum-flow empirical curves, which show Nu as a function of $\sqrt{Re}$ with a small, regular variation in Nu from compressibility or Mach number effects. The data showed increasing sensitivity to Kn as it increased to 0.077. The experimental Nu curves at $Kn = 0.077$ qualitatively verified two characteristics predicted by free-molecular-flow theoretical analysis. These are a shift to first-power dependence on Re and large separation of constant Mach number parametric curves due to rarefied gas-flow phenomena. Therefore, the experimental slip-flow correlation served as a bridge between continuum empirical relations and free-molecular theoretical results, but data between $0.10 < Kn < 2$ are required to complete this general correlation.

A complicated nonlinear dependence of the heat-transfer coefficient to the difference between cylinder and recovery temperature ΔT is reported. The heat-transfer coefficient h increased with increasing ΔT for $Kn < 0.02$; while for $Kn > 0.02$, h decreased with increasing ΔT. The Mach number had a secondary effect on this ΔT phenomenon. For cylinders operated at $\Delta T > 200^{\circ}$ F and over the entire range of this research, an increase in air temperature increased the heat-transfer coefficient. The preceding were second-order effects that caused deviations of up to 20 percent from the general correlation.

Finally, the application of these research results to hot-wire anemometry is discussed.

INTRODUCTION

Fine metal wires, 0.00005 to 0.001 inch in diameter, have been widely used in aerodynamic research as anemometers. The use of hot-wire anemometers for mean flow measurements began with the early work of King (ref. 1), while the investigation of fluctuations in airflows started with the classical research of Dryden and Kuethe (ref. 2). In every application, the sensitivity of the electrically heated anemometer to the flow properties is determined by the heat-transfer characteristics of cylinders in forced convection. Assuming potential flow over the wire, King derived an equation for steady flow that relates the electrical power input to the heat loss by convection:

$$I^2\Omega_w = (A + B\sqrt{U})(T_w - T_a) \tag{1}$$

where

$$A = alk$$

$$B = bl\sqrt{D_w \rho c_p k}$$

(All symbols are defined in appendix A.) In usual practice, the constants in King's equation, A and B, are obtained experimentally from a calibration curve of $I^2\Omega_w/(\Omega_w - \Omega_a)$ as a function of $\sqrt{U}$ for each wire used. The sensitivity predicted by King's equation is the basis for hot-wire-anemometer techniques that have become rather elaborate (e.g., ref. 3) in slow subsonic flows.

As aerodynamic research progressed into transonic and supersonic flows, it was natural to investigate the heat-loss characteristics of hot wires and to attempt extension of this research tool. In order to describe the influence of flow parameters over a wide range, recent investigators have used dimensionless groups to generalize heat-loss correlations. Hot-wire heat-loss studies not only supply anemometer sensitivity, but also have furnished the bulk of the heat-transfer measurements for cylinders in slip and near-free-molecule flows. Interest in this phase of aerodynamics has grown greatly as it has become necessary to compute heat transfer to missiles and satellites that fly at high altitudes. Though these objects generally fly at very high speeds, the actual flow over the body is subsonic in many cases, because shock waves occur near forward surfaces. This investigation follows some excellent research in this field during the past eight years; therefore, it is appropriate to outline the problem studied here in terms of what previous workers have established.

5111

5111

CS-1 back

Review of Previous Investigations

The Reynolds number (based on cylinder diameter) and Mach number are the usual dimensionless groups chosen to specify the regimes for airflow over normal cylinders. Figure 1 is a convenient summary of recent heat-transfer experiments with normal cylinders. The Mach number of the ordinate is based on free-stream velocity and static temperature; the abscissa is the Reynolds number based on the cylinder diameter and on free-stream density, velocity, and viscosity. The shaded areas indicate the experimental ranges of previous work, and these areas are keyed by numbers to the reference list of this report (refs. 4 to 16). Figure 1 also shows the research region of this paper.

The two constant Knudsen number lines in figure 1 provide a guide to the flow regimes. Though the boundaries of free-molecule, slip, and continuum flows probably are not sharply defined, reference 15 proposed the following definitions for flow over normal cylinders:

(1) Continuum flow: $Kn < 0.001$

(2) Slip flow: $0.001 < Kn < 2$

(3) Free-molecule flow: $Kn > 2$

The Knudsen number Kn is defined as the ratio of the mean free path of the gas λ to the cylinder diameter D_w. Kinetic theory of gases relates the Knudsen number to the ratio of the Mach number to the Reynolds number; for air, this proportionality is as follows:

$$Kn \equiv \frac{\lambda}{D_w} \approx 1.45 \frac{M}{Re_t}\sqrt{\frac{T}{T_t}} \tag{2}$$

At atmospheric pressure with anemometer wires 0.0002 inch or smaller in diameter, the flow region for the hot wires in much of the early turbulence work would fall below M of 0.10 and between Re of 3 and 30.

King's equation can be written in terms of nondimensional groups as

$$Nu = A' + B' \sqrt{Pr}\sqrt{Re} \tag{1a}$$

The 0.5-power dependence on Reynolds number is well established in slow subsonic continuum flows (ref. 11). However, Lowell (ref. 10) was the first to point out that the Reynolds number alone does not correlate fine-wire heat-transfer data over an appreciable velocity range. He reported that the Mach number was a parameter at $M = 0.375$ and 0.575. Then, Laurence and Landes (ref. 9) found that their data correlated if Nu was plotted as a function of $\sqrt{Re}$, but the Mach number remained a parameter even in the range of $M = 0.1$, 0.2, and 0.3. Since the work being reviewed is limited to room-temperature airflows over cylinders (i.e., viscosity is constant), the use of both Re and M simply shows that ρD_w and U are not interchangeable in the product $\rho D_w U$. This has been noted by later investigators (refs. 12, 14, and 16). It is well established that the maximum separation of the constant Mach number lines on a plot of Nu against $\sqrt{Re}$ occurs at the lowest Mach numbers; in fact, by proper choice of fluid properties, this "Mach number effect" can be almost eliminated in supersonic flow (refs. 7, 8, 14, and 15).

5111

The Knudsen number was introduced as a correlating parameter in reference 14. The effect of ρ and D_w in the product ρD_w was found to be fully equivalent over the wide experimental range of reference 14. Since conditions of constant ρD_w are constant Knudsen number flows, the Knudsen and Reynolds numbers were shown to be the governing parameters in the incompressible range. The nonequivalence of ρD_w and U in attempted Reynolds number correlations was most pronounced for very fine wires that exhibited low sensitivity to velocity.

Nearly all the anemometer heat-loss investigators have varied the operating temperature of the wire (refs. 9, 10, 14, and 16). The most extensive research has been reported by reference 14, which found that the Nu varied with wire temperature at a given flow condition, and that this variation depended on both M and ρ. However, no simple correlation was found to cover all of the effects observed when the wire temperature was varied.

Reference 16 reports measurements of the nonlinear variation with wire temperature of the heat-transfer rate from hot wires from $M = 0.5$ to 2.5 and $Re = 18$ to 144. The reference proposed a nonlinear overheat ratio ξ defined as

$$h = h_0(1 - \xi \bar{a}_w) \tag{3}$$

where h_0 is the heat-transfer coefficient extrapolated to $\Delta T = 0$, and $\bar{a}_w \equiv (\Omega_w - \Omega_e)/\Omega_e$. The overheat ratio ξ was found to be a function of Mach and Reynolds numbers. Like reference 14, reference 16 found that the nonlinearity reverses under some flow conditions. That is, for some Reynolds numbers in the subsonic region the heat-transfer coefficient increased with increasing wire temperature; and, depending on M and Re, the heat-transfer coefficient was observed to decrease with increasing wire temperature under other flow conditions.

The work of reference 16 is the nearest approach to formulating clearly the important parameters affecting the nonlinear variation of heat-transfer rate with wire temperature. However, the results are limited to transonic and supersonic Mach numbers and to three values of Reynolds number. Additional data are required to verify the predicted trends at lower subsonic Mach numbers.

Objectives of This Research

The primary objective of this research was to examine the nonlinear variation of heat transfer with wire and air temperatures. The effect of wire temperature is complicated and not fully clarified by previous work, while there appears to be no systematic variation of air temperature in heat-transfer experiments from fine wires. Besides providing an additional insight into the nonlinearity of heat transfer with ΔT, data taken at various air temperatures are important for some hot-wire-anemometer applications (e.g., appendix E of ref. 17).

Furthermore, sufficient heat-transfer data from normal cylinders have been published in recent years that it should be possible to show clearly the effect of continuum, slip, and free-molecule flows on heat-transfer characteristics. An attempt to find a preliminary general correlation based on the results of this and earlier work is also an objective of this report.

APPARATUS AND PROCEDURE

Apparatus

Tunnel and air facility. - A sketch of the variable-density, low-turbulence tunnel used in this research is shown in figure 2. The incoming air passed through a cone-shaped filter screen covered with filter paper and wool felt. The air then entered the 6-inch-diameter inlet section where a total-pressure probe and heater control thermocouple were located. The tunnel contracted to the 1.50-inch-diameter circular test section in 6 inches; both the inlet and test sections were polished machined steel, "Pentrated" to prevent rust formation. Four static-pressure taps (1/64-in. holes) were located in the plane of the hot-wire probe. Static taps also extended along the length of the contracted area. As shown in the sketch, the hot-wire probe was mounted in a probe actuator that moved the wire out of the airflow into a small dead-air volume for protection when flow conditions were adjusted. A high-pressure valve packing gland acted as the vacuum seal but allowed the in and out motion of the probe. This simple feature was the primary reason for the long test life of the fine tungsten wire probe (number 109) reported here; the design evolved during the breaking of the first 108 wires.

The tunnel was serviced by the central laboratory air facilities. Test-section static pressure could be varied between 3 and 110 inches of mercury absolute. Mass-flow rate was independently adjustable; in this manner, the corresponding test-section Mach number could be varied between 0 and 0.85. For low mass-flow rates, the air mass flow was metered with a calibrated sonic orifice. The measured tunnel total and static pressures were used to calculate the Mach number assuming isentropic relations for all mass flow above 0.014 pound per second. A water U-tube manometer was used for total-static differences less than 2 inches of mercury; all other pressure readings were read from calibrated mercury manometers. Pressures were measured to at least three significant figures on both water and mercury manometers. Some uncontrollable fluctuations occurred in the inlet air supply, which may have resulted in a random error in reading of the third significant figure.

5111

The total temperature of the air could be varied between -10° and 300° F by alternate use of refrigerator coils and electrical heaters. Total temperature was calculated from the measured recovery temperature of a calibrated thermocouple located in the probe test-section plane (see fig. 2). This temperature was read to the nearest half degree on a self-balancing indicator. Although the tunnel and inlet piping were well insulated, it was difficult to control the air total temperature as closely as desired over all the flow conditions. Deviations from the nominal air temperatures in day-to-day operation were ±10° F. However, the air temperature listed in table I is probably accurate within ±1° F of the total air temperature for each data point; uncertainty in total air temperature did not contribute significantly to uncertainty of the calculated Nusselt numbers except for wire temperatures only 50° F above recovery temperature. The effect of air-temperature fluctuations during any tunnel flow setting was minimized by making a linear interpolation between the two temperatures measured at the beginning and end of each set of six wire heat-loss measurements.

Probe design and tungsten wire. - A sketch of the probe used throughout this research is shown in figure 3. Several features of this design bear mentioning. One of the prime requirements is that the wire-supporting prongs do not substantially interfere with the airflow over the wire. Evidence that the design used met the requirement has been supplied by reference 12. Several probes of similar design were used in an experimental determination of the effect of yaw angle of attack on fine-wire heat transfer in reference 12, which concluded that no effect of probe interference could be noted in the results. Another important feature is that the four-wire lead design has matched metal junctions; that is, all unlike metal contacts occur symmetrically. Since the probe body was occasionally in a large temperature gradient (e.g., 300° F at fine-wire supports to 80° F at lead connector), it was important that no unbalanced thermocouple electromotive force exist in the probe, especially when the wire was operated only 50° F above air temperature. Although some of the early probe designs did not satisfy this requirement, the probe reported here did not show any direct-current unbalance at zero power input for all operating temperatures. Finally, the four-lead-wire design and the use of a Kelvin double bridge minimized the electrical resistance of the probe and its influence on the accuracy of the hot-wire heat-loss measurements. This point is clarified further in the discussion of anemometer electrical equipment.

Tungsten wire with a nominal diameter of 0.0002 inch served as the heat-transfer element of the probe. The mounting technique is described in reference 9. Briefly, the wire is copper-plated at the ends for ease in soldering to the Inconel prongs; a high-temperature soft solder (m.p., 650° F) was used. One of the major drawbacks in the use of fine wires as heat-transfer elements is the uncertainty in the wire diameter (e.g., see ref. 9). In an attempt to decrease this uncertainty, electron micrographs were taken of samples from the spool of wire used on probe 109. These photographs are shown in figure 4; each is a different wire sample. An average diameter was calculated from several diameter measurements near the central position of each photograph. The necked-down section of sample C was not included in this average, which was 0.00022 inch. It can only be hoped that any wire sample as irregular as sample C would be eliminated after its room-temperature resistance was measured. That is, annealed tungsten wires of equal lengths have nearly identical resistance if the wire diameter is uniform. Many probes were discarded as a control procedure when their measured resistance deviated ±5 percent from the average. Though the average diameter obtained from these samples is not necessarily the diameter of the 0.077-inch-long sample used in probe 109, the average is more probable than the manufacturer's nominal diameter, and 0.00022 inch was used in all calculations.

One of the most important physical properties of tungsten for the calculation of heat loss is the relation between temperature and electrical resistance. Early in the research it was apparent that each wire required calibrating if consistent data of the temperature loading effect on heat-transfer coefficient were to be obtained. Therefore, a small calibration heater was constructed, a sketch of which is given in figure 5. Several wires were silver-soldered to probes so the solder junction was unaffected at 650° F. These wires were then annealed by supplying sufficient current to heat the wire to about twice their room-temperature resistance for 30 minutes. The annealing caused the room-temperature resistance to drop several percent, but after 30 minutes no further change was observed. The probes were then inserted into the heater, and a complete calibration curve was obtained from 32° to 600° F. Two sample curves are given in figure 6(a). In all cases, a 1-milliampere detection current was used with the Kelvin bridge; therefore, negligible heating above air temperature resulted from the resistance measurement.

A least-square solution for the best parabola through these points gave the coefficients shown in figure 6(a); the curve was represented by $\Omega_w = \Omega_0[1 + \alpha(T_w - 32) + \beta(T_w - 32)^2]$. From ten such complete resistance-temperature calibration curves, an average value of the second-order coefficient β was calculated to be 3.40×10^{-7} $(^{\circ}F)^{-2}$. Then a partial calibration curve was measured for the soft-soldered wire reported here (probe 109). As shown in figure 6(b), a least-square parabola was determined from the data points assuming $\beta = 3.40\times10^{-7}$ $(^{\circ}F)^{-2}$; the resulting empirical equation was used for all calculations to relate measured wire resistance to wire temperature.

5111

Anemometer electrical equipment. - A sketch of the primary circuit is shown in figure 7. The desired operating wire resistance was set on a Leeds and Northrup Kelvin Double Bridge (Model 4285) to four significant figures. With the switch in "hot" position the constant-average-temperature anemometer circuit varied the power input to the bridge until the wire was heated to the desired resistance and the "error" or galvanometer signal was a minimum. A hand-balanced volt-range potentiometer connected to the potential leads of the double bridge was used to measure the voltage across the hot wire. The power input to the wire element could be reproduced at a given flow setting to at least three significant figures in this manner. To measure the resistance of the unheated wire, the anemometer circuit was switched to "cold" position. This supplied the bridge with about 1-milliampere detection current, and the resistance was found by varying the bridge resistance until a 1.65-microvolt-per-millimeter galvanometer indicated balance.

The use of the Kelvin bridge and four-lead probes made it possible to measure the resistance and voltage drop of only the wire element, solder junction, and support prongs. Since the combined resistance of the junctions and prongs was less than 0.2 ohm, these lead resistances were less than 3 percent of the measured resistances in the worst case.

Procedure

The tunnel was operated at nominal Mach numbers of 0.05, 0.10, 0.20, 0.30, and so on to 0.80. At each Mach number, six static-density settings were used corresponding to nominal wire Knudsen numbers of 0.00916, 0.0143, 0.0256, 0.0416, 0.0555, and 0.0770. Most of these combinations were set at all four nominal total air temperatures of tunnel operation: 0°, 80°, 180°, and 280° F. An important feature of the test procedure was the somewhat random schedule of data taking. The run numbers in tables I and II are chronological. As will be emphasized in the RESULTS section, this procedure decreases the probability of systematic error in the measurements.

After the tunnel had been set at the desired condition and the probe moved into the test section, the manometer readings and test-section total temperature were recorded. The unheated or recovery resistance of the wire was measured next. Then, five or six hot-wire resistances were set and the voltage across the wire was recorded at each setting. About 5 minutes were required for all these heat-loss measurements. Finally, the recovery resistance and manometer-temperature readings were recorded again to complete the procedure.

The measured wire recovery resistance was used as a check of the wire temperature-resistance calibration. At no time during the reported runs did the measured Ω_e differ from that predicted by figure 6(b), nor the calculated T_e by more than 1 percent and on the average within 0.5 percent; T_e was calculated from the measured air total temperature in a manner discussed in the next section.

DIMENSIONLESS GROUPS OF CORRELATION

In this section, the dimensionless groups used in correlating the data are related to the physical measurements. An energy balance considering convection, conduction, and radiation for a hot wire in steady operation is

$$Q_P = Q_C + Q_K + Q_R \tag{4}$$

The heat input per unit time is simply

$$Q_P = J'I^2\Omega_w \tag{5}$$

The convective heat-loss rate defines the heat-transfer coefficient h:

$$Q_C = h\pi D_w l(T_w - T_e) \tag{6}$$

Equation (6) has equilibrium or recovery temperature T_e of an insulated wire in the temperature difference $(T_w - T_e)$. Therefore, as the wire temperature approaches its recovery value, the convective heat-transfer rate goes to zero. Figure 8 (from ref. 10) is the equilibrium temperature ratio used to obtain T_e from the measured air total temperature. It is well established that, for Knudsen numbers less than 0.10, the equilibrium temperature ratio for normal wires in both slip and continuum flow is a function only of Mach number (refs. 10 and 13 to 16).

The conduction loss rate to the supporting prongs Q_K is discussed in detail in appendix B. The radiation rate Q_R was calculated to be less than 0.1 percent of the power input Q_P, and no correction for radiation was made. However, since the heat loss to the supports was appreciable, an "end-loss" correction was made.

The Nusselt number is defined as

$$Nu = \frac{hD_w}{k} \tag{7}$$

The air thermal conductivity k has been evaluated at various temperatures by previous investigators. Some use static, others equilibrium or recovery, or total temperature; frequently in engineering work an arithmetic average "film" temperature is used (ref. 11). The guiding principle for empirical data fitting is, of course, to obtain the best correlation. The DISCUSSION section shows that the nonlinear temperature effect on heat-transfer coefficient of both air and wire temperature is too complicated in the slip-flow region for any of these choices to eliminate either "Mach number" or temperature effects. Therefore, for convenience, the air conductivity has been evaluated at total air temperature (k_t). Since the tunnel was operated at set values of total temperature, this choice introduces no Mach number vairation into the Nusselt number correlation at constant Knudsen number:

$$Nu_t = \frac{hD_w}{k_t} \tag{7a}$$

The Nusselt number can be expressed in terms of heat loss using equation (6):

$$Nu_t = \frac{Q_C}{\pi l k_t (T_w - T_e)} \tag{8}$$

The convective heat loss Q_C is the difference between the measured power input Q_P and a calculated correction for Q_K. A convenient way to make this correction is to define an uncorrected Nusselt number Nu_t'', which is completely determined from measured quantities:

$$Nu_t'' \equiv \frac{Q_P}{\pi l k_t (T_w - T_e)} = \frac{J' I^2 \Omega_w}{\pi l k_t (T_w - T_e)} \tag{9}$$

Two published end-loss correction procedures were used, as discussed in appendix B; each gave a correction factor ψ, defined as

$$\psi = \frac{Nu_t}{Nu_t''} \tag{10}$$

5111

Therefore, the tabulated Nusselt numbers were obtained from

$$Nu_t = \psi \frac{J'I^2\Omega_w}{\pi l k_t(T_w - T_e)} \tag{11}$$

The wire temperature was obtained from measured Ω_w and the resistance-temperature calibration:

$$\Omega_w = \Omega_0\left[1 + \alpha(T_w - 32) + \beta(T_w - 32)^2\right] \tag{12}$$

The equilibrium wire temperature was calculated from figure 8 and the measured total air temperature. The air conductivity k_t was taken from reference 18. All calculations were performed with an IBM 653 digital computer.

The Reynolds number Re_t for the wire was defined by the free-stream (or static) density and velocity; the air viscosity was evaluated at total air temperature (ref. 18):

$$Re_t = \frac{\rho U D_w}{\mu_t} \tag{13}$$

The Knudsen number was calculated from free-stream density and the wire diameter using the formula suggested by reference 14:

$$Kn = \frac{\lambda}{D_w} = \frac{1.5870\times10^{-8}}{\rho D_w} \tag{14}$$

The constant 1.5870×10^{-8} has the units pounds(mass)×square feet. Equation (14) assumes that the mean free path for air λ is given by elementary kinetic theory and that $\rho\lambda$ is a constant.

The Mach number was calculated from the velocity measured with a sonic orifice and static temperature:

$$M = \frac{U}{49.02\sqrt{T}} \tag{15}$$

The measured total-static pressures were used in the isentropic relations ($\gamma = 1.40$) for high-range mass flows to find Mach number.

Finally, the dimensionless turbulent intensity v'/U is known to affect the heat transfer from normal cylinders. However, the excellent work of reference 19 has shown that intensities as high as 20 percent have negligible effect on heat transfer from fine wires if the scale of turbulence is large compared with cylinder diameter. The intensity of turbulence varied in the test section but was always less than 1 percent. The scale was large compared with D_w. Therefore, turbulence was not a factor in these tests.

RESULTS

Twenty-three plots using all 1100 data points are presented in this section. These figures are intended to show the general consistency and the scope of the data. In the following section, these plots are used to point out some of the complicated effects observed in slip flow. Figure 9 shows the Nusselt number variation with Mach number for specified values of Knudsen number and wire and air temperatures. Figure 9(a) gives results for increasing wire temperatures at a total air temperature of 0° F. Similarly, figures 9(b), (c), and (d) are for air temperatures of 80°, 180°, and 280° F, respectively.

With the exception of the lowest wire temperature at each air temperature, the general consistency of the data is good. There are two experimental checks that can be used as a guide to data reliability. The first has already been discussed in the Procedure section; that is, the recovery resistance of the wire at a given air temperature and Mach number can be checked against the measured air temperature and the resistance-temperature calibration. The fact that these measurements usually checked predicted values within 0.5 percent is evidence that the critical Ω-T calibration did not vary during the course of the experiment. Another check for consistency is reproducibility. To demonstrate this feature, the chronological run numbers are shown with the data points in figure 9(b) for T_w of 583.8° F. The fact that the agreement between check points is good is evidence that the heat-transfer characteristics of the wire were unaffected by dirt accumulation, oxidation, or other uncontrollable factors during the experiment.

The data scatter at the lowest wire temperature for each air temperature is reasonable, because in equation (11) it is clear that constant percentage errors in T_w or T_e are magnified when the difference $(T_w - T_e)$ is small. However, the scatter at $Kn = 0.0770$ and also at $M > 0.50$ is puzzling. No satisfactory explanation for this scatter has been found. The high Knudsen number suggests that the poor correlation may be associated with the rarefied gas flow. For example, reference 20 calculated a "correction" for the temperature-jump phenomenon of slip flow. Accepted slip theory (ref. 21) was used to calculate the temperature jump. Then, by redefining the heat-transfer coefficient in terms of the difference between jump temperature and recovery temperature, a Nusselt number "correction" that depends only Knudsen number was obtained.

5111

The jump phenomenon does not account for the data scatter observed here at low wire temperatures, because the temperature jump is assumed proportional to $(T_w - T_e)$, going to zero as ΔT vanishes. Furthermore, the correction procedure has dubious value when the slip-flow region is approached from free-molecule flow predictions, because the procedure attempts to force data taken in slip flow to fit the form of continuum-flow observations. In this sense, the correction only confuses the over-all correlation and postpones the inevitable deviation from continuum Reynolds number correlations.

DISCUSSION

In this section some of the non-Reynolds-number effects evident in figure 9 are discussed. Then, the dependence of the Nusselt number on both wire and air temperature is considered. These complicated effects fortunately are relatively small compared with the dependence of Nusselt number on the aerodynamic environment. Therefore, the few generalizations that can be inferred from the data concerning these second-order temperature effects are discussed first. Then, a graphical Nusselt number correlation as a function of Reynolds and Knudsen (or Mach) numbers is presented for the slip-flow data of this research. An attempted general Nusselt number correlation for continuum, slip, and free-molecule flows follows, based on these and earlier data together with free-molecule flow theory. Finally, a fluctuation sensitivity equation for hot-wire anemometers is presented that applies to fine wires in subsonic slip flow.

Preliminary Discussion of Results

The following discussion of figure 9 attempts to point out the deviations from simple $\sqrt{Re}$ dependence of continuum flow that are evident in these slip-flow data. Later in this section, the heat-transfer characteristics of cylinders in continuum, slip, and free-molecule flows are considered. The discussion is limited to air at constant temperature where viscosity is constant. If the Nusselt number were a function only of $\sqrt{Re}$, lines of constant ρD_w on a logarithmic plot of Nu against U would form a family of parallel straight lines with a common slope of 0.50. The argument changes little if a family of constant Knudsen number lines on a log-log plot of Nusselt number against Mach number is considered. Two important deviations from this behavior should be noted in figure 9. The constant Knudsen number lines are linear only for Mach numbers less than 0.4. The decrease in slope and curvature that occurs around $M = 0.4$ is most pronounced at high Knudsen number where the sensitivity of heat-transfer coefficient to changes in Mach number almost disappears. Secondly, even the straight portions of these constant Kn curves exhibit slopes other than 0.50. For example, the slopes $(\Delta \log Nu_t)/(\Delta \log M)$ in figure 9(b) for $T_w = 583.8^\circ$ F from $M = 0.05$ to 0.4 increase with increasing Kn from 0.25 to 0.35.

Therefore, it is clear that no simple power dependence of Nu_t against Re_t should be expected to apply to these data over any appreciable range of variables. Furthermore, the wire and air temperatures can be expected to have only secondary influence on any correlation of the data, because the characteristics just discussed appear in all 23 parts of figure 9.

5111

Effect of Wire Temperature on Heat-Transfer Coefficient

Many cross plots are necessary in order to show clearly what effect varying the wire temperature has on the heat-transfer coefficient at a given flow condition. Figure 10(a), which presents cross plots of figure 9(a), is a plot of Nusselt number as a function of $(T_w - T_e)$ with Knudsen number as a parameter. All plots are for total air temperature of 0° F, and each plot is for a particular Mach number. Similarly, figures 10(b), (c), and (d), which are for total air temperatures of 80°, 180°, and 280° F, respectively, are cross plots of figures 9(b) to (d).

Consider figure 10(b) for $T_t = 80^\circ$ F and $M = 0.10$. The interesting feature is that the Nusselt number increases for the two lowest values of Knudsen number as the wire temperature is increased. For $Kn = 0.0256$ and 0.0416, Nu_t does not vary appreciably with ΔT, but at the two highest values of Kn, the heat-transfer coefficient decreases as the wire temperature increases. Furthermore, whether Nu_t increases or decreases, the dependence on wire temperature is greatest for ΔT less than 200° F and tends to vanish for ΔT greater than 200° F. This general picture is repeated for all the subsonic Mach numbers at $T_t = 80^\circ$ (fig. 10(b)). The two anomalous points at $M = 0.05$ are probably experimental errors. The percentage change in Nu_t from $\Delta T = 50^\circ$ F to the asymptotic value at $\Delta T > 200^\circ$ F is roughly 20 percent at all Mach numbers for both $Kn = 0.00916$ and $Kn = 0.0770$. There does appear to be a secondary Mach number effect that causes the reversal value of Kn (where the sign of the temperature dependence changes) to increase as M increases. For example, at $M = 0.10$, Nu_t is insensitive to ΔT at $Kn = 0.0256$ and 0.0416; but at $M = 0.60$ Nu_t is relatively insensitive to ΔT at higher Kn values (0.0416 and 0.0555).

Therefore, from figure 10(b), the wire temperature appears to affect the heat transfer in a manner primarily dependent on Kn and to a lesser extent on M, over the range of this experiment.

Figures 10(a), (c), and (d) essentially confirm what was observed at $T_t = 80^\circ$ F in figure 10(b). The temperature difference $(T_w - T_e)$ again appears to correlate the data into families of curves similar to figure 10(b). It is important to note that between $\Delta T = 50^\circ$ and 200° F at all air temperatures the maximum wire-temperature loading effect is evident, and at $\Delta T > 200^\circ$ F, Nu_t approaches an asymptote. Had a nondimensional temperature ratio like $\tau \left(\equiv \frac{T_w - T_e}{T_t}\right)$ been used, this regular feature would not have been observed. In figures 10(c) and (d), the increased air temperature tends to decrease the value of the Knudsen number where the sign of the wire-temperature loading effect reverses. That is, the $Kn = 0.0416$ and 0.0555 lines of both figures 10(c) and (d) show Nu_t increasing with increasing ΔT, while at $T_t = 80^\circ$ F these data were either unaffected or decreased as ΔT increased. This same effect of air temperature on the wire-temperature loading may also be seen in figure 10(a) for $T_t = 0^\circ$ F. Disregarding for the moment the $Kn = 0.00916$ and 0.0143 lines in figure 10(a), it is apparent that the insensitivity to ΔT at $M = 0.40$ to 0.80 persists at lower values of Kn in figure 10(a) than in figure 10(b). No explanation for the apparently anomolous behavior of the $Kn = 0.00916$ and 0.0143 curves in figure 10(a) has been discovered.

However, though the air temperature seems to have a secondary role in the wire-temperature loading phenomenon, it should not confuse the primary observation. That is, for $Kn < 0.02$, the heat-transfer coefficient increases with increasing ΔT up to $\Delta T \approx 200^\circ$ F, where it assumes an asymptotic value. On the other hand, for $Kn > 0.02$, the heat-transfer coefficient is unaffected or decreases with increasing ΔT to $\Delta T \approx 200^\circ$ F, where it again assumes an asymptotic value. The Mach number has a secondary role in this wire-temperature loading effect, generally causing the reversal Knudsen number to assume higher values (>0.02) as the Mach number increases in the subsonic range.

The trends reported here have been noted by previous investigators. The work of reference 16 was mentioned in the INTRODUCTION. The nonlinear overheat coefficient ξ defined by equation (3) is given as a function of Reynolds and Mach number by figure 8 of reference 16. For convenience, this figure is included herein as figure 11, and lines of constant Kn are superimposed. Now, it is clear from figure 10 that the heat-transfer coefficient observed in this research is not a linear function of ΔT (or related $\overline{a}_w$ or τ). However, the sign of the overheat coefficient ξ and its dependence on Kn and M is the important feature of figure 11. In general, in subsonic flow for low Kn, figure 11 predicts an increase in Nu_t with ΔT; a reversal of sign occurs between Kn = 0.015 and 0.020; while for Kn greater than these latter values, ξ predicts Nu_t will decrease with increasing ΔT. Furthermore, the Mach number has a secondary role causing the reversal value of Kn to increase. With the exception of the asymptotic behavior at large ΔT observed in this research, the work of reference 16 generally substantiates the results reported here. Since similar effects were noted in reference 14, there can be no doubt that these complicated wire-temperature effects are real, even though of second-order magnitude. Appendix B discusses the sole correction to the primary data (conduction loss) at some length to emphasize the fact that the wire-temperature loading effect cannot be traced to improper handling of the primary data.

Effect of Air Temperature on Heat-Transfer Coefficient

In order to isolate the effect of air temperature on the heat-transfer coefficient, it is of course necessary to eliminate the influence of wire-temperature loading. A logical way to accomplish this distinction would be to extrapolate the Nusselt number curves of figure 10 to $\Delta T = 0$. However, this is the region of maximum curvature, and extrapolation to zero overheat would be very uncertain. The asymptotic value of Nu_t for $\Delta T > 200^{\circ}$ F is a more direct Nu_t value that is independent of wire-temperature loading. Therefore, plots of the asymptotic Nu_t ($\Delta T > 200^{\circ}$ F) are presented in figure 12 as a function of total air temperature at various Mach numbers. Over the entire range of this experiment, the Nu_t decreases with increasing air temperature. The magnitude of this general trend in figure 12 appears to depend primarily on the value of the Nusselt number, being the order of 5 to 10 percent per 100° F for Nu_t between 3.0 and 4.0 but decreasing to 1 to 2 percent per 100° F near $Nu_t = 1.0$. No clear dependence of the air-temperature loading of Nu_t on either Mach or Knudsen number is discernible in this experimental range.

In figure 12, the Nusselt number decreases with increasing temperature, but it is not clear what dependence the heat-transfer coefficient h has on air temperature. Figure 13, which clarifies this point, is a copy of figure 12(b) for M = 0.50 with lines of constant heat-transfer coefficient superimposed. If the heat-transfer coefficient were constant and equal to the value observed in 80° F air, then Nu_t would vary with air temperature as shown by the dashed lines in figure 13. That is, the variation in air thermal conductivity k, which causes the T_t dashed-line dependence, is counterbalanced by an increase in heat-transfer coefficient h as the air temperature is increased. However, since h is not as temperature-dependent as k in this experimental range, the result is a net decrease in Nu_t with rising T_t.

Reference 6 reports good agreement of data taken at $1540^\circ < T_t < 3000^\circ$ F with the room-temperature correlation of reference 13. Thus, in the range of this work ($450 < Re < 3000$, $0.3 < M < 0.8$), air temperature had little effect on the Nusselt number, though there is a possibility that the high-temperature correlation is slightly lower than the room-temperature results. Therefore, it appears well established that increasing air temperature causes an increase in heat-transfer coefficient for all subsonic conditions where $Re > 1.0$.

The Prandtl number $c_p\mu/k$ varies from about 0.72 at 0° F to 0.68 at 280° F (ref. 18). Several correlations of Nu_t with Pr were attempted in order to eliminate the air-temperature effect shown in figure 13. However, none of these was successful, although plots of Nu_t/Pr_t^2 or Nu_t/Pr_t^3 did generally reduce the air-temperature dependence. The air-temperature range of this research is too small for any valid conclusions concerning Prandtl number correlations to be inferred.

Correlation of Slip-Flow Heat-Transfer Data

The heat-transfer characteristics of cylinders in slip flow are complicated by second-order dependence on body and air temperature. Nevertheless, a correlation of Nusselt number with the flow parameters is desirable as a first approximation in engineering work even though it does not account for the temperature phenomena. The Preliminary Discusssion of Results pointed out what deviations from simple $\sqrt{Re}$ dependence are evident in the data, but figure 9 is not a satisfactory substitute for the conventional correlation of Nu and $\sqrt{Re}$. Figure 14 is an attempt to find a useful correlation. It shows the logarithmic variation of Nu_t with Re_t; constant M and Kn parametric lines are shown solid and dashed, respectively. Data for $T_t \approx 80^\circ$ F and $T_w = 584^\circ$ F are plotted in this slip-flow correlation.

The increasing necessity for an additional parameter other than the Reynolds number to correlate these experimental heat-transfer data shows clearly on this plot as Re decreases. This additional parameter is either the Mach number or the Knudsen number. The graphical correlation (fig. 14) makes no distinction between $Nu = f(Re, M)$ or $Nu = f(Re, Kn)$, because both forms are shown. However, only one additional parameter (M or Kn) is independent (eq. (2)). The remainder of this section is devoted to showing that the use of Knudsen number as the additional parameter is preferable. Note that the Kn lines decrease in slope as

Kn increases. However, these constant Kn curves are approaching the slope of the constant Mach number lines at Kn = 0.00916. That is, ρD_w is approaching equivalence to U as required for simple Re correlation as Kn decreases; but the decreasing slopes of the Kn curves as Kn → 0.0770 cause a wide divergence of the constant Mach number lines that is most pronounced at low subsonic M (and low Re).

The preceding discussion of figure 14 emphasizes the fact that the failure of the Reynolds number alone to correlate the data, which has been termed a "Mach number effect" (e.g., p. 34 of ref. 22) and associated with compressibility, is, in fact, a rarefied-gas phenomenon and should be termed a "Knudsen number effect." This distinction is important and not just an arbitrary matter of viewpoint, even though equation (2) may make it so appear. When viewed as a rarefied-gas effect, the large separation of subsonic Mach number lines on a plot of Nu_t against Re_t loses its anomalous features and becomes theoretically predictable. Figure 15 was taken from an approximate slip-flow analysis published in 1953 (ref. 23). The qualitative agreement with the data in figure 14 is excellent, considering the approximations made in the theoretical analysis.

5111

Attempted General Correlation for Nusselt Number in Continuum, Slip, and Free-Molecule Flows

Figure 16 combines the correlation of the slip-flow data of this research (fig. 14) with the continuum experimental results of reference 13 and the free-molecular-flow theoretical predictions of references 15 and 24. A brief review of these latter reports is followed by a discussion of figure 16 as a whole.

The experimental range of reference 13 is shown in figure 1. The transient response of thermocouples in air was measured, and the results were correlated within 7.4-percent average deviation of a single observation by the following equation:

$$Nu_t = 0.431 \sqrt{Re_t^*} \qquad (16)$$

where Re_t^* is a Reynolds number defined by free-stream velocity, total-temperature viscosity, wire diameter, and a density based on static pressure and total temperature. In terms of the Reynolds number defined by equation (13), the Nusselt number correlation of reference 13 is

$$Nu_t = 0.431 \sqrt{Re_t}\left(\frac{T}{T_t}\right)^{1/2} \qquad (16a)$$

where

$$\frac{T}{T_t} = \left(1 + \frac{\gamma - 1}{2} M^2\right)^{-1}$$

The equation applies in range of the experiment: $250 < Re < 30{,}000$ and $0.1 < M < 0.9$. A partial plot of equation (16a) is shown in figure 17. The important feature is the small effect that changing the subsonic Mach number has on heat transfer at constant Reynolds number. This Mach number effect increases with increasing M and is practically zero below $M = 0.3$. It is reasonable to expect that a compressibility phenomenon would behave in this manner.

An equation for the free-molecular-flow heat transfer from an infinite cylinder in a diatomic gas stream was derived in reference 24. Evaluating all air properties at 80° F and assuming an accommodation coefficient of 0.90, this equation may be written as

$$Nu_t = 0.0297 \frac{g(s)}{Kn} \left(\frac{T}{T_t}\right)^{1/2} \tag{17}$$

where $g(s)$ is a defined function of Mach number plotted in figure 18. Equation (17) applies to all $Kn > 2$. Figure 19 is a plot of equation (17) for $Kn > 2$; it also gives the predictions of slip theory for $Kn < 2$. Although several of the essential features of this free-molecule analysis have been confirmed experimentally, equation (17) has not been tested over an appreciable range of variables. However, free-molecule-analysis theoretical predictions are generally believed reliable. The two essential features of figure 19 for $Kn > 2$ are the first-power dependence on Re and the large separation of subsonic M lines.

Returning to figure 16, the slip-flow experimental data extrapolate smoothly into the continuum-flow empirical curve. However, the slip-flow correlation at $Kn = 0.0770$ cannot be extrapolated to the free-molecule-flow correlation at $Kn = 2$. Nevertheless, several of the trends required by the rarefied-gas analysis are evident in the data. The slip-flow data constant M lines increase in slope and may be approaching first-power Re_t dependence at $Kn = 0.0770$. Furthermore, the increasing Kn dependence causes a spread of the constant M lines at $Kn = 0.0770$ that is most pronounced at low subsonic M. Before the attempted correlation in figure 16 can be reliably extended below $Re = 1.0$, it will be necessary to obtain experimental data between Kn of 0.10 and 10.0. Until these data are published, the theoretical curves from the approximate slip-flow analysis of reference 23 between Kn of 0.04 and 2 shown in figure 19 may be used as a first approximation together with the free-molecule-flow prediction for $Kn > 2$.

Finally, the suggested curve of reference 11 is shown in figure 16 for easy comparison. The low Reynolds number data used to obtain this curve were for very low velocities (Kn < 0.01). Furthermore, the attempted general correlation and the reference 11 correlation are not comparable, strictly speaking, because total air temperature was used for calculating conductivity and viscosity in the proposed correlation, while an average "film" temperature was used in reference 11.

Hot-Wire-Anemometer Sensitivity

5111

One application of the heat-transfer correlations presented in the preceding section is for hot-wire-anemometer sensitivity. King's equation (1) sensitivity for wire Re < 250 is a crude approximation because the Knudsen number effect complicates the Reynolds number correlation. In the following paragraphs, a sensitivity equation based on dimensionless group correlations is proposed. However, as in the past, the only reliable hot-wire sensitivity is a direct calibration of the particular wire over the flow range of operation. The sensitivity equation serves as a guide to performing this calibration.

The Nusselt number correlation given in figure 14 may be expressed in a general manner as

$$Nu_t = f(M, Kn, \Delta T, T_t) \tag{18}$$

The dependence on ΔT and T_t causes up to 20-percent deviations from figure 14 in a complicated manner. The following derivation assumes that the anemometer wire operates at constant temperature (e.g., see ref. 9). This eliminates the functional dependence of Nu_t on ΔT. It is convenient to express the remaining T_t dependence in equation (18) with a dimensionless temperature ratio τ:

$$\tau = \frac{T_w - \eta T_t}{T_t} = \frac{\Delta T}{T_t} \tag{19}$$

The recovery temperature ratio η (fig. 8) will be assumed a function only of Mach number; this is true for Kn < 0.10.

The general sensitivity for a constant-temperature anemometer wire to fluctuating flow velocity, density, and total temperature may be written as

$$2I\Omega_w\,dI = \frac{\partial}{\partial U}\left[\frac{\pi}{J}\,l k_t Nu_t(T_w - \eta T_t)\right]dU + \frac{\partial}{\partial \rho}\left[\frac{\pi}{J}\,l k_t Nu_t(T_w - \eta T_t)\right]d\rho + \frac{\partial}{\partial T_t}\left[\frac{\pi}{J}\,l k_t Nu_t(T_w - \eta T_t)\right]dT_t \tag{20}$$

Recalling that it is assumed that the wire temperature is maintained constant by a fluctuating feedback current, denoted by i (=dI), then equation (20) becomes

$$i = \frac{I}{200}\left[-\left(1 + \frac{\gamma - 1}{2} M^2\right)\frac{M}{\tau}\frac{\partial\eta}{\partial M} - \frac{\eta}{\tau}(\gamma - 1)M^2 + \left(1 + \frac{\gamma - 1}{2} M^2\right)\frac{\partial \log Nu}{\partial \log M}\right]$$

$$\times \frac{100\delta U}{U} + \frac{I}{200}\left(-\frac{\partial \log Nu}{\partial \log Kn}\right)\frac{100\delta\rho}{\rho} + \frac{I}{200}\left(\frac{\partial \log k}{\partial \log T_t} - \frac{\eta}{\tau} - \frac{\tau + \eta}{Nu}\frac{\partial Nu}{\partial \tau}\right)\frac{100\delta T}{T_t} \tag{21}$$

Appendix C gives the derivation of equation (21), which relates the fluctuating current i of a constant-temperature anemometer wire to the fluctuating flow variables velocity fluctuation δU, density fluctuation $\delta\rho$, and total-air-temperature fluctuation δT. The average wire current I refers to an infinitely long wire if the sensitivity slopes are taken from Nu_t rather than Nu_t'' plots. The second-order dependence of the general correlation (fig. 14) on air and wire temperatures complicates generalizations concerning the major sensitivity slopes: $\frac{\partial \log Nu}{\partial \log M}$, $\frac{\partial \log Nu}{\partial \log Kn}$, and $\frac{\partial Nu}{\partial \tau}$. However, since over a small range of variables each of the logarithmic slopes is linear and approximately independent of the magnitude of the independent variable, it is possible to make two limited generalizations. Figure 20 gives the measured slopes from figure 9(b) for T_w of 583.8° F and its cross plot; these terms are applicable at $T_t \approx 80°$ F and $\Delta T > 200°$ F.

The utility of equation (21) is limited by the lack of a precise universal correlation. However, if the turbulent velocity intensity is the quantity of interest in airflows of $M < 0.4$, equation (21) simplifies considerably. Under these circumstances, density fluctuations are frequently negligible; and, unless heat is added to or taken from the airstream, the total-air-temperature fluctuations are also negligible. The predominant term in the velocity sensitivity is $(\partial \log Nu)/(\partial \log M)$, and this term is as easily obtained experimentally as the usual King's equation calibration curve, perhaps requiring only a larger range of velocity variation.

Finally, it should be pointed out that reference 22 presents sensitivity equations similar to equation (21) for constant-current anemometry, with special emphasis on supersonic-flow applications. In subsonic and transonic applications, equation (21) has the advantage that the Reynolds number was not chosen as an independent variable (M and Kn, rather than M and Re). The use of Reynolds number introduces additional terms in the velocity sensitivity.

CONCLUDING REMARKS

The following conclusions can be drawn from the heat-transfer measurements for cylinders in slip flow presented in this report:

1. An attempted Nusselt number correlation for heat transfer from normal cylinders in subsonic continuum, slip, and free-molecule airflows is given as figure 16. Slip-flow experimental data of this paper extrapolate into existing continuum-flow experimental data for low values of Knudsen number ($Kn < 0.01$). The slip-flow data qualitatively verify trends predicted by free-molecule-flow theory ($Kn > 2$) at Kn approaching 0.10; but extrapolation does not give quantitative agreement. Further experiments in the transition region between slip and free-molecule flows are necessary to complete the general correlation.

2. Empirical equations that give the Nusselt number as a constant power of Reynolds number, familiar in continuum flow, are progressively in error for $Re < 250$ because of increasing Kn dependence in the slip-flow region. The correlation of Nusselt number for this slip-flow experiment is shown graphically in figure 14 as a function of Reynolds and Knudsen or Mach numbers. This dependence is too complicated for an empirical equation with engineering utility, although simple equations have previously been proposed in both continuum and free-molecule flows.

3. The approximate slip-flow analysis of reference 23 correctly predicts the trends observed but fails to fit the data quantitatively.

4. For air temperatures between 80° and 280° F, the heat-transfer coefficient h increases with increasing temperature difference ΔT at low Kn (<0.02). This nonlinearity in h with ΔT has commonly been observed in continuum-flow experiments. However, with air temperatures between 0° and 280° F, at high Kn (>0.02) the heat-transfer coefficient decreases with increasing ΔT. In both cases, the effect of ΔT was greatest for ΔT below 200° F, tending to disappear at ΔT greater than 200° F. A secondary Mach number effect causes the reversal Knudsen number of about 0.02 to shift to larger values as M increases. The major trends are corroborated by the work of reference 16.

5. For wires operated at ΔT greater than 200° F, an increase of air temperature causes the heat-transfer coefficient h to increase. This occurs for all flow conditions of this research. The increase in air thermal conductivity with total air temperature tends to cancel the variation of Nusselt number $Nu_t (=hD_w/k_t)$ with air temperature. However, Nu_t decreases slightly with increasing air temperature because the thermal conductivity has a greater temperature-dependence than the heat-transfer coefficient in the range of this research.

6. Constant-temperature hot-wire-anemometer sensitivity to velocity, density, and total-air-temperature fluctuations is extremely complicated with the probe in subsonic slip flow. General sensitivity equations together with a few generalizations observed in this research have been presented. However, individual calibration of wires in the flow range of interest is the only reliable technique for subsonic applications because (a) King's law is a very special case of hot-wire sensitivity ($Kn < 0.001$, $M < 0.3$), and (b) complicated nonlinearity of heat transfer with wire and air temperature prevents accurate generalizations using dimensionless groups.

Lewis Flight Propulsion Laboratory
National Advisory Committee for Aeronautics
Cleveland, Ohio, August 28, 1958

APPENDIX A

SYMBOLS

A	King's equation intercept (eq. (1)), $A = alk$
A'	dimensionless King's equation intercept (eq. (1a)), $A' = a/\pi \Omega_0 \alpha$
A_w	cross-sectional area of wire, sq ft
a,b	dimensionless empirical constants (eq. (1))
a^*	dimensionless term in eq. (B24)
a_s	speed of sound
$\bar{a}_w$	resistance ratio, $(\Omega_w - \Omega_e)/\Omega_e$
B	King's equation slope (eq. (1)), $B = bl\sqrt{D_w \rho c_p k}$
B_1,B_2	empirical constants (eq. (B16))
B'	dimensionless King's equation slope (eq. (1a)), $B' = b/\pi \Omega_0 \alpha$
B^*	dimensionless term defined by eq. (B18)
C	ratio of heat lost by conduction to supports to heat lost to air by convection (eq. (B13))
c_p	isobaric specific heat
D_s	support diameter, ft or in.
D_w	wire diameter, ft or in.
e,G	dimensionless terms defined by eq. (B20)
g_c	conversion factor to engineering units, (lb(M))(ft)/lb(F)-sec^2
h	convective heat-transfer coefficient (eq. (6))
h_0	heat-transfer coefficient extrapolated to $\Delta T = 0$
I	wire current, amp
J	conversion of Btu to ft-lb(F)

J'	conversion of watts to Btu/sec, 9.484×10^{-4}
K_s	thermal conductivity of Inconel support, Btu/(sec)(ft)(°F)
K_w	thermal conductivity of tungsten wire, Btu/(sec)(ft)(°F)
Kn	Knudsen number, λ/D_w
k	thermal conductivity of air, Btu/(sec)(ft)(°F)
l	length of wire, ft
M	Mach number
Nu	Nusselt number, hD_w/k
Nu"	Nusselt number uncorrected for heat loss to supports (eq. (9))
Pr	Prandtl number, $c_p\mu/k$
Q	length-average heating rate, Btu/sec
q	heating rate per unit length, Btu/(ft)(sec)
Re	Reynolds number, $\rho D_w U/\mu$
$Re_{f,s}$	Reynolds number of support, $\rho U D_s/\mu_{f,s}$
S	dimensionless term defined by eq. (B25)
T	static or free-stream air temperature
ΔT	temperature difference, $T_w - T_e$
T_a	air temperature
T_e	recovery or equilibrium wire temperature
T_t	total air temperature
T_w	length-average wire temperature
$T_{w,\infty}$	length-average temperature of infinitely long wire, $T_{w,\infty} \equiv \sigma_1/\sigma$
t^*	dimensionless ratio (eq. (B18))
t_w	local wire temperature at any point x

U	free-stream air velocity, ft/sec
v'	rms turbulent velocity, ft/sec
x	any position along length of wire, $x = 0$ at wire center
Y	dimensionless term defined by eq. (B18)
z	factor in end-loss correction procedure, defined by eq. (B19)
α	first-order coefficient of electrical resistance - temperature relation (eq. (12)), $^{\circ}F^{-1}$
β	second-order coefficient of electrical resistance - temperature relation (eq. (12)), $^{\circ}F^{-2}$
γ	ratio of specific heats, 1.4 for air
δ	perturbation component
η	recovery temperature ratio, $\eta \equiv T_e/T_t$
λ	mean free path of air, ft
μ	air viscosity, lb(M)/(ft)(sec)
ξ	nonlinear overheat coefficient (eq. (3))
ρ	air density, lb(M)/cu ft
σ	coefficient defined in eq. (B7)
σ_1	coefficient defined in eq. (B8)
τ	temperature ratio, $\tau \equiv (T_w - T_e)/T_t$
ψ	end-loss correction ratio, $\psi \equiv Nu/Nu''$
Ω_a	length-average wire resistance at air temperature T_a, ohms
Ω_e	length-average wire resistance at recovery air temperature T_e, ohms
Ω_w	length-average wire resistance at hot-wire temperature T_w, ohms
Ω_0	length-average wire resistance at 32° F, ohms
ω	wire resistance per unit length, ohms/ft

5111

Subscripts:

C	convection
f	film temperature, $T_f \equiv (T_s + T_e)/2$
K	conduction
m	measured
P	production
R	radiation
s	support (except a_s)
t	total air temperature T_t
w	wire or cylinder
O	evaluated at 32° F (except h_O)

APPENDIX B

CORRECTIONS FOR CONDUCTION TO SUPPORTS

Linear Correction

The steady-state heat transfer from a hot wire having negligible radiant heat loss is treated by Lowell in reference 10, where equations for making precise corrections for finite wire length are presented. Except for a minor innovation, the following analysis is that of reference 10.

The energy-balance equation at any cross section x for this problem is simply

$$q_P = q_C + q_K \tag{B1}$$

The convection heat loss per unit length of wire at x can be expressed as

$$q_C = hD_w\pi(t_w - T_e) = \pi k_t Nu_t(t_w - T_e) \tag{B2}$$

The expression for conduction of heat to the supports can be simplified if it is assumed that the heat flow through the wire is one-dimensional and that the wire thermal conductivity K_w is not affected by temperature:

$$q_K = -K_w A_w \frac{d^2 t_w}{dx^2} \tag{B3}$$

Neglecting the second-order term $\beta(t_w - 32)^2$, the resistance per unit length of wire can be written in terms of the local wire temperature:

$$\omega = \omega_0[1 + \alpha(t_w - 32)] \tag{B4}$$

where ω_0 is the resistance per unit length in ohms per inch at 32° F. Substituting equations (B2) to (B4) into (B1),

$$J'I^2\omega_0[1 + \alpha(t_w - 32)] = \pi k_t Nu_t(t_w - T_e) - K_w A_w \frac{d^2 t_w}{dx^2} \tag{B5}$$

5111

5111

Equation (B5) can be written more simply as

$$\frac{d^2t_w}{dx^2} - \sigma t_w = -\sigma_1 \tag{B6}$$

where the constants are defined as follows:

$$\sigma \equiv \frac{\pi k_t Nu_t - J'I^2\omega_0\alpha}{K_w A_w} \tag{B7}$$

$$\sigma_1 \equiv \frac{\pi k_t Nu_t T_e + J'I^2\omega_0\alpha\left(\frac{1}{\alpha} - 32\right)}{K_w A_w} \tag{B8}$$

The lengthwise variation of $k_t Nu_t$ or its equivalent hD_w is ignored; that is, h is assumed unaffected by t_w or T_e.

Equation (B6) is a second-order, ordinary differential equation with constant coefficients. The following boundary conditions are used to find the temperature distribution along the wire length:

(1) The wire is symmetrical; therefore, at the center of the wire (at $x = 0$), the temperature gradient must be zero: $\left.\frac{dt_w}{dx}\right|_{x=0} = 0$.

(2) The temperature at each support, $x = \pm l/2$, is $T_{w,s}$ (an as yet undetermined temperature, but physically it is known that $T_e \geq T_{w,s} \geq T_w$).

The solution of equation (B6) satisfying these conditions is

$$t_w = T_{w,\infty} - (T_{w,\infty} - T_{w,s})\frac{\cosh \sigma^{1/2} x}{\cosh \frac{\sigma^{1/2}}{2} l} \tag{B9}$$

The measured mean resistance Ω_w is related to the length-average wire temperature $(\omega_0 l = \Omega_0)$:

$$\Omega_w = \Omega_0[1 + \alpha(T_w - 32)] \tag{B10}$$

Here, T_w is obtained from integration of (B9) over the wire length:

$$T_w = T_{w,\infty} - \frac{T_{w,\infty} - T_{w,s}}{\frac{\sigma^{1/2} l}{2}} \tanh \frac{\sigma^{1/2} l}{2} \tag{B11}$$

Having obtained the wire-temperature distribution, the next step is to write an energy balance on the entire wire. The power input is now written in terms of equation (B10), the convection loss in terms of (B11), and the conduction loss in terms of the derivative of (B9) evaluated at the point of attachment $(x = l/2)$:

$$J'I^2\omega_0[1 + \alpha(T_w - 32)]$$
$$= \pi k_t Nu_t(T_w - T_e) + \frac{2K_w A_w \sigma^{1/2}}{l}(T_{w,\infty} - T_{w,s})\tanh \frac{\sigma^{1/2} l}{2} \tag{B12}$$

At this point, it is convenient to define a quantity C as the ratio of the heat lost by conduction to the supports to that lost directly to the airstream by convection:

$$C \equiv \frac{4K_w A_w}{l^2} \frac{(T_{w,\infty} - T_{w,s})\left(\frac{\sigma^{1/2} l}{2}\right)\tanh \frac{\sigma^{1/2} l}{2}}{\pi k_t Nu_t(T_w - T_e)} \tag{B13}$$

Equation (B12) can be expressed in terms of C as follows:

$$J'I^2\omega_0[1 + \alpha(T_w - 32)] = \pi k_t Nu_t(T_w - T_e)(1 + C) \tag{B14}$$

The only unknown in C (other than Nu_t) is the temperature at the support $T_{w,s}$. An energy balance on the support is made to determine $T_{w,s}$. The problem is analogous to the wire treatment just outlined except that the heat input is the conduction from the wire, the output is convection from the support, and the electrical power input is assumed zero in the supports. Solving this energy balance for $T_{w,s}$ and approximating $\tanh(\sigma^{1/2} l/2)$ as 1.0 give the following:

$$T_{w,s} = \frac{2Nu_{f,s}^{1/2}k_{f,s}^{1/2}K_s^{1/2}D_s T_e + K_w D_w^2 \sigma^{1/2} T_{w,\infty}}{2Nu_{f,s}^{1/2}k_{f,s}^{1/2}K_s^{1/2}D_s + K_w D_w^2 \sigma^{1/2}} \tag{B15}$$

5111

Since the objective of the foregoing analysis of the heat transfer from the support was to determine $T_{w,s}$ in terms of known quantities (so that ultimately the end loss ratio C could be found), it appears that the introduction of $Nu_{f,s}$ in equation (B15) has simply replaced one unknown by another. Fortunately, the Nusselt number of the support can be adequately represented by the following empirical relation, because the support is large and in continuum flow:

$$Nu_{f,s} = B_1 + B_2(Re_{f,s})^n \tag{B16}$$

where

$$Re_{f,s} = \frac{\rho U D_s}{\mu_{f,s}}$$

Equation (B16) neglects the small Mach number effect observed at Re > 250. Following are values of n, B_1, and B_2 from reference 11 (p. 260, table 10-4):

$Re_{f,s}$ range	n	B_1	B_2
0.1 - 1000	0.52	0.32	0.43
1000 - 50,000	.60	0	.24

Equations (B13), (B15), and (B16) can be combined with equation (B14); the only unknown quantity is the corrected wire Nusselt number Nu_t. Lowell (ref. 10) has shown that the combination of essentially the equations just mentioned can be written as

$$C = \frac{1 - t^*(1 + C)}{B^*\left[(1 + C)^{-1} - t^*\right] + Y\left[(1 + C)^{-1} - t^*\right]^{1/2} - 1} \tag{B17}$$

where

$$\left.\begin{aligned} t^* &\equiv \frac{T_w - T_e}{\left(\frac{1}{\alpha} - 32\right) + T_w} \\ B^* &\equiv \frac{l k_t Nu_t''}{(B_1 + B_2 Re_{f,s}^n)^{1/2} K_s^{1/2} k_{f,s}^{1/2} D_s} \\ Y &\equiv \left(\frac{k_t}{K_w}\right)^{1/2} \frac{l}{D_w} (Nu_t'')^{1/2} \end{aligned}\right\} \tag{B18}$$

A more usable form of equation (B17) was derived by Lowell after reference 10 was published. Another form of the ratio of corrected to uncorrected Nusselt number was defined as follows:

$$\frac{Nu_f}{Nu_f''} = \frac{1}{1 + C} \equiv (1 - t^*)\left(\frac{t^*}{1 - t^*} + z^2\right) \tag{B19}$$

Then, by letting

$$\left.\begin{aligned} e &\equiv Y(1 - t^*)^{1/2} \\ G &\equiv B^*(1 - t^*) \end{aligned}\right\} \tag{B20}$$

an algebraically simpler expression for equation (B19) is obtained:

$$Gz + e = \frac{1}{z - z^3} \tag{B21}$$

The procedure used to calculate Nu_t for table I was to solve (B21) for the root of z between $z = 0.5$ and $z = 1.0$. This solution is straightforward once the physical constants in both G and e are evaluated. The following values were used in the electronic digital computor data-reduction program:

Tungsten wire: $l = 0.077$ in.

$D_w = 2.2 \times 10^{-4}$ in.

$\alpha = 2.24 \times 10^{-3}\ {}^{\circ}F^{-1}$

$K_w = 3.43 \times 10^{-2}$ Btu/(sec)(ft)(°F)

Inconel support: $D_s = 0.027$ in. (at point of attachment)

$K_s = 2.19 \times 10^{-3}$ Btu/(sec)(ft)(°F)

Air properties: $\left.\begin{aligned} \mu_{f,s} &\approx \mu_t \\ k_{f,s} &\approx k_t \end{aligned}\right\}$ (ref. 18)

Another method of making end-loss corrections on hot-wire data has been widely used by investigators at other laboratories. Essentially, it is a limiting case of the more general method just outlined. Kovásznay originally published the method (without derivation) in reference 7; reference 25 gives a more complete presentation.

The problem is identical to that treated by Lowell, except that Kovásznay uses the mathematically simpler boundary condition $T_{w,s} = T_e$. Since the recovery temperature T_e is immediately available, equations (B7) and (B12) can be solved without further ado for Nu_f. A further simplification can be gained if the reference temperature of the calibration of wire temperature and resistance is taken at T_e rather than at 32° F as in the previous section. If these substitutions are made in equations (B13) and (B14), it can be shown that the following equation is the desired solution for ψ:

$$\frac{Nu_t}{Nu_t''} = \frac{\frac{\bar{a}_w}{a^*} + \bar{a}_w}{1 + \bar{a}_w} \tag{B22}$$

where

$$\bar{a}_w = \frac{\Omega_w - \Omega_e}{\Omega_e} \tag{B23}$$

$$\frac{\bar{a}_w}{a^*} = 1 - S\left(\frac{a^*}{\bar{a}_w}\right)^{1/2} \tanh \frac{1}{S}\left(\frac{\bar{a}_w}{a^*}\right)^{1/2} \tag{B24}$$

$$S = \frac{D_w}{l}\left(\frac{K_w}{k_t}\right)^{1/2} Nu_t''^{-1/2}(1 + \bar{a}_w)^{1/2} \tag{B25}$$

This procedure was also used in the data-reduction program. The results of this end-loss correction agreed with those obtained using equation (B21) within a small fraction of 1 percent of Nu_t for all flow conditions of this research. Therefore, the probe supports did act effectively as an infinite sink. That is, the wire-support junction was effectively maintained at recovery temperature, $T_e \approx T_{w,s}$.

Nonlinear Correction

The linear correction procedures just outlined are rather elaborate. However, the methods differ only in the manner used to treat the temperature of the wire-support junction. Both procedures assume that the wire has no second-order temperature dependence ($\beta = 0$), that the heat-transfer coefficient is not dependent on wire temperature, and that the wire thermal conductivity is constant. Generally, none of these

5111

CS-5

assumptions are true. So, it is conceivable that the end-loss correction is incorrect and that this mistake causes the nonlinearity of Nu_t with ΔT and T_t. An excellent discussion of this problem is published in reference 16. Mechanically integrated solutions of the nonlinear equation that includes β, ξ (eq. (3)), and $K_w = f(t_w)$ are compared with the linear solution, and it is concluded that the linear solution of Kovásznay differs by only 1/2 percent from the nonlinear solutions for any realistic probe design. Therefore, the procedure used to correct for finite wire length in this report is adequate.

APPENDIX C

DERIVATION OF HOT-WIRE-ANEMOMETER SENSITIVITY EQUATIONS

Assume that the general heat-loss characteristics of normal cylinders are known in terms of Nusselt number corrected for conduction loss to supports. Specifically, the Nusselt number is a function of the Mach and Knudsen (or Reynolds) numbers, and the effect of air temperature at constant wire temperature is assumed described by a single parameter τ:

$$Nu_t = f(M,Kn,\tau) \tag{C1}$$

$$\tau = \frac{T_w - T_e}{T_t} \tag{C2}$$

The subscript t on Nu and k will be dropped here and understood throughout appendix C. The recovery temperature ratio η will be assumed to be independent of Kn, as in figure 8; this is valid at least to $Kn = 0.10$:

$$\eta = \frac{T_e}{T_t} = f(M) \tag{C3}$$

The heat loss from a wire may be written as

$$J'I^2\Omega_w = \pi l k(T_w - \eta T_t)Nu \tag{C4}$$

Equation (C4) assumes that Nu is corrected for finite wire length so that I^2 is the square of the measured wire current times the end-loss correction factor, ψI_m^2. Naturally, if a calibration curve for a particular wire is being used, it is possible to set $\psi = 1$ and correlate data as Nu''.

It will be assumed that the hot-wire resistance (and temperature) is maintained constant by a fluctuating feedback current:

$$2J'I\Omega_w\,dI = \frac{\partial}{\partial U}\left[\pi l k(T_w - \eta T_t)Nu\right]dU + \frac{\partial}{\partial \rho}\left[\pi l k(T_w - \eta T_t)Nu\right]d\rho + \frac{\partial}{\partial T_t}\left[2 l k(T_w - \eta T_t)Nu\right]dT \tag{C5}$$

If the fluctuating current dI is set equal to i and small finite flow fluctuations are approximated by δ to replace the derivatives, equation (C5) can be written as

$$i = \left[\frac{\pi l}{2J'I\Omega_w} kNuT_t\left(-\frac{\partial\eta}{\partial U}\right) + \frac{\pi l}{2J'I\Omega_w} kNu\eta\left(-\frac{\partial T_t}{\partial U}\right) + \frac{\pi l}{2J'I\Omega_w} k(T_w - \eta T_t)\frac{\partial Nu}{\partial U}\right]\delta U$$

$$+ \left[\frac{\pi l}{2J'I\Omega_w} k(T_w - \eta T_t)\frac{\partial Nu}{\partial \rho}\right]\delta\rho$$

$$+ \left[\frac{\pi l}{2J'I\Omega_w}(T_w - \eta T_t)Nu\frac{\partial k}{\partial T_t} - \frac{\pi l}{2J'I\Omega_w} kNu\eta + \frac{\pi l}{2J'I\Omega_w} k(T_w - \eta T_t)\frac{\partial Nu}{\partial T_t}\right]\delta T_t \tag{C6}$$

It will be convenient to introduce the following dimensionless groups to generalize equation (C6) for numerical evaluation of the various sensitivity derivatives:

$$\frac{\partial}{\partial\rho} = \frac{\partial Kn}{\partial\rho}\frac{\partial}{\partial Kn} = -\frac{Kn}{\rho}\frac{\partial}{\partial Kn} \tag{C7}$$

$$\frac{\partial}{\partial U} = \frac{\partial M}{\partial U}\frac{\partial}{\partial M} = \frac{1 + \frac{\gamma - 1}{2}M^2}{a_s}\frac{\partial}{\partial M} \tag{C8}$$

$$\frac{\partial T_t}{\partial U} = \frac{U}{c_p g_c J} \tag{C9}$$

$$\frac{\partial}{\partial T_t} = \frac{\partial\tau}{\partial T_t}\frac{\partial}{\partial\tau} = -\frac{\tau + \eta}{T_t}\frac{\partial}{\partial\tau} \tag{C10}$$

Substituting (C7) to (C10) into equation (C6) and recalling that $M = \frac{U}{a_s}$ and $\frac{I}{2Nu} = \frac{\pi l}{2JI\Omega_w} k(T_w - \eta T_t)$, the following form may be written:

$$i = \frac{I}{2}\left[-\left(1 + \frac{\gamma - 1}{2}M^2\right)\frac{M}{\tau}\frac{\partial\eta}{\partial M} - \frac{\eta}{T_w - \eta T_w}\frac{U^2}{c_p g_c J} + \left(1 + \frac{\gamma - 1}{2}M^2\right)\frac{M}{Nu}\frac{\partial Nu}{\partial M}\right]\frac{\delta U}{U}$$

$$+ \frac{I}{2}\left(-\frac{Kn}{Nu}\frac{\partial Nu}{\partial Kn}\right)\frac{\partial\rho}{\rho} + \frac{I}{2}\left(\frac{T_t}{k}\frac{\partial k}{\partial T_t} - \frac{\eta T_t}{T_w - \eta T_t} - \frac{\tau + \eta}{Nu}\frac{\partial Nu}{\partial\tau}\right)\frac{\partial T_t}{T_t} \tag{C11}$$

Replacing $\left(\frac{u}{v}\frac{\partial v}{\partial u}\right)$ by $\frac{\partial \log v}{\partial \log u}$ and using a familiar identity, the sensitivity equation can be written in its final form, which is given as equation (21) of the text.

REFERENCES

1. King, Louis Vessot: On the Convection of Heat from Small Cylinders in a Stream of Fluid. Proc. Roy. Soc. (London), ser. A, vol. 214, no. 14, Nov. 12, 1914, pp. 373-432.

2. Dryden, H. L., and Kuethe, A. M.: The Measurement of Fluctuations of Air Speed by the Hot-Wire Anemometer. NACA Rep. 320, 1929.

3. Corrsin, Stanley: Extended Applications of the Hot-Wire Anemometer. NACA TN 1864, 1949.

4. Carbon, M. W., Kutsch, H. J., and Hawkins, G. A.: The Response of Thermocouples to Rapid Gas-Temperature Changes. Trans. ASME, vol. 72, no. 5, July 1950, pp. 655-657.

5. Fiock, Ernest: Ninth Monthly Report of Progress on the Development of Thermocouple Pyrometers for Gas Turbines. NBS, Sept. 6, 1946.

6. Glawe, George E., and Johnson, Robert C.: Experimental Study of Heat Transfer to Small Cylinders in a Subsonic, High-Temperature Gas Stream. NACA TN 3934, 1957.

7. Kovásznay, Leslie S. G., and Törmarck, Sven I. A.: Heat Loss of Hot-Wires in Supersonic Flow. Bumblebee Rep. No. 127, Dept. Aero., The Johns Hopkins Univ., Apr. 1950. (Contract NOrd 8036 with BuOrd., U. S. Navy.)

8. Laufer, J., and McClellan, R.: Measurement of Heat Transfer from Fine Wires in Supersonic Flows. Jour. Fluid Mech., vol. 1, pt. 3, Sept. 1956, pp. 276-289.

9. Laurence, James C., and Landes, L. Gene: Auxiliary Equipment and Techniques for Adapting the Constant-Temperature Hot-Wire Anemometer to Specific Problems in Air-Flow Measurements. NACA TN 2843, 1952.

10. Lowell, Herman H.: Design and Applications of Hot-Wire Anemometers for Steady-State Measurements at Transonic and Supersonic Airspeeds. NACA TN 2117, 1950.

11. McAdams, William H.: Heat Transmission. Third ed., ch. 10, McGraw-Hill Book Co., Inc., 1954.

12. Sandborn, Virgil A., and Laurence, James C.: Heat Loss from Yawed Hot Wires at Subsonic Mach Numbers. NACA TN 3563, 1955.

13. Scadron, Marvin D., and Warshawsky, Isidore: Experimental Determination of Time Constants and Nusselt Numbers for Bare-Wire Thermocouples in High-Velocity Air Streams and Analytic Approximation of Conduction and Radiation Errors. NACA TN 2599, 1952.

14. Spangenberg, W. G.: Heat-Loss Characteristics of Hot-Wire Anemometers at Various Densities in Transonic and Supersonic Flow. NACA TN 3381, 1955.

15. Stalder, Jackson R., Goodwin, Glen, and Creager, Marcus O.: Heat Transfer to Bodies in a High-Speed Rarefied-Gas Stream. NACA Rep. 1093, 1952. (Supersedes NACA TN 2438.)

16. Winovich, Warren, and Stine, Howard A.: Measurements of the Nonlinear Variation with Temperature of Heat-Transfer Rate from Hot Wires in Transonic and Supersonic Flow. NACA TN 3965, 1957.

17. Mickelsen, William R., and Baldwin, Lionel V.: Aerodynamic Mixing Downstream from Line-Source of Heat in High-Intensity Sound Field. NACA TN 3760, 1956.

18. Hilsenrath, Joseph, et al.: Tables of Thermal Properties of Gases. Cir. 564, NBS, Nov. 1, 1955.

19. Van Der Hegge Zijnen, B. G.: Heat Transfer from Horizontal Cylinders to a Turbulent Air Flow. Appl. Sci. Res., sec. A, vol. 7, nos. 2-3, 1958, pp. 205-223.

20. Collis, D. C., and Williams, M. J.: Two-Dimensional Forced Convection from Cylinders at Low Reynolds Numbers. Rep. A. 105, Res. & Dev. Branch, Aero. Res. Labs. (Australia), Nov. 1957.

21. Kennard, Earle H.: Kinetic Theory of Gases. McGraw-Hill Book Co., Inc., 1938, pp. 312-315.

22. Morkovin, M. V.: Fluctuations and Hot-Wire Anemometry in Compressible Flows. AGARDograph 24, North Atlantic Treaty Organization, AGARD, Nov. 1956.

23. Sauer, F. M., and Drake, R. M., Jr.: Forced Convection Heat Transfer from Horizontal Cylinders in a Rarefied Gas. Jour. Aero. Sci., vol. 20, no. 3, Mar. 1953, pp. 175-180.

24. Stalder, Jackson R., Goodwin, Glen, and Creager, Marcus O.: A Comparison of Theory and Experiment for High-Speed Free-Molecule Flow. NACA Rep. 1032, 1951. (Supersedes NACA TN 2244.)

25. Kovásznay, L. S. G.: Turbulence Measurements. Vol. IX of Physical Measurements in Gas Dynamics and Combustion, sec. F, pt. 1, R. Ladenburg, ed., Princeton Univ. Press, 1954, pp. 213-285.

TABLE I. - RESULTS OF STUDY OF HEAT TRANSFER FROM CYLINDERS IN SUBSONIC SLIP FLOW

M	Kn	Re_t	T_t	T_w	Nu_t''	Nu_t	Run[a]
0.0488	0.0753	0.9763	12.9	33.6	1.054	0.7396	342
		.9814	11.5	86.6	.9479	.6534	343
		.9874	9.9	183.6	.9212	.6402	344
0.0490	0.0143	4.677	272.9	333.2	1.361	1.089	319
		4.679	272.7	383.9	1.402	1.133	320
		4.685	272.1	483.4	1.429	1.170	321
		4.689	271.8	583.8	1.450	1.199	322
		4.693	271.4	620.0	1.456	1.208	323
	0.0748	0.9973	8.5	33.6	1.058	0.7428	420
		.9952	9.0	86.6	.9783	.6803	421
		.9930	9.6	183.6	.9360	.6538	422
		.9909	10.2	383.9	.9031	.6301	423
		.9888	10.7	483.4	.8897	.5961	424
		.9866	11.3	583.8	.8802	.5915	425
0.0492	0.0142	5.239	8.4	33.6	2.002	1.596	348
		5.222	9.3	86.6	1.797	1.424	349
		5.206	10.1	183.6	1.715	1.370	350
		5.190	10.9	383.9	1.698	1.384	351
		5.174	11.7	483.4	1.698	1.394	352
		5.158	12.5	583.4	1.700	1.407	353
	0.0551	1.308	71.5	133.2	1.021	0.7364	85
				183.6	1.003	.7278	86
				283.2	.9908	.7280	87
				383.9	.9819	.7281	88
				483.4	.9619	.7147	89
				583.8	.9504	.7061	90
0.0495	0.0744	0.9724	72.5	132.0	0.9212	0.6468	1
				183.0	.9094	.6426	2
				234.5	.9082	.6471	3
				285.1	.9008	.6450	4
				332.6	.8960	.6441	5
				386.5	.8871	.6390	6
				437.3	.8815	.6359	7
				488.0	.8712	.6273	8
				538.5	.8638	.6201	9
				590.2	.8572	.6120	10
				640.4	.8439	.5926	11
0.0496	0.0570	1.331	3.5	33.6	1.101	0.7804	396
		1.329	3.9	86.6	1.069	.7614	397
		1.324	4.8	183.6	1.028	.7374	398
		1.321	5.4	383.9	1.010	.7344	399
		1.318	6.1	483.4	1.002	.7258	400
		1.255	18.9	583.8	.9929	.7182	401
0.0498	0.0259	2.603	283.8	333.2	1.090	0.8420	309
		2.611	282.5	383.9	1.114	.8697	310
		2.618	281.3	483.4	1.141	.9045	311
		2.626	280.0	583.8	1.151	.9224	312
		2.634	278.7	620.0	1.149	.9233	313
0.0500	0.0143	5.067	88.5	133.2	1.607	1.270	145
				183.6	1.459	1.145	146
				283.2	1.599	1.289	147
				383.9	1.590	1.295	148
				483.4	1.594	1.310	149
				583.8	1.595	1.321	150
0.0501	0.0259	2.951	5.6	33.6	1.517	1.155	360
		2.941	6.5	86.6	1.418	1.078	361
		2.929	7.6	183.6	1.374	1.056	362
		2.918	8.5	383.9	1.361	1.069	363
		2.907	9.5	483.4	1.362	1.078	364
		2.897	10.5	583.8	1.357	1.079	365
	0.0406	1.706	184.9	233.1	1.065	0.8019	217
		1.708	184.5	283.2	1.053	.7974	218
		1.710	184.0	383.9	1.037	.7938	219
		1.712	183.6	483.4	1.031	.7970	220
		1.716	182.9	583.8	1.031	.8042	221
		1.717	182.7	620.1	1.032	.8070	222
0.0502	0.00922	7.896	89.0	133.2	1.903	1.541	151
				183.6	1.898	1.548	152
				283.2	1.875	1.545	153
				383.9	1.885	1.570	154
				483.4	1.886	1.584	155
				583.8	1.891	1.599	156
	0.0412	1.864	8.5	33.6	1.201	0.8709	378
		1.856	9.6	86.6	1.185	.8668	379
		1.848	10.7	183.6	1.165	.8644	380
		1.840	11.8	383.9	1.145	.8661	381
		1.832	13.0	483.4	1.135	.8622	382
		1.824	14.1	583.8	1.130	.8597	383
0.0503	0.0255	2.867	87.5	133.2	1.303	0.9931	133
				183.6	1.325	1.022	134
				283.2	1.299	1.013	135
				383.9	1.291	1.018	136
				483.4	1.287	1.023	137
				583.8	1.281	1.025	138
0.0506	0.0442	1.662	85.0	133.2	1.081	0.7928	109
				183.6	1.086	.8050	110
				283.2	1.066	.7994	111
				383.9	1.051	.7947	112
				483.4	1.037	.7891	113
				583.8	1.031	.7883	114
0.0507	0.0253	2.762	196.6	233.1	1.281	0.9981	223
		2.770	195.5	283.2	1.244	.9717	224
		2.779	194.4	383.9	1.236	.9768	225
		2.787	193.2	483.4	1.235	.9858	226
		2.795	192.1	583.8	1.237	.9967	227
		2.804	191.0	620.1	1.235	.9974	228
0.0508	0.0403	1.711	265.5	333.2	0.9844	0.7457	288
		1.716	264.2	383.9	.9849	.7514	289
		1.721	262.9	483.4	.9922	.7671	290
		1.726	261.7	583.8	.9945	.7769	291
		1.732	260.4	620.0	.9988	.7830	292
0.0513	0.0575	1.202	274.3	333.2	0.8821	0.6358	283
		1.206	272.9	383.9	.8667	.6447	284
		1.209	271.8	483.4	.8680	.6540	285
		1.213	270.1	583.8	.8678	.6606	286
		1.216	269.2	620.0	.8656	.6606	287
	0.0782	0.8818	283.1	333.2	0.7475	0.5332	278
		.8855	281.3	383.9	.7538	.5431	279
		.8893	279.5	483.4	.7603	.5562	280
		.8931	277.6	583.8	.7589	.5608	281
		.8969	275.8	620.0	.7557	.5595	282
0.0516	0.0582	1.234	187.2	233.1	0.8849	0.6398	193
		1.233	187.6	283.2	.9112	.6692	194
		1.232	188.0	383.9	.9110	.6789	195
		1.231	188.3	483.4	.9036	.6799	196
		1.229	188.7	583.8	.8987	.6815	197
		1.228	189.0	620.1	.8965	.6814	198
0.0529	0.0142	5.159	182.7	233.1	1.596	1.286	235
		5.168	182.1	283.2	1.581	1.280	236
		5.176	181.5	383.9	1.567	1.281	237
		5.185	180.8	483.4	1.565	1.291	238
		5.193	180.2	583.8	1.569	1.305	239
		5.202	179.6	620.1	1.576	1.315	240
0.0531	0.0792	0.9231	189.1	233.1	0.8635	0.6211	169
		.9249	188.0	283.2	.8398	.6051	170
		.9268	187.1	383.9	.8097	.5867	171
		.9287	186.2	483.4	.8003	.5846	172
		.9305	185.3	583.8	.7923	.5820	173
		.9324	184.4	620.1	.7882	.5793	174
0.0637	0.0261	3.665	13.3	33.6	1.804	1.417	354
		3.660	13.7	86.6	1.539	1.189	355
		3.654	14.1	183.6	1.466	1.141	356
		3.649	14.5	383.9	1.442	1.146	357
		3.643	14.9	483.4	1.431	1.144	358
		3.637	15.3	583.8	1.427	1.148	359
0.0870	0.0439	2.873	86.0	133.2	1.239	0.9354	127
				183.6	1.246	.9501	128
				283.2	1.221	.9415	129
				383.9	1.203	.9355	130
				483.4	1.184	.9272	131
				583.8	1.172	.9224	132
0.0969	0.0740	2.029	-0.3	33.6	1.171	0.8423	336
		2.006	2.5	86.6	1.157	.8404	337
		1.984	5.3	183.6	1.099	.8028	338
		1.963	8.2	383.9	1.050	.7746	339
		1.942	11.0	483.4	1.026	.7523	340
		1.921	13.8	583.8	1.032	.7566	341
0.0973	0.0394	3.676	10.6	33.6	1.882	1.488	372
				86.6	1.535	1.185	373
				183.6	1.429	1.106	374
				383.9	1.373	1.080	375
				483.4	1.356	1.073	376
				583.8	1.339	1.062	377
0.0979	0.0736	2.026	3.7	33.6	1.231	0.8964	414
		2.021	4.4	86.6	1.149	.8334	415
		2.016	5.0	183.6	1.096	.8004	416
		2.010	5.7	383.9	1.050	.7736	417
		2.006	6.3	483.4	1.034	.7592	418
		2.001	7.0	583.8	1.018	.7321	419

[a]Run numbers were assigned in advance planning of the experiment to correspond to particular conditions. Therefore, data are missing in cases where experimental problems made it impossible to follow this plan.

5111

CS-6

TABLE I. - Continued. RESULTS OF STUDY OF HEAT TRANSFER FROM CYLINDERS IN SUBSONIC SLIP FLOW

M	Kn	Re_t	T_t	T_w	Nu_t''	Nu_t	Run
0.0990	0.0259	5.199	277.5	333.2	1.279	1.014	314
		5.208	276.7	383.9	1.351	1.086	315
		5.217	276.0	483.4	1.391	1.135	316
		5.226	275.3	583.8	1.406	1.158	317
		5.235	274.5	620.0	1.407	1.162	318
	0.0549	2.628	72.5	133.2	1.207	0.9042	91
				183.6	1.180	.8881	92
				283.2	1.152	.8764	93
				383.9	1.131	.8669	94
				483.4	1.113	.8579	95
				583.8	1.098	.8486	96
0.0993	0.0256	5.804	13.8	33.6	2.068	1.658	366
		5.802	13.9	86.6	1.780	1.409	367
		5.800	14.0	183.6	1.684	1.342	368
		5.798	14.1	383.9	1.645	1.336	369
		5.797	14.2	483.4	1.634	1.336	370
		5.795	14.2	583.8	1.621	1.332	371
0.0997	0.0407	3.397	188.5	233.1	1.222	0.9438	211
		3.406	187.5	283.2	1.242	.9696	212
		3.415	186.5	383.9	1.234	.9744	213
		3.424	185.6	483.4	1.227	.9784	214
		3.433	184.6	583.8	1.221	.9811	215
		3.442	183.6	620.1	1.216	.9787	216
0.1000	0.0569	2.707	-4.0	33.6	1.232	0.8958	390
		2.692	-2.5	86.6	1.273	.9442	391
		2.676	-1.0	183.6	1.224	.9159	392
		2.661	.4	383.9	1.193	.9081	393
		2.646	1.9	483.4	1.174	.8953	394
		2.631	3.3	583.8	1.156	.8793	395
0.1008	0.0255	5.704	89.5	133.2	1.553	1.220	522
				183.6	1.548	1.226	523
				283.2	1.559	1.253	524
				383.9	1.556	1.264	525
				483.4	1.550	1.269	526
				583.8	1.549	1.278	527
	0.0564	2.440	259.8	333.2	0.9797	0.7410	273
		2.443	259.5	383.9	1.016	.7797	274
		2.445	259.1	483.4	1.022	.7942	275
		2.447	258.7	583.8	1.021	.8015	276
		2.449	258.3	620.0	1.020	.8024	277
0.1009	0.0250	5.586	188.1	233.1	1.534	1.229	229
		5.602	187.1	283.2	1.529	1.232	230
		5.618	186.0	383.9	1.523	1.241	231
		5.634	185.0	483.4	1.513	1.243	232
		5.650	183.9	583.8	1.511	1.251	233
		5.666	182.8	620.1	1.507	1.250	234
0.1010	0.00917	15.92	90.0	133.2	1.996	1.826	1065
				183.6	2.194	1.821	1066
				283.2	2.278	1.920	1067
				383.9	2.310	1.968	1068
				483.4	2.329	2.000	1069
				583.8	2.337	2.020	1070
	0.0749	1.960	79.5	132.0	1.127	0.8328	13
				183.0	1.064	.7836	14
				234.5	1.050	.7776	15
				285.1	1.023	.7585	16
				332.6	1.016	.7565	17
				386.5	.9997	.7457	18
				437.3	.9886	.7388	19
				488.0	.9792	.7328	20
				538.5	.9671	.7234	21
				590.2	.9585	.7165	22
				640.4	.9523	.7110	23
0.1012	0.0411	3.368	269.4	333.2	1.076	0.8283	299
		3.367	269.5	383.9	1.133	.8864	300
		3.365	269.8	483.4	1.161	.9218	301
		3.364	270.0	583.8	1.169	.9386	302
		3.363	270.1	620.0	1.172	.9441	303
0.1019	0.0255	5.780	87.0	133.2	1.592	1.256	139
				183.6	1.623	1.295	140
				283.2	1.590	1.281	141
				383.9	1.566	1.273	142
				483.4	1.556	1.274	143
				583.8	1.543	1.272	144
	0.0766	1.928	85.0	133.2	1.112	0.8202	37
				183.6	1.057	.7782	38
				233.1	1.038	.7673	39
				283.2	1.023	.7598	40
				333.2	1.010	.7528	41
				383.9	.9956	.7433	42
				433.0	.9823	.7343	43
				483.4	.9722	.7276	44
				533.0	.9625	.7206	45
				583.8	.9480	.7081	46
0.1020	0.00916	16.91	2.0	33.6	2.653	2.194	984
		16.90	2.1	86.6	2.555	2.121	985
			2.2	183.6	2.505	2.101	986
		16.89	·2.3	383.9	2.507	2.143	987
	0.00917	16.89	2.4	483.4	2.509	2.160	988
		16.88	2.5	583.8	2.509	2.172	989
0.1024	0.0445	3.336	85.0	133.2	1.342	1.028	115
				183.6	1.294	.9931	116
				283.2	1.274	.9896	117
				383.9	1.251	.9798	118
				483.4	1.229	.9682	119
				583.8	1.214	.9612	120
	0.0757	1.866	185.5	233.1	1.006	0.7488	163
		1.873	185.3	283.2	.9663	.7188	164
		1.879	185.1	383.9	.9621	.7252	165
		1.886	184.9	483.4	.9455	.7178	166
		1.893	184.7	583.8	.9320	.7116	167
		1.900	184.5	620.1	.9244	.7062	168
0.1029	0.0415	3.360	280.4	333.2	1.119	0.8688	293
		3.371	278.9	383.9	1.144	.8972	294
		3.383	277.5	483.4	1.160	.9216	295
		3.394	276.0	583.8	1.164	.9340	296
		3.406	274.5	620.0	1.166	.9383	297
0.1032	0.0776	1.776	281.9	333.2	0.9775	0.7403	247
		1.788	278.9	383.9	.9868	.7539	248
		1.801	276.0	483.4	.9093	.6919	249
		1.816	272.3	583.8	.9002	.6904	250
		1.829	269.4	620.0	.8909	.6838	251
0.1039	0.0143	10.48	90.5	133.2	1.661	1.319	1035
				183.6	1.827	1.482	1036
				283.2	1.913	1.581	1037
				383.9	1.936	1.617	1038
				483.4	1.941	1.635	1039
				583.8	1.952	1.657	1040
	0.0580	2.495	184.4	233.1	1.068	0.8042	181
		2.498	183.9	283.2	1.083	.8243	182
		2.501	183.5	383.9	1.072	.8259	183
		2.504	183.0	483.4	1.061	.8248	184
		2.507	182.6	583.8	1.052	.8230	185
		2.510	182.1	620.1	1.047	.8214	186
0.1069	0.0141	11.54	-2.0	33.6	2.202	1.778	935
				86.6	2.180	1.774	936
				183.6	2.128	1.750	937
				383.9	2.117	1.776	938
				483.4	2.110	1.782	939
				583.8	2.103	1.786	940
0.1614	0.0613	3.948	6.0	33.6	1.543	1.179	324
		3.934	6.9	86.6	1.437	1.095	325
		3.919	7.9	183.6	1.355	1.038	326
		3.904	8.9	383.9	1.283	.9957	327
		3.890	9.9	483.4	1.258	.9789	328
		3.875	10.9	583.8	1.235	.9809	329
0.1956	0.0139	21.29	-2.0	33.6	2.919	2.441	923
				86.6	2.790	2.339	924
				183.6	2.680	2.264	925
				383.9	2.611	2.241	926
				483.4	2.603	2.248	927
				583.8	2.576	2.235	928
	0.0251	11.75	-2.0	33.6	2.153	1.733	917
		11.76	-2.2	86.6	2.172	1.767	918
			-2.4	183.6	2.076	1.702	919
		11.77	-2.6	383.9	2.029	1.692	920
		11.78	-2.8	483.4	2.001	1.679	921
			-5.0	583.8	1.983	1.672	922
0.1957	0.0746	3.909	11.4	33.6	1.574	1.207	330
		3.894	12.4	86.6	1.375	1.039	331
		3.880	13.4	183.6	1.290	.9792	332
		3.866	14.3	383.9	1.213	.9514	333
		3.852	15.3	483.4	1.186	.9121	334
		3.838	16.3	583.8	1.164	.8938	335
0.1972	0.0735	3.619	259.0	333.2	1.087	0.8386	252
		3.622	258.6	383.9	1.091	.8479	253
		3.625	258.3	483.4	1.079	.8465	254
		3.628	257.9	583.8	1.070	.8457	255
		3.632	257.5	620.0	1.066	.8444	256
0.1986	0.00908	33.03	-3.5	33.6	3.458	2.942	947
	0.00909	33.00	-3.2	86.6	3.334	2.846	948
		32.97	-2.9	183.6	3.209	2.760	949
	0.00910	32.94	-2.6	383.9	3.181	2.779	950
	0.00911	32.91	-2.3	483.4	3.163	2.779	951
		32.88	-2.0	583.8	3.163	2.794	952

TABLE I. - Continued. RESULTS OF STUDY OF HEAT TRANSFER FROM CYLINDERS IN SUBSONIC SLIP FLOW

M	Kn	Re_t	T_t	T_w	Nu''_t	Nu_t	Run
0.1987	0.0400	6.708	267.9	333.2	1.358	1.086	304
		6.720	287.1	383.9	1.409	1.139	305
		6.732	266.4	483.4	1.425	1.185	306
		6.743	265.6	583.8	1.417	1.168	307
		6.755	264.9	620.0	1.419	1.173	308
0.1989	0.00916	31.09	90.0	133.2	2.496	2.088	1053
				183.6	2.798	2.383	1054
				283.2	2.904	2.506	1055
				383.9	2.933	2.554	1056
				483.4	2.942	2.580	1057
				583.8	2.951	2.602	1058
0.1996	0.0559	5.147	79.0	133.2	1.464	1.138	97
				183.6	1.359	1.052	98
				283.2	1.374	1.081	99
				383.9	1.335	1.057	100
				483.4	1.302	1.036	101
				583.8	1.277	1.020	102
0.1997	0.0745	3.840	90.0	133.2	1.412	1.093	49
				183.6	1.250	.9540	50
				233.1	1.221	.9351	51
				283.2	1.201	.9231	52
				333.2	1.185	.9145	53
				383.9	1.162	.8979	54
				433.0	1.140	.8826	55
				483.4	1.123	.8700	56
				533.0	1.112	.8634	57
				583.8	1.110	.8639	58
				620.1	1.090	.8467	59
0.1998	0.0254	10.79	192.0	620.1	1.792	1.518	748
	0.0255	10.74	194.4	383.9	1.835	1.530	745
		10.76	193.6	483.4	1.817	1.527	746
		10.77	192.8	583.8	1.798	1.520	747
	0.0256	10.71	196.0	233.1	1.556	1.249	743
0.1999	0.0402	7.503	-2.0	33.6	1.776	1.388	857
		7.499	-1.8	86.6	1.742	1.371	858
		7.494	-1.6	183.6	1.675	1.331	859
		7.490	-1.4	383.9	1.628	1.316	860
	0.0403	7.486	-1.2	483.4	1.605	1.305	861
		7.482	-1.0	583.8	1.585	1.294	862
0.2004	0.0143	20.08	90.5	133.2	2.120	1.740	1029
				183.6	2.334	1.951	1030
				283.2	2.412	2.045	1031
				383.9	2.431	2.082	1032
				483.4	2.433	2.098	1033
				583.8	2.436	2.114	1034
0.2008	0.0251	10.64	287.0	483.4	1.744	1.463	724
		10.65	286.5	583.8	1.753	1.482	725
		10.65	286.0	620.0	1.757	1.489	726
	0.0252	10.62	288.0	333.2	1.484	1.202	722
		10.63	287.5	383.9	1.679	1.390	723
0.2019	0.0257	11.24	90.0	133.2	1.908	1.546	528
				183.6	1.940	1.587	529
				283.2	1.931	1.597	530
				383.9	1.918	1.601	531
				483.4	1.892	1.589	532
				583.8	1.891	1.599	533
0.2025	0.0411	6.713	194.1	233.1	1.547	1.240	205
		6.727	193.3	283.2	1.545	1.247	206
		6.740	192.5	383.9	1.512	1.230	207
		6.754	191.8	483.4	1.488	1.220	208
		6.768	191.0	583.8	1.465	1.209	209
		6.781	190.3	620.1	1.454	1.202	210
0.2032	0.0567	4.803	271.6	333.2	1.217	0.9572	268
		4.819	270.1	383.9	1.224	.9701	269
		4.836	268.6	483.4	1.213	.9701	270
		4.853	267.2	583.8	1.205	.9710	271
		4.870	265.7	620.0	1.206	.9746	272
0.2034	0.0582	5.237	7.8	33.6	1.665	1.290	384
		5.222	8.6	86.6	1.540	1.189	385
		5.209	9.2	183.6	1.454	1.129	386
		5.193	10.0	383.9	1.384	1.091	387
		5.179	10.7	483.4	1.350	1.067	388
		5.175	10.8	583.8	1.326	1.049	389
0.2048	0.0761	4.052	-0.7	33.6	1.458	1.100	408
		4.037	.3	86.6	1.366	1.030	409
		4.021	1.3	183.6	1.287	.9749	410
		4.006	2.3	383.9	1.218	.9320	411
		3.991	3.2	483.4	1.192	.9127	412
		3.976	4.2	583.8	1.161	.8847	413
0.2050	0.0407	7.196	91.8	133.2	1.702	1.357	262
		7.185	92.3	183.6	1.652	1.322	263
		7.174	92.7	283.2	1.616	1.306	264
		7.164	93.2	383.9	1.587	1.293	265
		7.153	93.7	483.4	1.562	1.281	266
		7.142	94.1	583.8	1.541	1.271	267
0.2068	0.0769	3.856	88.0	132.0	1.465	1.140	25
				183.0	1.321	1.018	26
				234.5	1.262	.9719	27
				285.1	1.229	.9485	28
				332.6	1.197	.9248	29
				386.5	1.168	.9036	30
				437.3	1.147	.8879	31
				488.0	1.130	.8761	32
				538.5	1.124	.8735	33
				590.2	1.119	.8724	34
				640.4	1.103	.8592	35
0.2072	0.0570	4.949	183.5	233.1	1.382	1.089	187
		4.960	182.7	283.2	1.273	.9971	188
		4.970	182.0	383.9	1.313	1.047	189
		4.980	181.2	483.4	1.283	1.029	190
		4.990	180.5	583.8	1.263	1.020	191
		5.000	179.7	620.1	1.251	1.011	192
0.2081	0.0754	3.793	179.0	233.1	1.128	0.8584	157
		3.801	178.7	283.2	1.162	.8961	158
		3.809	178.4	383.9	1.133	.8808	159
		3.817	178.1	483.4	1.113	.8715	160
		3.825	177.8	583.8	1.091	.8591	161
		3.833	177.5	620.1	1.079	.8499	162
0.2357	0.0435	7.739	85.8	133.2	1.710	1.363	121
				183.6	1.657	1.326	122
				283.2	1.610	1.299	123
				383.9	1.568	1.275	124
				483.4	1.537	1.256	125
				583.8	1.510	1.240	126
0.2921	0.0252	15.22	284.0	333.2	1.675	1.378	727
		15.22	284.2	383.9	1.818	1.518	728
		15.21	284.5	483.4	1.907	1.615	729
	0.0253	15.20	284.8	583.8	1.946	1.663	730
			285.0	620.0	1.962	1.682	731
	0.0716	5.474	20.4	33.6	4.287	3.725	402
		5.557	16.4	86.6	1.916	1.534	403
		5.643	12.4	183.6	1.528	1.198	404
		5.731	8.3	383.9	1.364	1.071	405
		5.821	4.3	483.4	1.314	1.030	406
		5.914	.2	583.8	1.282	1.003	407
0.2926	0.0391	10.11	194.5	233.1	1.533	1.228	611
			194.6	283.2	1.649	1.343	612
			194.7	383.9	1.633	1.344	613
	0.0392	10.11	194.8	483.4	1.613	1.337	614
		10.10	194.9	583.8	1.599	1.334	615
			195.0	620.1	1.586	1.325	616
0.2959	0.00911	48.30	-2.0	583.8	3.584	3.196	983
		48.26	-1.7	483.4	3.585	3.181	982
	0.00912	48.22	-1.4	383.9	3.598	3.175	981
	0.00913	48.18	-1.1	183.6	3.675	3.199	980
		48.14	-.8	86.6	3.788	3.273	979
	0.00914	48.10	-0.5	33.6	3.880	3.336	978
0.2964	0.0402	10.96	-3.0	33.6	1.982	1.577	839
			-2.9	86.6	1.913	1.529	840
		10.95	-2.8	183.6	1.882	1.523	841
	0.0403	10.95	-2.7	383.9	1.816	1.493	842
			-2.6	483.4	1.771	1.462	843
		10.94	-2.5	583.8	1.746	1.447	844
0.2972	0.00901	49.08	-4.0	33.6	4.035	3.481	953
		49.05	-3.8	86.6	3.807	3.290	954
	0.00902	49.02	-3.6	183.6	3.703	3.225	955
		48.99	-3.4	383.9	3.631	3.206	956
	0.00903	48.97	-3.2	483.4	3.605	3.200	957
		48.94	-3.0	583.8	3.611	3.221	958

5111

TABLE I. - Continued. RESULTS OF STUDY OF HEAT TRANSFER FROM CYLINDERS IN SUBSONIC SLIP FLOW

M	Kn	Re_t	T_t	T_w	Nu_t''	Nu_t	Run
0.2975	0.0752	5.172	282.7	333.2	1.234	0.9730	257
				383.9	1.214	.9614	258
				483.4	1.178	.9387	259
				583.8	1.159	.9299	260
				620.0	1.153	.9271	261
0.2979	0.0550	7.674	82.3	133.2	1.617	1.278	103
				183.6	1.581	1.256	104
				283.2	1.526	1.222	105
				383.9	1.479	1.191	106
				483.4	1.437	1.163	107
				583.8	1.405	1.141	108
0.2980	0.0142	29.57	89.0	133.2	2.434	2.031	1023
				183.6	2.674	2.268	1024
				283.2	2.715	2.329	1025
				383.9	2.762	2.393	1026
				483.4	2.758	2.405	1027
				583.8	2.758	2.419	1028
0.2983	0.0142	31.23	-3.0	33.6	3.172	2.675	929
		31.25	-3.2	86.6	3.151	2.676	930
		31.27	-3.4	183.6	3.044	2.605	931
		31.29	-3.6	383.9	2.990	2.598	932
		31.30	-3.8	483.4	2.962	2.589	933
		31.32	-4.0	583.8	2.941	2.582	934
	0.0253	15.91	194.4	583.8	2.059	1.766	741
		15.92	194.0	620.1	2.039	1.751	742
	0.0254	15.86	196.0	233.1	1.776	1.452	737
		15.89	195.2	383.9	2.062	1.742	739
		15.90	194.8	483.4	2.067	1.761	740
0.2987	0.00922	45.74	89.0	133.2	2.911	2.475	1059
				183.6	3.236	2.794	1060
				283.2	3.314	2.893	1061
				383.9	3.339	2.938	1062
				483.4	3.339	2.956	1063
				583.8	3.356	2.988	1064
0.2990	0.0739	5.714	80.4	133.2	1.437	1.115	61
				183.6	1.361	1.055	62
				233.1	1.330	1.035	63
				283.2	1.311	1.025	64
				333.2	1.298	1.019	65
				383.9	1.268	.9970	66
				433.0	1.245	.9796	67
				483.4	1.226	.9662	68
				533.0	1.210	.9553	69
				583.8	1.194	.9438	70
				620.1	1.180	.9328	71
0.2994	0.0399	9.843	284.0	483.4	1.557	1.288	699
		9.851	283.5	583.8	1.565	1.307	700
		9.859	283.0	620.0	1.558	1.304	701
	0.0400	9.827	285.0	333.2	1.442	1.163	697
		9.835	284.5	383.9	1.513	1.236	698
0.3005	0.0254	16.67	89.5	133.2	2.184	1.800	534
				183.6	2.190	1.818	535
				283.2	2.183	1.832	536
				383.9	2.159	1.827	537
				483.4	2.142	1.824	538
				583.8	2.132	1.827	539
0.3012	0.0253	17.63	0.4	383.9	2.247	1.898	890
		17.64	.2	483.4	2.223	1.890	891
		17.65	0	583.8	2.205	1.884	892
	0.0254	17.60	1.0	33.6	2.428	1.986	887
		17.61	.8	86.6	2.352	1.934	888
		17.62	.6	183.6	2.287	1.899	889
0.3019	0.0591	7.574	0	33.6	1.739	1.356	815
		7.570	.2	86.6	1.640	1.279	816
	0.0592	7.565	0.4	183.6	1.567	1.232	817
		7.561	.6	383.9	1.487	1.185	818
		7.557	.8	483.4	1.451	1.161	819
		7.552	1.0	583.8	1.421	1.138	820
0.3021	0.0564	7.037	282.0	333.2	1.141	0.8888	671
	.0565	7.019	283.5	383.9	1.271	1.013	672
	.0566	7.002	285.0	483.4	1.305	1.056	673
	0.0567	6.997	285.5	583.8	1.306	1.066	674
		6.991	286.0	620.0	1.312	1.074	675
0.3040	0.0565	7.232	186.0	233.1	1.479	1.178	199
		7.236	185.9	283.2	1.472	1.179	200
		7.241	185.6	383.9	1.439	1.164	201
		7.245	185.4	483.4	1.396	1.135	202
		7.250	185.2	583.8	1.372	1.122	203
		7.254	184.9	620.1	1.365	1.118	204

M	Kn	Re_t	T_t	T_w	Nu_t''	Nu_t	Run
0.3088	0.0750	5.536	181.0	233.1	1.295	1.010	175
		5.542	180.8	283.2	1.270	.9949	176
		5.548	180.6	383.9	1.250	.9888	177
		5.554	180.4	483.4	1.218	.9698	178
		5.559	180.2	583.8	1.188	.9501	179
		5.565	180.0	620.1	1.178	.9430	180
0.3183	0.0444	10.09	88.5	133.2	1.763	1.413	486
				183.6	1.790	1.448	487
				283.2	1.753	1.432	488
				383.9	1.730	1.426	489
				483.4	1.704	1.414	490
0.3948	0.00919	59.46	88.0	133.2	3.334	2.871	1071
				183.6	3.549	3.089	1072
				283.2	3.644	3.206	1073
				383.9	3.672	3.254	1074
				483.4	3.683	3.284	1075
				583.8	3.659	3.278	1076
0.3961	0.0242	23.94	-8.0	33.6	2.699	2.237	881
		23.95	-8.1	86.6	2.684	2.240	882
		23.96	-8.2	183.6	2.586	2.177	883
			-8.3	383.9	2.488	2.124	884
		23.97	-8.4	483.4	2.523	2.172	885
		23.98	-8.5	583.8	2.406	2.073	886
0.3977	0.0410	14.15	-6.0	33.6	2.174	1.753	833
		14.14	-5.9	86.6	2.097	1.698	834
			-5.8	183.6	2.005	1.636	835
		14.13	-5.7	383.9	1.926	1.596	836
	0.0411	14.13	-5.6	483.4	1.881	1.565	837
			-5.5	583.8	1.842	1.538	838
0.3982	0.0776	7.082	91.0	133.2	1.498	1.172	426
				183.6	1.369	1.063	427
				283.2	1.376	1.085	428
				383.9	1.332	1.057	429
				483.4	1.295	1.032	430
				583.8	1.260	1.007	431
0.3986	0.00911	63.76	-4.0	483.4	3.919	3.500	994
	.00912	63.67	-3.5	383.9	3.915	3.477	993
	.00913	63.58	-3.0	183.6	4.017	3.523	992
	.00914	63.49	-2.5	86.6	4.166	3.628	991
	.00915	63.40	-2.0	33.6	4.459	3.881	990
0.3987	0.0766	7.556	0.5	33.6	1.713	1.332	767
	0.0767	7.554	0.6	86.6	1.593	1.237	768
		7.552	.7	183.6	1.491	1.163	769
		7.550	.8	383.9	1.389	1.094	770
		7.547	.9	483.4	1.351	1.066	771
		7.545	1.0	583.8	1.320	1.041	772
0.3991	0.0141	41.31	-6.0	33.6	3.559	3.037	941
				86.6	3.421	2.929	942
				183.6	3.273	2.821	943
				383.9	3.226	2.822	944
				483.4	3.196	2.811	945
				583.8	3.172	2.803	946
	0.0254	20.81	190.0	620.1	2.189	1.892	754
	0.0255	20.71	192.4	483.4	2.209	1.895	752
		20.76	191.2	583.8	2.194	1.893	753
	0.0256	20.67	173.6	383.9	2.209	1.880	751
	0.0257	20.57	196.0	233.1	1.869	1.538	749
0.4000	0.0407	13.60	87.8	133.2	1.898	1.537	492
				183.6	1.914	1.563	493
				283.2	1.880	1.550	494
				383.9	1.851	1.538	495
				483.4	1.816	1.519	496
				583.8	1.794	1.509	497
0.4003	0.0143	38.71	88.0	133.2	2.689	2.268	1041
				183.6	2.925	2.503	1042
				283.2	2.993	2.591	1043
				383.9	2.999	2.617	1044
				483.4	2.994	2.629	1045
				583.8	2.984	2.634	1046
0.4004	0.0574	9.645	89.5	133.2	1.712	1.366	444
				183.6	1.646	1.316	445
				283.2	1.593	1.285	446
				383.9	1.561	1.269	447
				483.4	1.542	1.262	448
				583.8	1.492	1.225	449

TABLE I. - Continued. RESULTS OF STUDY OF HEAT TRANSFER FROM CYLINDERS IN SUBSONIC SLIP FLOW

M	Kn	Re_t	T_t	T_w	Nu''_t	Nu_t	Run
0.4007	0.0565	9.116	281.5	333.1	1.241	0.9801	666
				383.9	1.349	1.085	667
				483.4	1.399	1.143	668
				583.8	1.398	1.151	669
				620.0	1.386	1.144	670
0.4008	0.0408	12.99	192.2	583.8	1.720	1.447	621
			192.0	620.1	1.712	1.444	622
	0.0409	12.97	193.0	233.1	1.647	1.333	617
			192.8	283.2	1.705	1.395	618
		12.98	192.6	383.9	1.739	1.442	619
			192.4	483.4	1.732	1.448	620
0.4010	0.0256	21.64	89.0	133.2	2.355	1.959	540
				183.6	2.384	1.999	541
				283.2	2.359	1.996	542
				383.9	2.339	1.996	543
				483.4	2.309	1.982	544
				583.8	2.289	1.976	545
0.4013	0.0402	12.84	282.0	333.2	1.350	1.080	702
				383.9	1.568	1.287	703
				483.4	1.652	1.377	704
				583.8	1.678	1.412	705
				620.0	1.677	1.414	706
0.4024	0.0749	6.911	283.0	333.2	1.027	0.7852	646
		6.908	283.2	383.9	1.141	.8950	647
		6.905	283.5	483.4	1.185	.9451	648
		6.902	283.8	583.8	1.186	.9550	649
	0.0750	6.899	284.0	620.0	1.185	0.9571	650
0.4028	0.0742	7.503	91.3	133.2	1.494	1.167	73
				183.6	1.458	1.144	74
				233.1	1.437	1.134	75
				283.2	1.405	1.111	76
				333.2	1.377	1.092	77
				383.9	1.258	.9878	78
				433.0	1.316	1.047	79
				483.4	1.288	1.025	80
				533.0	1.269	1.011	81
				583.8	1.251	.9977	82
				620.1	1.240	.9893	83
0.4032	0.0250	20.74	282.0	333.2	1.958	1.641	732
		20.69	283.5	383.9	2.064	1.747	733
	0.0251	20.68	283.7	483.4	2.071	1.768	734
			283.8	583.8	2.113	1.820	735
		20.67	284.0	620.0	2.120	1.831	736
0.4056	0.0141	38.02	184.5	233.1	2.215	1.857	1113
	0.0142	37.99	184.9	283.2	2.583	2.211	1114
		37.96	185.3	383.9	2.848	2.480	1115
		37.93	185.7	483.4	2.862	2.510	1116
		37.90	186.1	583.8	2.855	2.518	1117
		37.87	186.5	620.1	2.860	2.527	1118
0.4072	0.0585	10.10	-2.0	33.6	1.843	1.451	809
	0.0586	10.10	-1.8	86.6	1.777	1.405	810
		10.09	-1.6	183.6	1.699	1.354	811
		10.08	-1.4	383.9	1.602	1.293	812
		10.07	-1.2	483.4	1.558	1.262	813
	0.0587	10.07	-1.0	583.8	1.519	1.232	814
0.4074	0.0577	9.334	192.0	233.1	1.346	1.058	599
				283.2	1.277	1.002	600
				383.9	1.454	1.178	601
				483.4	1.445	1.181	602
				583.8	1.430	1.177	603
				620.1	1.422	1.172	604
0.4415	0.0570	10.13	194.5	233.1	1.158	0.8870	552
		10.17	192.4	283.2	1.290	1.014	553
		10.21	190.3	383.9	1.301	1.037	554
		10.25	188.2	483.4	1.275	1.023	555
		10.30	186.1	583.8	1.260	1.018	556
		10.34	184.0	620.1	1.248	1.009	557
0.4717	0.0647	9.212	280.0	620.0	1.228	0.9970	645
	0.0648	9.200	280.8	583.8	1.241	1.006	644
		9.190	281.5	483.4	1.249	1.004	643
	0.0649	9.179	282.2	383.9	1.230	0.9761	642
	.0650	9.167	283.0	333.2	1.085	.8381	641
0.4793	0.00910	75.19	-5.0	33.6	4.549	3.966	995
		75.17	-5.0	86.6	4.390	3.840	997
				183.6	4.267	3.760	998
				383.9	4.161	3.712	999
				483.4	4.128	3.700	1000
0.4931	0.00910	77.03	-5.0	33.6	4.587	4.002	996
0.4951	0.0143	46.77	87.0	133.2	2.698	2.277	1047
				183.6	3.044	2.615	1048
				283.2	3.145	2.735	1049
				383.9	3.158	2.768	1050
				483.4	3.149	2.777	1051
				583.8	3.136	2.780	1052
0.4965	0.0143	49.35	-3.0	33.6	3.605	3.081	959
				86.6	3.520	3.023	960
				183.6	3.469	3.007	961
				383.9	3.384	2.973	962
				483.4	3.357	2.966	963
				583.8	3.315	2.940	964
0.4968	0.0249	28.31	-6.0	33.6	2.871	2.397	893
				86.6	2.788	2.339	894
				183.6	2.702	2.286	895
				383.9	2.578	2.211	896
				483.4	2.525	2.175	897
				583.8	2.484	2.148	898
0.4974	0.0398	17.80	-8.0	33.6	2.270	1.842	845
		17.79	-7.8	86.6	2.217	1.809	846
		17.78	-7.6	183.6	2.146	1.768	847
		17.77	-7.4	383.9	2.050	1.713	848
		17.76	-7.2	483.4	2.011	1.689	849
		17.75	-7.0	583.8	1.986	1.675	850
0.4981	0.0255	26.34	87.0	133.2	2.377	1.980	546
				183.6	2.467	2.077	547
				283.2	2.464	2.095	548
				383.9	2.445	2.096	549
				483.4	2.418	2.086	550
				583.8	2.387	2.068	551
0.4986	0.0403	16.70	84.0	133.2	1.936	1.572	498
				183.6	1.971	1.616	499
				283.2	1.967	1.632	500
				383.9	1.885	1.571	501
				483.4	1.907	1.604	502
				583.8	1.877	1.587	503
0.4992	0.0388	18.49	-24.0	33.6	2.295	1.863	869
	0.0389	18.46	-23.6	86.6	2.274	1.860	870
		18.44	-23.2	183.6	2.132	1.752	871
		18.42	-22.8	383.9	2.027	1.688	872
	0.0390	18.40	-22.4	483.4	1.978	1.654	873
		18.38	-22.0	583.8	1.935	1.623	874
0.4998	0.0573	11.26	190.0	233.1	1.283	1.001	581
				283.2	1.476	1.185	582
				383.9	1.499	1.220	583
				483.4	1.492	1.225	584
				583.8	1.480	1.223	585
				620.1	1.476	1.223	586
0.5005	0.0254	25.45	188.0	233.1	2.019	1.677	755
		25.41	188.8	283.2	2.150	1.808	756
	0.0255	25.37	189.6	383.9	2.226	1.896	757
		25.33	190.4	483.4	2.258	1.941	758
		25.29	191.2	583.8	2.271	1.966	759
		25.26	192.0	620.1	2.283	1.982	760
0.5006	0.0401	15.62	280.0	333.2	1.403	1.128	707
		15.63	280.0	383.9	1.711	1.419	708
	0.0402	15.60	281.0	483.4	1.728	1.448	709
		15.57	282.0	583.8	1.733	1.464	710
		15.55	283.0	620.0	1.740	1.474	711
0.5010	0.0565	11.11	282.0	333.2	1.327	1.059	676
				383.9	1.433	1.163	677
				483.4	1.456	1.196	678
				583.8	1.448	1.198	679
				620.0	1.441	1.195	680
0.5016	0.0761	9.316	0.5	33.6	1.828	1.439	773
				86.6	1.654	1.294	774
				183.6	1.544	1.213	775
				383.9	1.437	1.139	776
				483.4	1.397	1.110	777
				583.8	1.360	1.080	778
0.5048	0.0411	15.80	191.0	620.1	1.780	1.508	829
	0.0412	15.75	192.6	283.2	1.765	1.451	824
		15.76	192.2	383.9	1.836	1.533	825
		15.78	191.8	483.4	1.829	1.539	626
		15.79	191.4	583.8	1.788	1.512	628
	0.0413	15.74	193.0	233.1	1.653	1.340	623

5111

5111

TABLE I. - Continued. RESULTS OF STUDY OF HEAT TRANSFER FROM CYLINDERS IN SUBSONIC SLIP FLOW

M	Kn	Re_t	T_t	T_w	Nu_t^*	Nu_t	Run
0.5051	0.0578	11.73	89.5	133.2	1.767	1.418	450
				183.6	1.731	1.395	451
				283.2	1.660	1.347	452
				383.9	1.608	1.314	453
				483.4	1.566	1.286	454
				583.8	1.529	1.260	455
0.5056	0.0570	12.55	-4.0	33.6	2.068	1.657	803
				86.6	1.917	1.534	804
				183.6	1.764	1.414	805
				383.9	1.676	1.363	806
				483.4	1.622	1.322	807
				583.8	1.579	1.289	808
0.5061	0.0141	46.30	182.0	233.1	2.392	2.023	1119
		46.25	182.6	283.2	2.716	2.336	1120
		46.20	183.2	383.9	2.970	2.596	1121
	0.0142	46.14	183.8	483.4	3.012	2.653	1122
		46.09	184.4	583.8	3.024	2.679	1123
		46.04	185.0	620.1	3.013	2.673	1124
0.5087	0.0556	11.79	184.0	620.1	1.265	1.025	563
	.0557	11.77	185.2	583.8	1.273	1.031	562
	.0558	11.74	186.4	483.4	1.300	1.046	561
	.0559	11.71	187.6	383.9	1.330	1.064	560
	.0560	11.69	188.8	283.2	1.218	.9488	559
	.0561	11.66	190.0	233.1	1.237	.9583	558
0.5195	0.00924	75.32	86.0	133.2	3.480	3.009	1077
				183.6	3.692	3.225	1078
				283.2	3.892	3.442	1079
				383.9	3.914	3.486	1080
				483.4	3.919	3.510	1081
0.5214	0.0773	9.012	89.0	133.2	1.626	1.289	432
				183.6	1.510	1.192	433
				283.2	1.431	1.136	434
				383.9	1.398	1.118	435
				483.4	1.354	1.087	436
				583.8	1.307	1.051	437
0.5651	0.0563	13.96	-4.5	33.6	2.136	1.720	791
				86.6	1.993	1.604	792
				183.6	1.872	1.515	793
				383.9	1.755	1.437	794
				483.4	1.715	1.410	795
				583.8	1.667	1.373	796
0.5906	0.0398	18.09	276.0	333.2	1.555	1.269	712
	.0399	18.04	277.5	383.9	1.697	1.407	713
	0.0400	17.99	279.0	483.4	1.765	1.483	714
		17.95	280.5	583.8	1.768	1.498	715
	0.0401	17.91	282.0	620.0	1.775	1.509	716
0.5915	0.0250	29.73	180.0	233.1	1.935	1.599	1095
		29.71	180.4	283.2	2.139	1.798	1096
	0.0251	29.68	180.8	383.9	2.330	1.994	1097
		29.66	181.2	483.4	2.365	2.042	1098
		29.64	181.6	583.8	2.360	2.050	1099
		29.62	182.0	620.1	2.344	2.040	1100
0.5926	0.0247	33.07	-8.8	483.4	2.596	2.242	903
		33.09	-9.0	583.8	2.565	2.225	904
	0.0248	33.00	-8.0	33.6	2.930	2.453	899
		33.01	-8.2	86.6	2.875	2.421	900
		33.03	-8.4	183.6	2.751	2.333	901
		33.05	-8.6	383.9	2.646	2.275	902
0.5933	0.0253	30.76	82.0	133.2	2.223	1.837	1005
				183.6	2.422	2.035	1006
				283.2	1.249	.9677	1007
				383.9	2.481	2.130	1008
				483.4	2.458	2.123	1009
				583.8	2.431	2.111	1010
0.5943	0.0587	13.25	83.0	133.2	1.606	1.271	468
				183.6	1.679	1.348	469
				283.2	1.649	1.337	470
				383.9	1.611	1.316	471
				483.4	1.573	1.292	472
				583.8	1.538	1.268	473
0.5958	0.0571	13.07	188.8	233.1	1.460	1.163	587
				283.2	1.508	1.214	588
				383.9	1.528	1.248	589
				483.4	1.520	1.252	590
				583.8	1.498	1.241	591
				620.1	1.501	1.247	592

M	Kn	Re_t	T_t	T_w	Nu_t^*	Nu_t	Run
0.5977	0.0143	57.24	-3.8	86.6	3.677	3.171	966
		57.29	-4.1	183.6	3.605	3.136	967
		57.34	-4.4	383.9	3.518	3.102	969
		57.39	-4.7	483.4	3.475	3.078	970
		57.44	-5.0	583.8	3.429	3.051	971
	0.0144	57.19	-3.5	33.6	3.758	3.226	965
0.5983	0.0750	9.696	277.2	583.8	1.244	1.009	654
		9.699	277.0	620.0	1.233	1.002	655
	0.0751	9.683	278.0	333.2	1.108	0.8598	651
		9.686	277.8	383.9	1.210	.9584	652
		9.691	277.5	483.4	1.250	1.006	653
0.5996	0.0144	54.48	84.0	133.2	2.880	2.448	1083
				183.6	3.148	2.714	1084
				283.2	3.278	2.861	1085
				383.9	3.320	2.922	1086
				483.4	3.302	2.923	1087
				583.8	3.297	2.934	1088
0.6001	0.0569	14.51	-6.0	33.6	2.100	1.687	797
				86.6	1.981	1.593	798
				183.6	1.871	1.514	799
				383.9	1.754	1.437	800
				483.4	1.697	1.393	801
				583.8	1.657	1.363	802
0.6005	0.0775	10.10	89.5	133.2	1.611	1.275	438
				183.6	1.517	1.199	439
				283.2	1.441	1.146	440
				383.9	1.394	1.115	441
				483.4	1.345	1.079	442
				583.8	1.305	1.050	443
0.6011	0.0406	18.49	189.0	233.1	1.711	1.393	630
	0.0407	18.47	189.6	283.2	1.902	1.578	631
		18.45	190.2	383.9	1.880	1.574	632
		18.43	190.8	483.4	1.851	1.560	633
	0.0408	18.41	191.4	583.8	1.818	1.541	634A
		18.39	192.0	620.1	1.801	1.528	634B
0.6017	0.0742	11.13	-5.0	33.6	1.819	1.431	761
			-4.8	86.6	1.703	1.338	762
	0.0743	11.12	-4.6	183.6	1.612	1.275	763
		11.12	-4.4	383.9	1.489	1.188	764
		11.11	-4.2	483.4	1.444	1.154	765
	0.0744	11.10	-4.0	583.8	1.406	1.124	766
0.6030	0.0565	12.94	280.0	333.2	1.341	1.073	681
				383.9	1.450	1.179	682
				483.4	1.469	1.209	683
				583.8	1.465	1.215	684
				620.0	1.465	1.218	685
0.6049	0.0400	20.79	-10.0	383.9	2.095	1.756	854
				483.4	2.048	1.724	855
				583.8	2.006	1.694	856
	0.0401	20.73	-9.0	33.6	2.306	1.876	851
		20.75	-9.2	86.6	2.248	1.839	852
		20.77	-9.6	183.6	2.184	1.803	853
0.6050	0.0405	19.48	83.5	133.2	1.983	1.616	504
				183.6	2.013	1.656	505
				283.2	2.006	1.668	506
				383.9	1.969	1.650	507
				483.4	1.945	1.640	508
				583.8	1.898	1.607	509
0.6142	0.0237	35.49	-10.0	33.6	2.855	2.383	905
				86.6	2.941	2.482	906
				183.6	2.845	2.420	907
				383.9	2.717	2.342	908
				483.4	2.643	2.287	909
				583.8	2.572	2.232	910
0.6897	0.0250	34.93	81.0	133.2	2.291	1.902	1011
				183.6	2.475	2.085	1012
				283.2	2.541	2.169	1013
				383.9	2.547	2.193	1014
				483.4	2.522	2.184	1015
				583.8	2.484	2.162	1016
0.6920	0.0255	32.85	179.6	283.2	2.274	1.924	1102
		32.88	179.2	383.9	2.364	2.027	1103
		32.90	178.8	483.4	2.369	2.047	1104
		32.93	178.4	583.8	2.361	2.052	1105
		32.96	178.0	620.1	2.363	2.058	1106
	0.0256	32.83	180.0	233.1	2.024	1.682	1101

TABLE I. - Concluded. RESULTS OF STUDY OF HEAT TRANSFER FROM CYLINDERS IN SUBSONIC SLIP FLOW

M	Kn	Re_t	T_t	T_w	Nu''_t	Nu_t	Run
0.6932	0.0557	15.05	186.0	233.1	1.502	1.202	593
				283.2	1.542	1.247	594
				383.9	1.524	1.245	595
				483.4	1.513	1.245	596
				583.8	1.493	1.236	597
				620.1	1.496	1.243	598
0.7008	0.0408	20.73	184.0	620.1	1.823	1.550	640
	.0409	20.67	185.5	583.8	1.841	1.562	639
	.0410	20.61	187.0	483.4	1.874	1.582	638
	0.0411	20.55	188.5	383.9	1.876	1.571	637
		20.57	188.0	233.1	1.735	1.415	635
	0.0412	20.49	190.0	283.2	1.808	1.492	636
0.7012	0.0573	15.42	81.3	133.2	1.671	1.330	474
				183.6	1.705	1.372	475
				283.2	1.685	1.371	476
				383.9	1.647	1.351	477
				483.4	1.607	1.325	478
				583.8	1.572	1.300	479
0.7019	0.0761	12.19	-3.7	183.6	1.568	1.235	781
			-3.8	383.9	1.454	1.156	782
			-3.9	483.4	1.407	1.120	783
		12.20	-4.0	583.8	1.368	1.088	784
	0.0762	12.18	-3.5	33.6	1.746	1.365	779
			-3.6	86.6	1.670	1.309	780
0.7035	0.0400	20.55	274.0	333.2	1.616	1.326	717
	0.0402	20.50	275.5	383.9	1.748	1.455	718
		20.44	277.0	483.4	1.787	1.504	719
	0.0403	20.39	278.3	583.8	1.793	1.522	720
	.0404	20.34	280.0	620.0	1.792	1.524	721
0.7060	0.0402	23.26	-11.0	33.6	2.330	1.898	863
		23.28	-11.2	86.6	2.322	1.908	864
		23.29	-11.4	183.6	2.222	1.840	865
		23.30	-11.6	383.9	2.117	1.777	866
		23.32	-11.8	483.4	2.060	1.735	867
		23.33	-12.0	583.8	2.017	1.705	868
0.7077	0.0563	14.67	276.0	333.2	1.291	1.027	687
		14.68	275.8	383.9	1.396	1.130	688
		14.69	275.5	483.4	1.466	1.207	689
			275.2	583.8	1.480	1.229	690
		14.70	275.0	620.0	1.479	1.232	691
0.7091	0.0753	10.99	276.5	333.2	1.153	0.9013	656
			276.4	383.9	1.232	.9792	657
			276.2	483.4	1.248	1.004	658
		11.00	276.1	583.8	1.238	1.004	659
			276.0	620.0	1.228	.9981	660
0.7127	0.0237	37.88	80.3	133.2	2.299	1.909	1017
				183.6	2.582	2.185	1018
				283.2	3.611	2.234	1019
				383.9	2.808	2.250	1020
				483.4	2.899	2.542	1021
				583.8	2.521	2.196	1022
0.7158	0.0408	21.99	82.0	133.2	1.967	1.621	510
				183.6	2.145	1.778	511
				283.2	2.036	1.698	512
				383.9	1.997	1.677	513
				483.4	1.957	1.652	514
				583.8	1.919	1.627	515
	0.0582	16.22	-8.5	583.8	1.599	1.309	826
		16.20	-8.1	483.4	1.646	1.345	825
	0.0583	16.19	-7.7	383.9	1.702	1.388	824
		16.17	-7.3	183.6	1.818	1.465	823
	0.0584	16.15	-6.9	86.6	1.907	1.526	822
		16.13	-6.5	33.6	1.999	1.595	821
0.7240	0.0762	11.36	184.2	483.4	1.261	1.011	567
		11.35	184.6	583.8	1.246	1.006	568
	0.0763	11.35	185.0	620.1	1.242	1.005	569
0.7373	0.0754	12.17	77.0	133.2	1.470	1.147	456
				183.6	1.477	1.163	457
				283.2	1.442	1.146	458
				383.9	1.414	1.133	459
				483.4	1.366	1.099	460
				583.8	1.372	1.112	461
0.7582	0.0141	69.57	-8.5	33.6	3.786	3.353	972
				86.6	3.849	3.334	973
				183.6	3.796	3.317	974
				383.9	3.685	3.281	975
				483.4	3.636	3.233	976

M	Kn	Re_t	T_t	T_w	Nu''_t	Nu_t	Run
0.7635	0.0559	15.59	275.2	583.8	1.465	1.216	695
			275.0	620.0	1.491	1.243	696
	0.0560	15.57	276.0	333.2	1.430	1.155	692
			275.8	383.9	1.467	1.196	693
		15.58	275.5	483.4	1.474	1.214	694
0.7714	0.0759	11.57	276.0	333.2	1.173	0.9194	661
			275.9	383.9	1.238	.9850	662
			275.8	483.4	1.241	.9982	663
		11.58	275.6	583.8	1.233	1.000	664
			275.5	620.0	1.224	.9948	665
0.7799	0.0570	15.99	183.0	233.1	1.430	1.136	605
			183.2	283.2	1.493	1.202	606
		15.98	183.4	383.9	1.525	1.246	607
		15.97	183.6	483.4	1.511	1.244	608
	0.0571	15.96	184.0	620.1	1.488	1.235	610
	.0572	15.91	183.8	583.8	1.506	1.249	609
0.7827	0.0772	11.83	185.0	233.1	1.234	0.9575	575
		11.82	185.4	283.2	1.131	.8710	576
		11.81	185.8	383.9	1.293	1.031	577
	0.0773	11.80	186.2	483.4	1.254	1.005	578
		11.79	186.6	583.8	1.233	.9944	579
	0.0774	11.78	187.0	620.1	1.222	0.9872	580
0.7831	0.0386	26.32	-27.2	86.6	2.368	1.949	876
		26.34	-27.4	183.6	2.285	1.897	877
		26.36	-27.6	383.9	2.154	1.809	878
		26.37	-27.8	483.4	2.073	1.745	879
		26.39	-28.0	583.8	2.014	1.699	880
	0.0387	26.31	-27.0	33.6	2.452	2.009	875
0.7844	0.0408	22.47	176.5	233.1	1.599	1.290	1089
		22.46	176.6	283.2	1.830	1.512	1090
			176.7	383.9	1.871	1.566	1091
		22.45	176.8	483.4	1.860	1.570	1092
			176.9	583.8	1.844	1.565	1093
	0.0409	22.44	177.0	620.1	1.831	1.557	1094
0.7857	0.0254	36.12	176.0	233.1	2.018	1.678	1107
		36.10	176.2	283.2	2.290	1.940	1108
		36.09	176.4	383.9	2.394	2.055	1109
		36.08	176.6	483.4	2.396	2.072	1110
	0.0255	36.06	176.8	583.8	2.400	2.089	1111
		36.05	177.0	620.1	2.386	2.081	1112
0.7865	0.0249	40.63	-12.5	33.6	2.896	2.423	911
				86.6	2.883	2.429	912
				183.6	2.848	2.425	913
				383.9	2.764	2.388	914
				483.4	2.702	2.344	915
				583.8	2.629	2.287	916
0.7870	0.0570	17.70	-11.0	33.6	1.988	1.585	827
			-11.1	86.6	1.945	1.561	828
		17.71	-11.2	183.6	1.859	1.504	829
			-11.3	383.9	1.729	1.413	830
		17.72	-11.4	483.4	1.669	1.367	831
			-11.5	583.8	1.618	1.326	832
0.7888	0.0733	13.09	78.5	133.2	1.454	1.133	462
				183.6	1.498	1.182	463
				283.2	1.466	1.169	464
				383.9	1.426	1.144	465
				483.4	1.384	1.116	466
				583.8	1.347	1.089	467
0.7899	0.0557	17.23	80.0	133.2	1.672	1.331	480
				183.6	1.740	1.405	481
				283.2	1.721	1.405	482
				383.9	1.693	1.393	483
				483.4	1.650	1.365	484
				583.8	1.605	1.332	485
0.7928	0.0401	24.00	81.0	133.2	2.039	1.669	516
				183.6	2.111	1.748	517
				283.2	2.080	1.739	518
				383.9	2.023	1.701	519
				483.4	1.993	1.687	520
				583.8	1.947	1.654	521
0.7944	0.0734	13.78	-6.0	33.6	1.854	1.464	785
				86.8	1.753	1.385	786
				183.6	1.645	1.307	787
				383.9	1.514	1.212	788
				483.4	1.465	1.175	789
				583.8	1.420	1.138	790

5111

5111

TABLE II. - ORGANIZATION OF RESULTS FOR NOMINAL VALUES OF PARAMETERS

Nominal Knudsen number, Kn	Nominal Mach number, M								
	0.05	0.10	0.20	0.30	0.40	0.50	0.60	0.70	0.80
Run numbers[a] for $T_t \approx 0^\circ$ F									
0.0770	342 420	336 414	330 408	402	767	773	761	779	785
0.0555	396	390	324 384	815	809	791 803	797	821	827
0.0416	378	372	857	839	833	845 869	851	863	875
0.0256	354 360	366	917	887	881	893	899 905	---	911
0.0143	348	935	923	929	941	959	965	---	972
0.00916	---	984	947	953 978	990	995	---	---	---
Run numbers[a] for $T_t \approx 80^\circ$ F									
0.0770	1	13 37	25 49	61	73 426	432	438	456	462
0.0555	85	91	97	103	444	450	468	474	480
0.0416	109	115 127	121 262	486	492	498	504	510	516
0.0256	133	139 522	528	534	540	546	1005	1011 1017	---
0.0143	145	1035	1029	1023	1041	1047	1083	----	---
0.00916	151	1065	1053	1059	1071	1077	----	----	---
Run numbers[a] for $T_t \approx 180^\circ$ F									
0.0770	169	163	157	175	---	---	---	567	575
0.0555	193	181	187	199	552 599	558 581	587	593	605
0.0416	217	211	205	611	617	623	630	635	1089
0.0256	223	229	743	737	749	755	1095	1101	1107
0.0143	235	---	---	---	1113	1119	----	----	----
Run numbers[a] for $T_t \approx 280^\circ$ F									
0.0770	278	247	252	257	646	---	651	656	661
0.0555	283	273	268	671	666	641 676	681	687	692
0.0416	288	293 299	304	697	702	707	712	717	---
0.0256	309	314	722	727	732	---	---	---	---
0.0143	319	---	---	---	---	---	---	---	---

[a]Each run number is the first of a group of runs in table I at the indicated nominal values of M, Kn, and T_t.

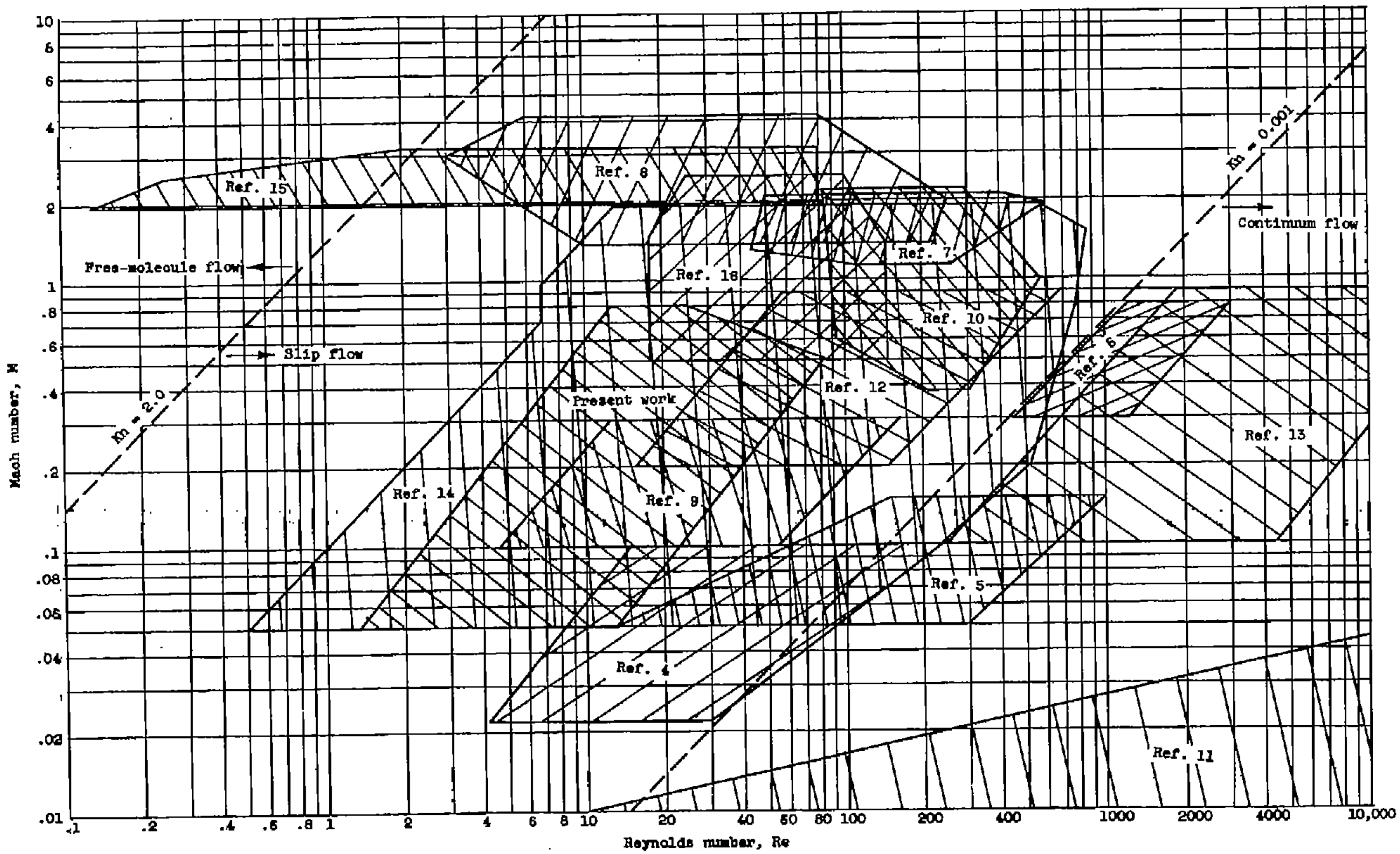

Figure 1. - Comparison of Mach and Reynolds number ranges of heat-transfer experiments with normal cylinders. Flow regions after reference 15.

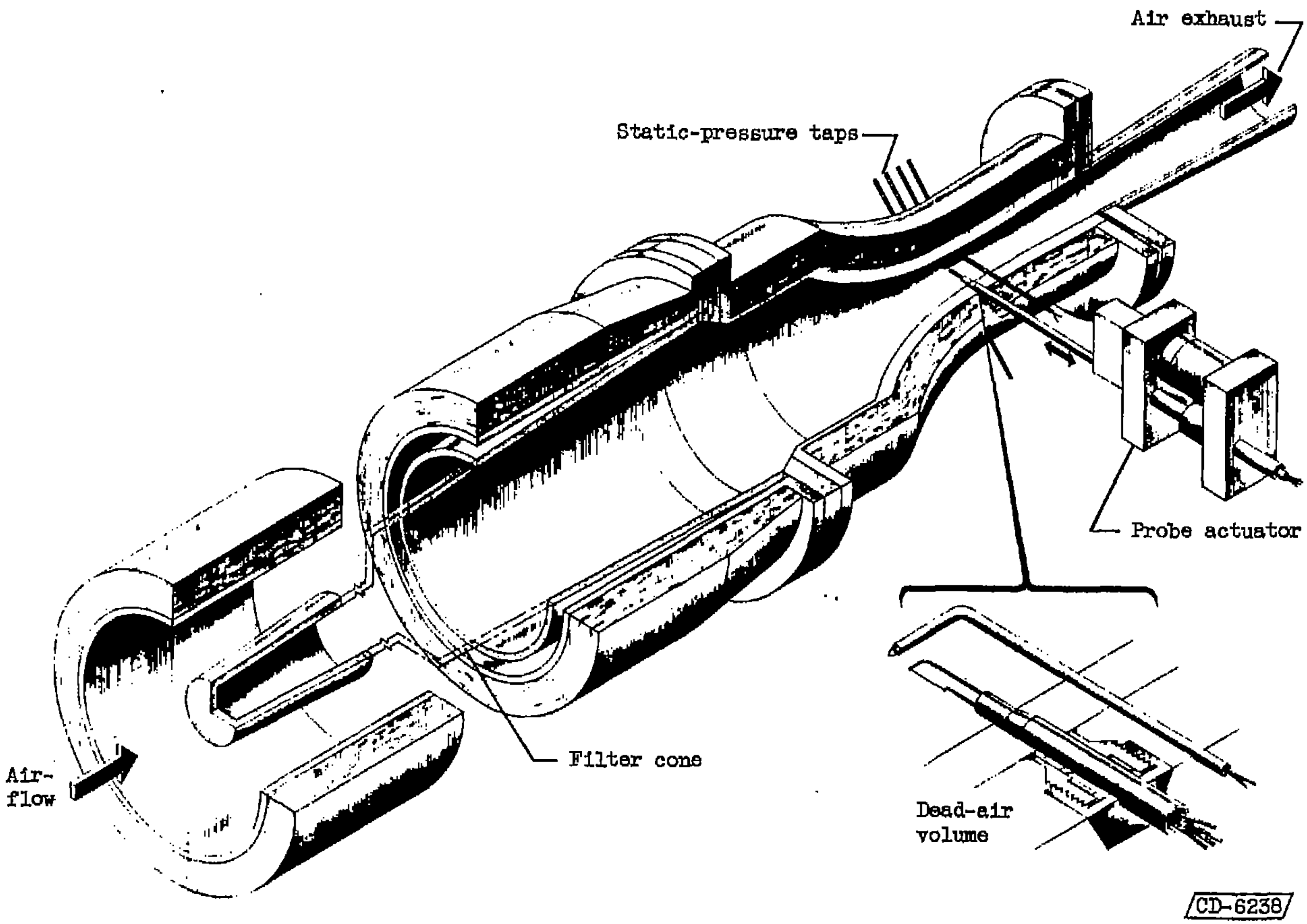

Figure 2. - Variable-density subsonic tunnel.

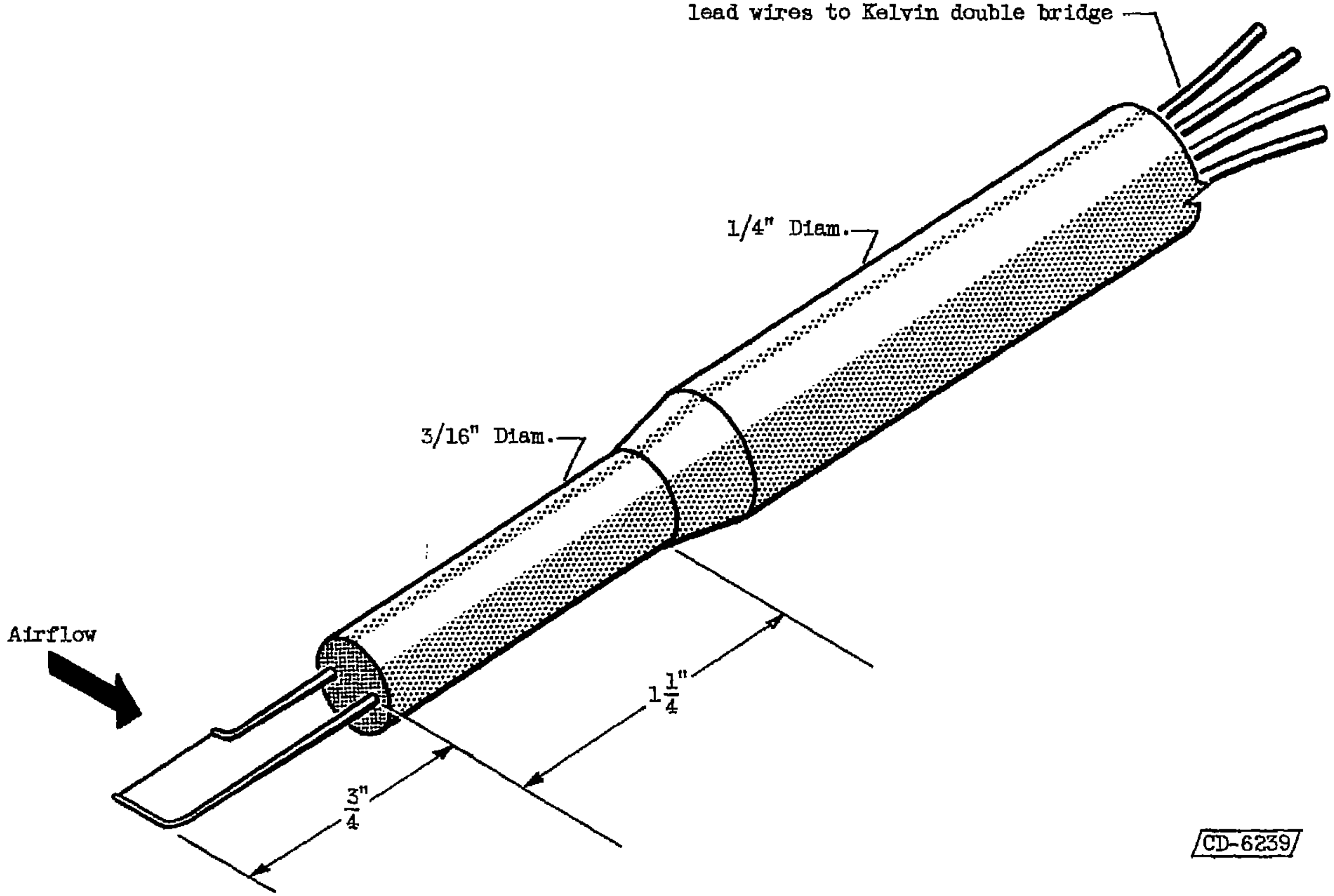

Figure 3. - Tungsten-wire supporting probe.

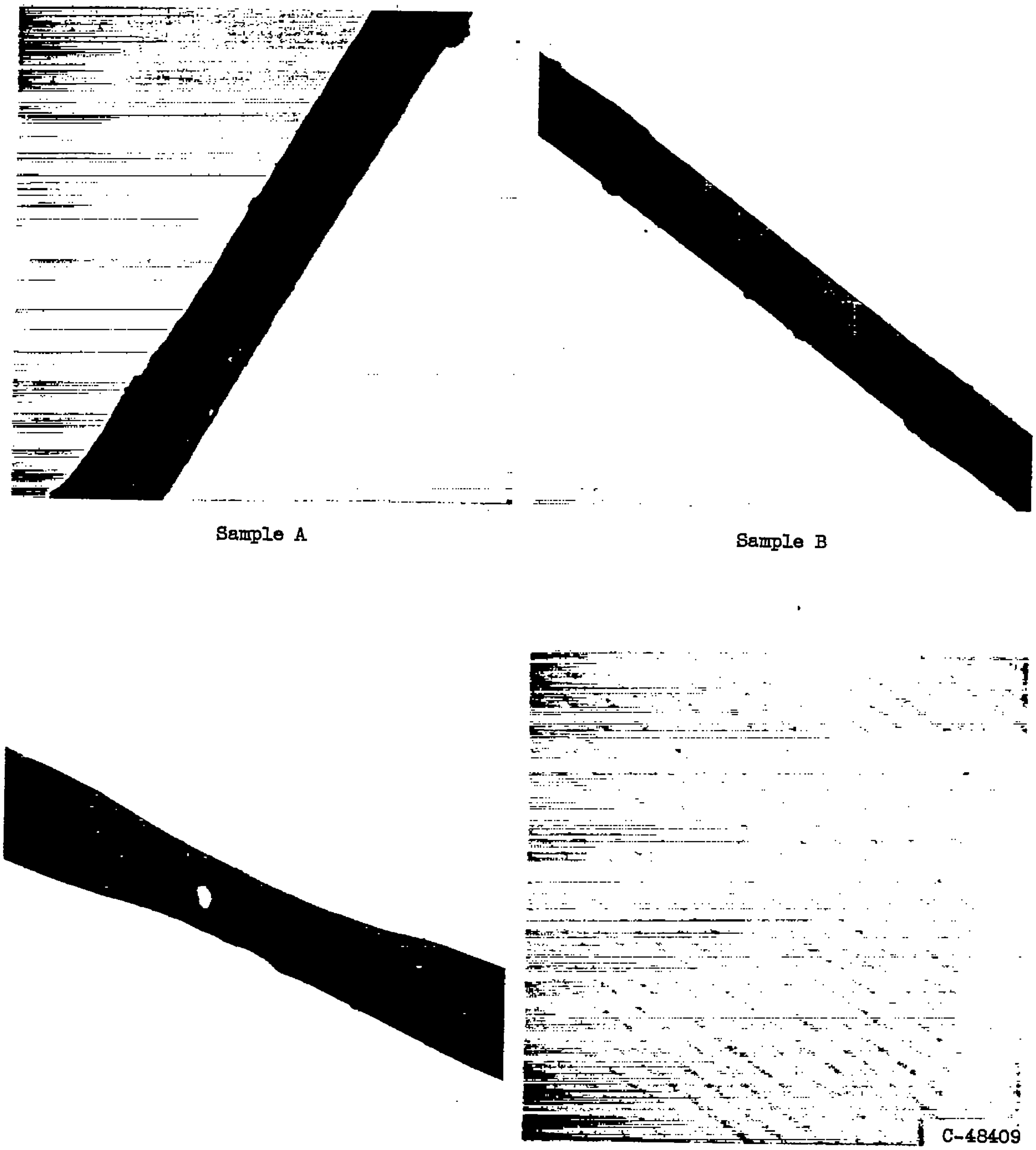

Sample A

Sample B

Sample C

Scale factor; 600 grates = 1 millimeter

Figure 4. - Electron photomicrographs of tungsten wire.

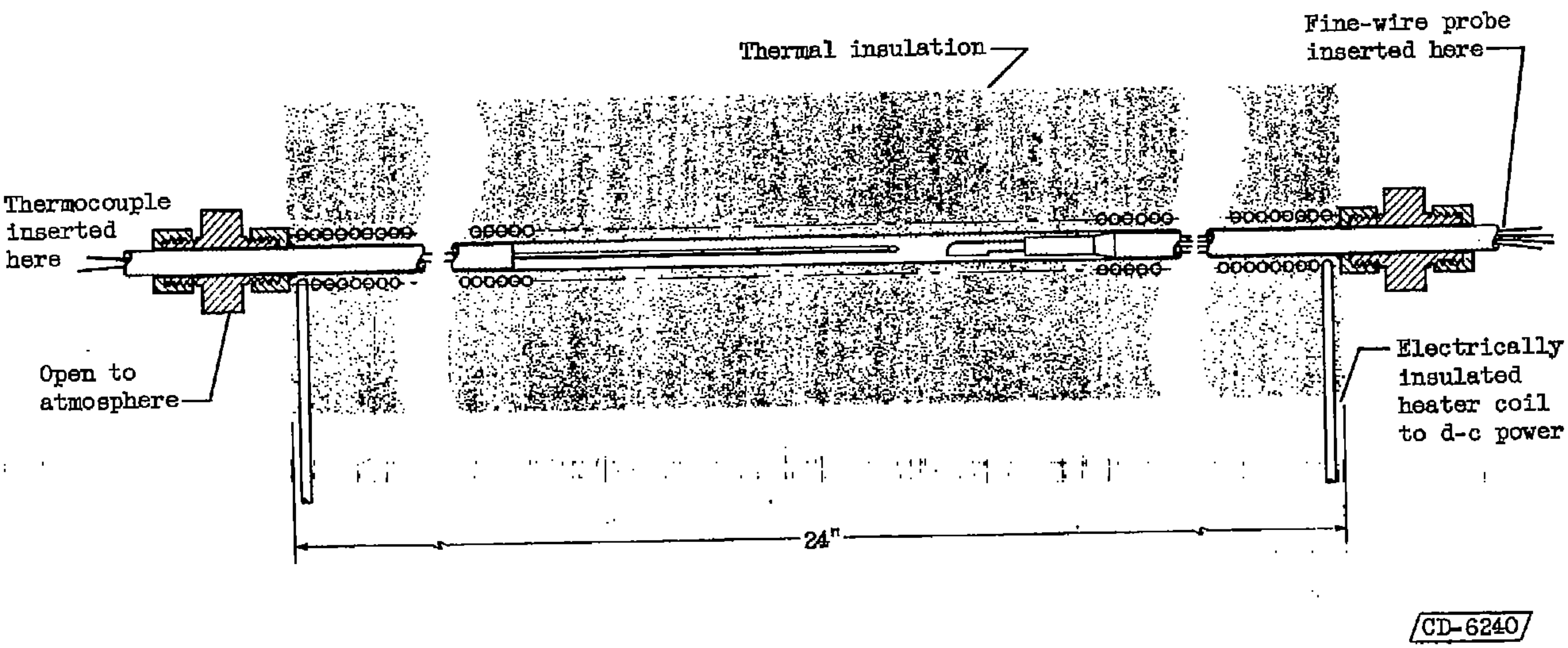

Figure 5. - Resistance-temperature calibration tank.

5111

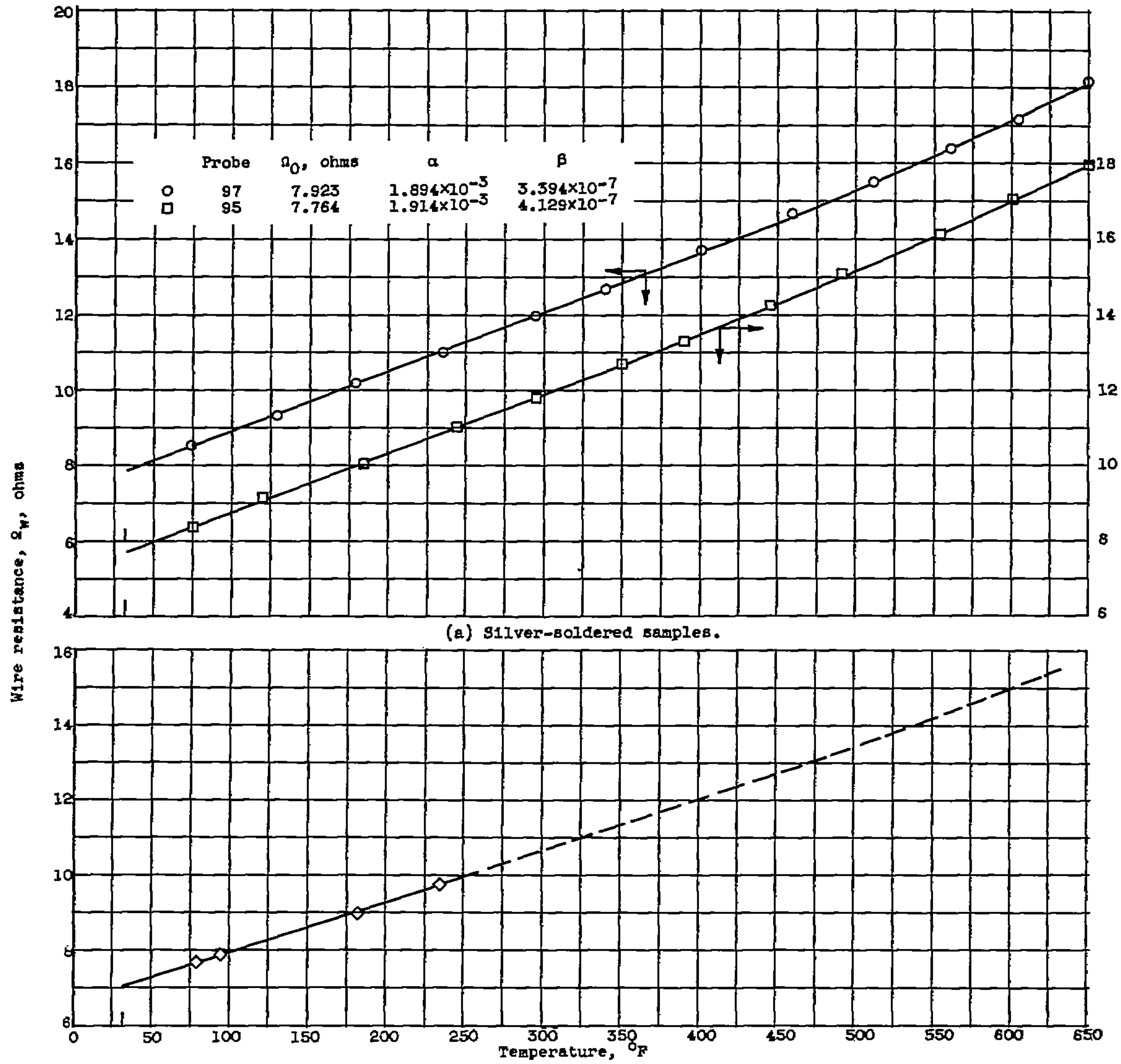

(b) Probe 109: Ω_0 = 7.054 ohms; α = 1.833×10^{-3}; assumed β = 3.40×10^{-7}.

Figure 6. - Calibration of wire electrical resistance and temperature.

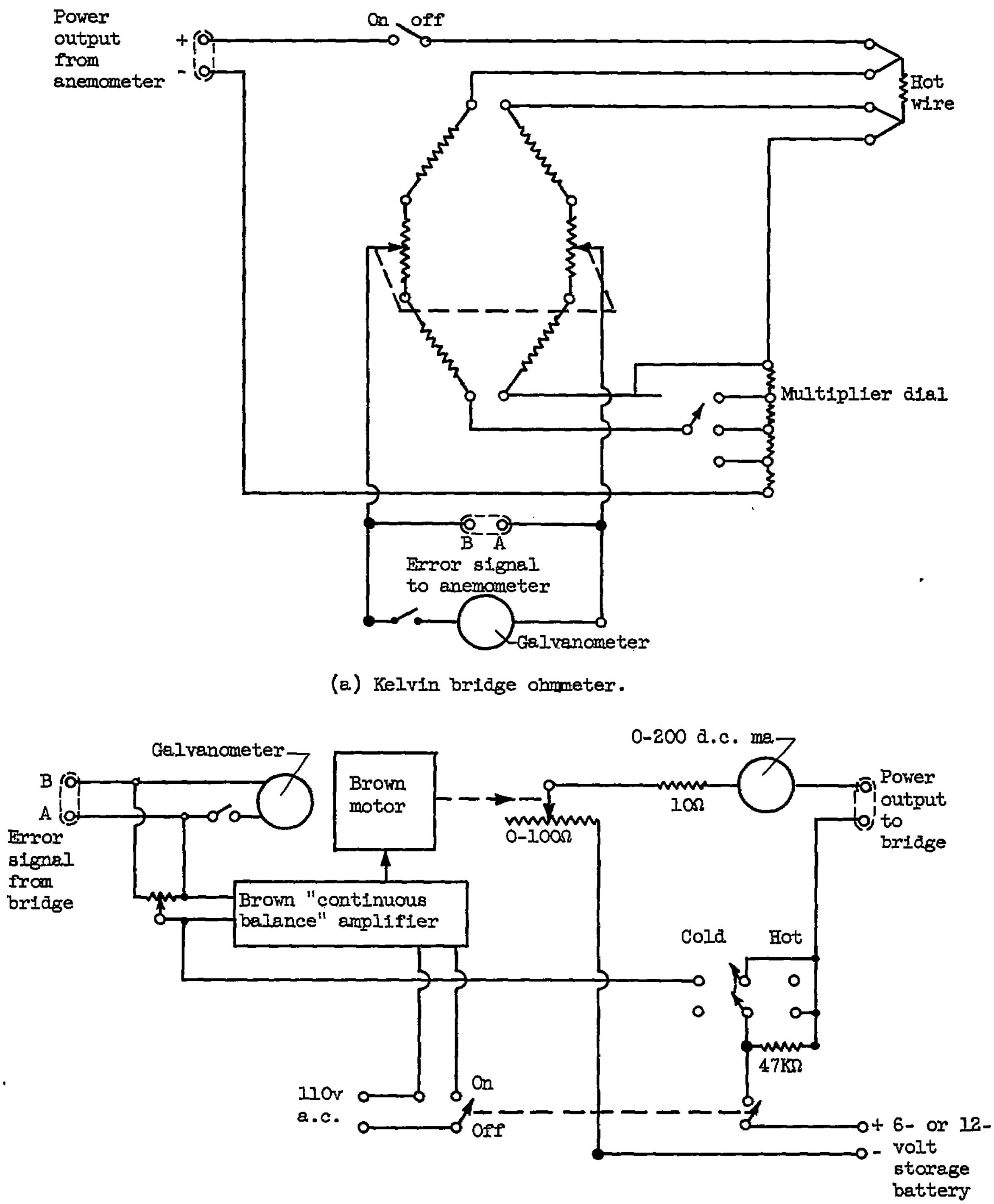

(a) Kelvin bridge ohmmeter.

(b) Constant-average-temperature anemometer.

Figure 7. - Anemometer electrical equipment.

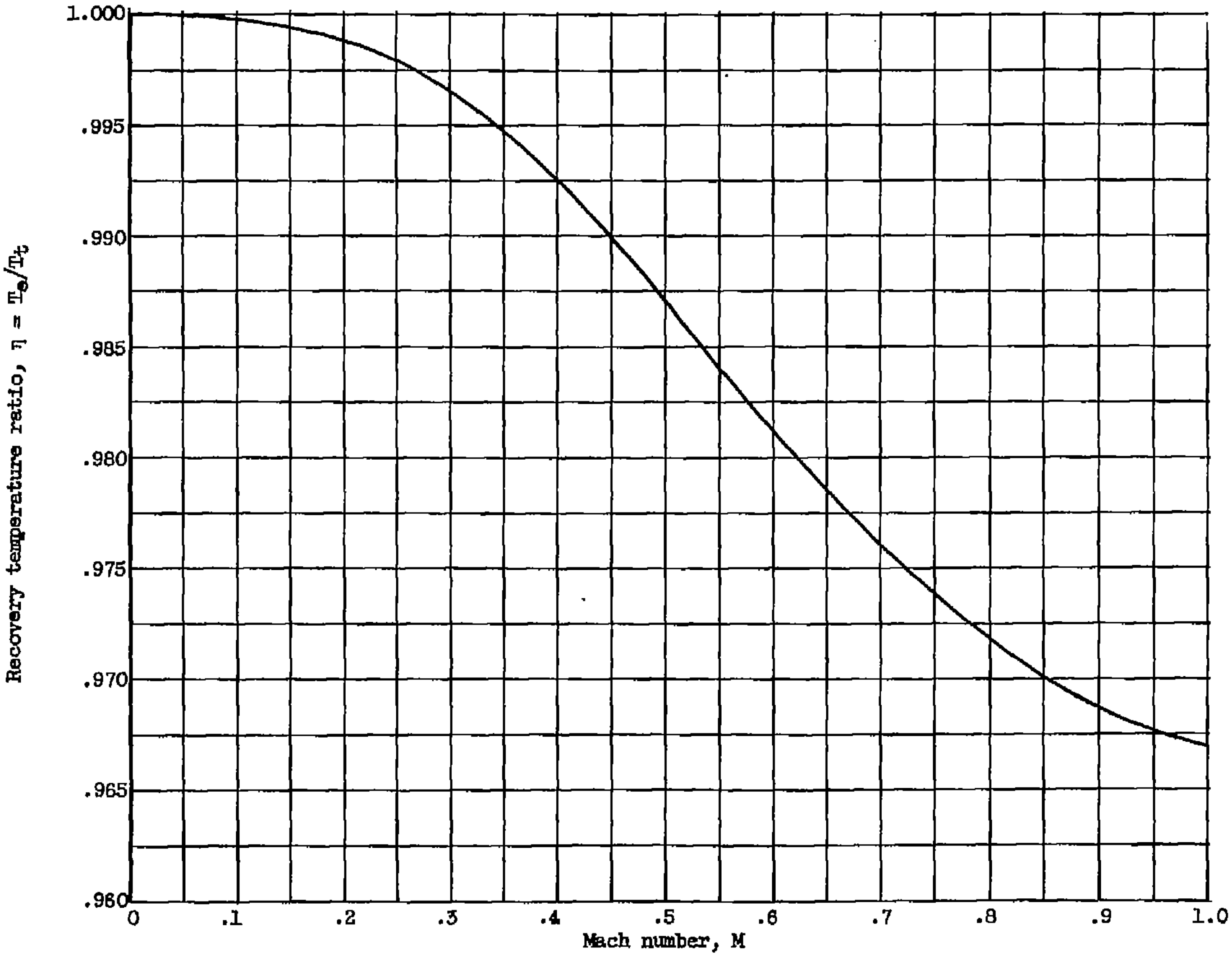

Figure 8. - Recovery temperature ratio as function of Mach number.

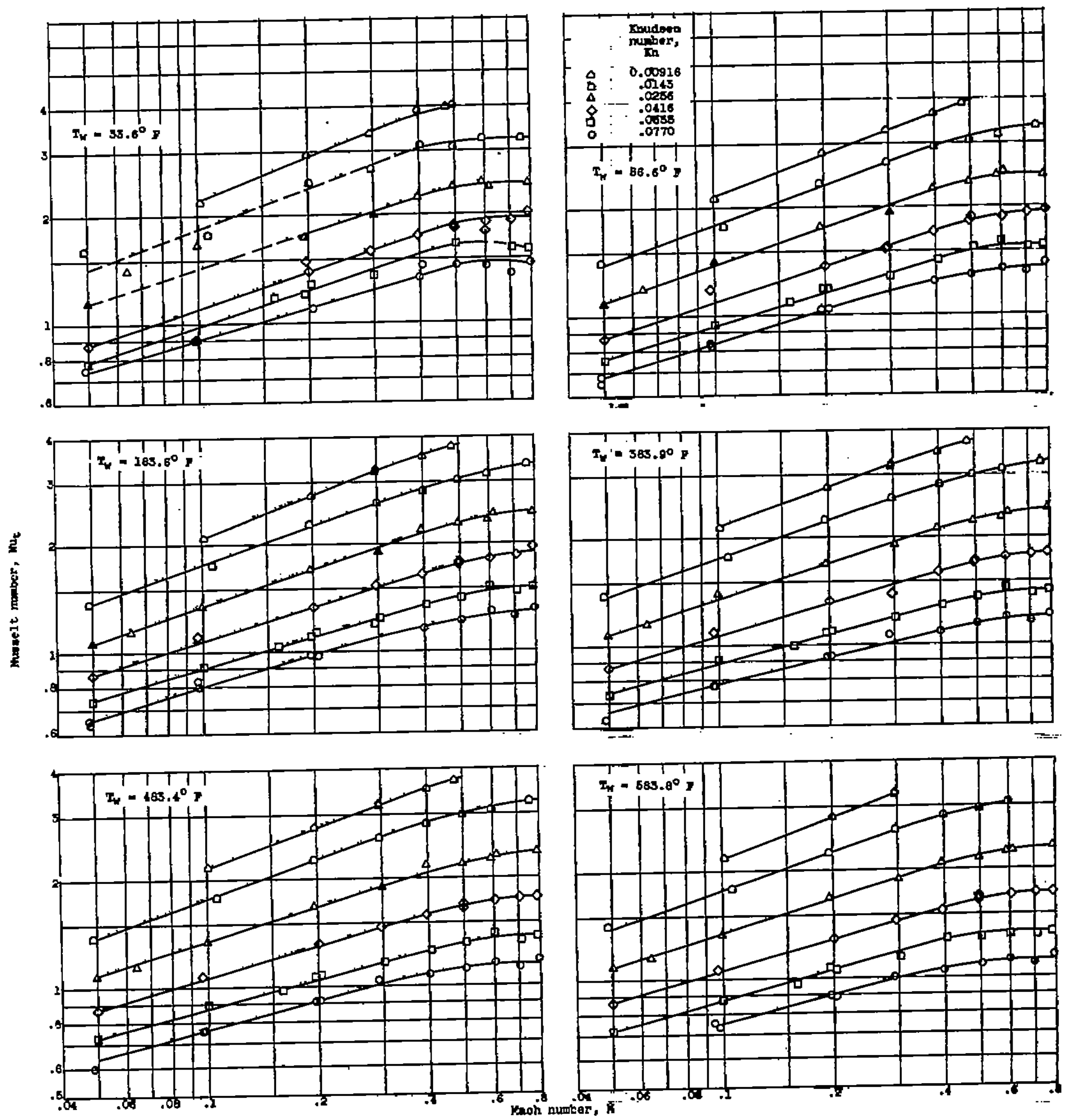

(a) Total air temperature, 0° F.

Figure 9. - Variation of Nusselt number with Mach number for constant Knudsen number and constant total air and cylinder temperatures.

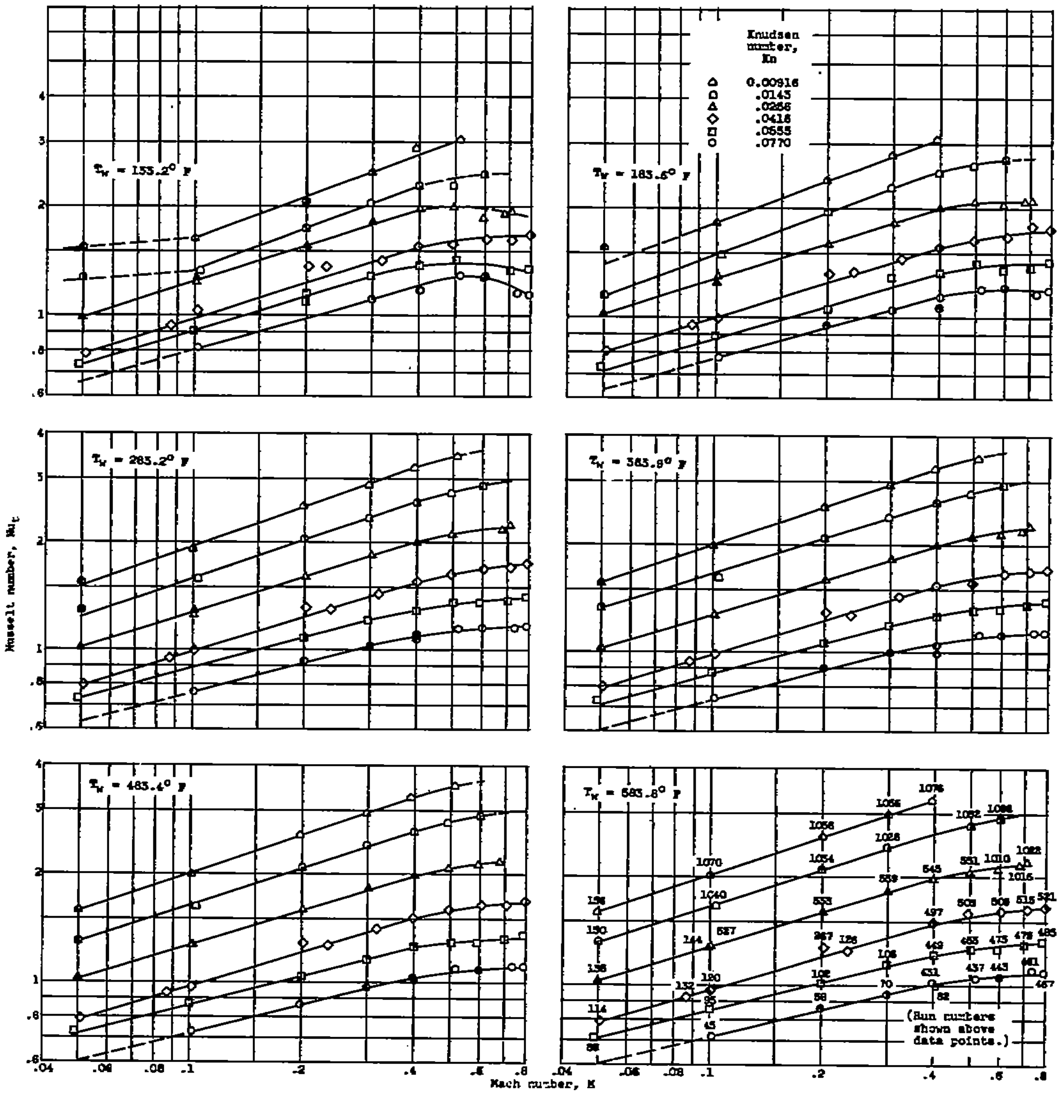

(b) Total air temperature, 80° F.

Figure 9. - Continued. Variation of Nusselt number with Mach number for constant Knudsen number and constant total air and cylinder temperatures.

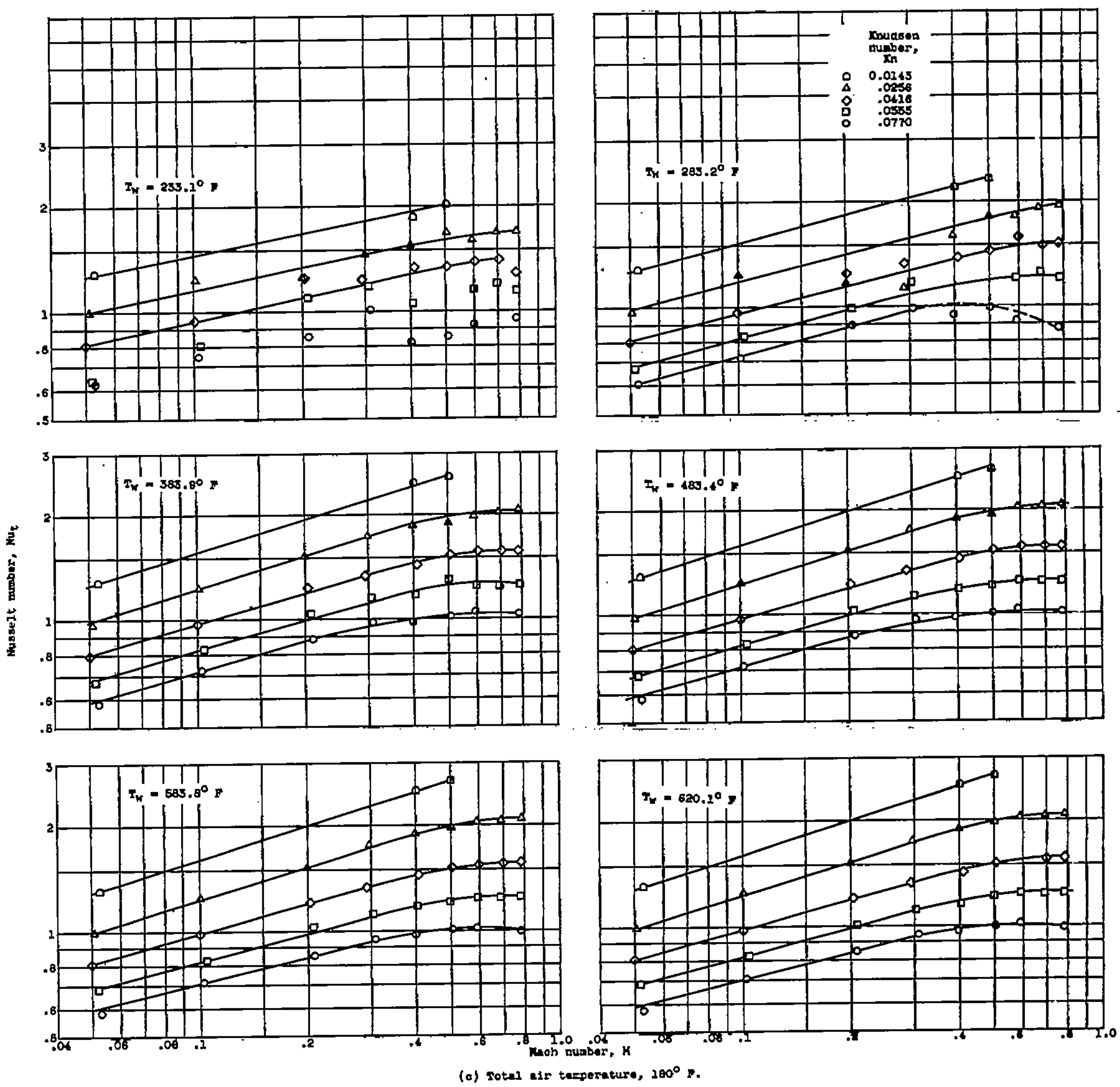

Figure 8. - Continued. Variation of Nusselt number with Mach number for constant Knudsen number and constant total air and cylinder temperatures.

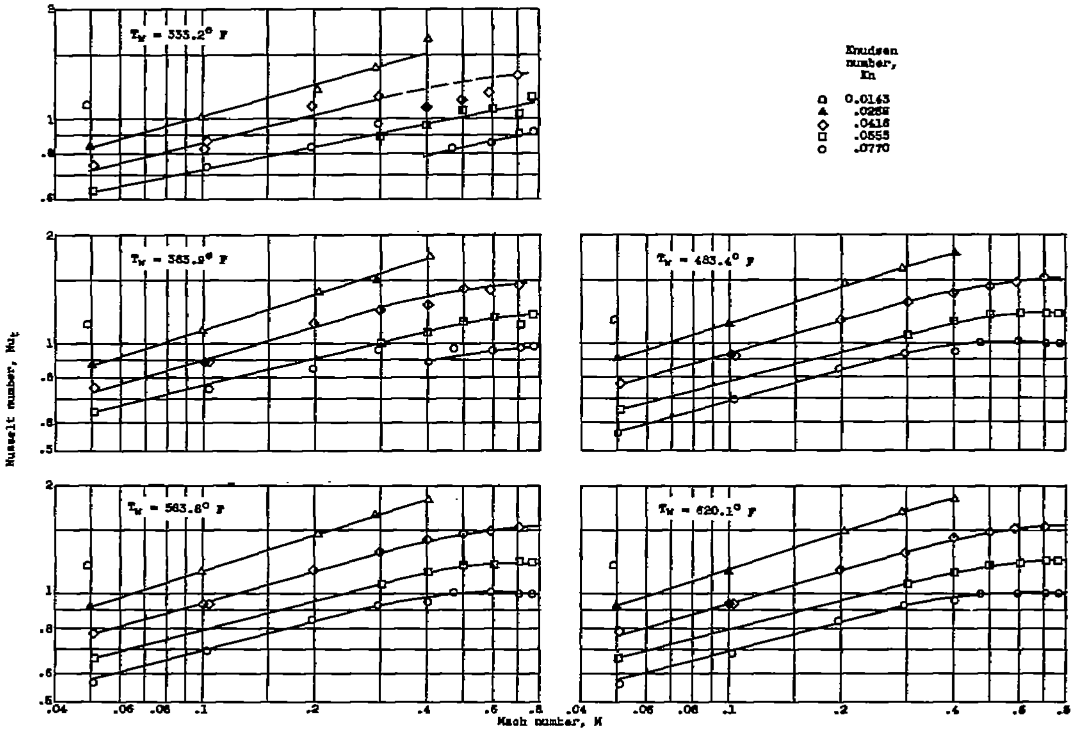

(d) Total air temperature, 280° F.

Figure 9. - Concluded. Variation of Nusselt number with Mach number for constant Knudsen number and constant total air and cylinder temperatures.

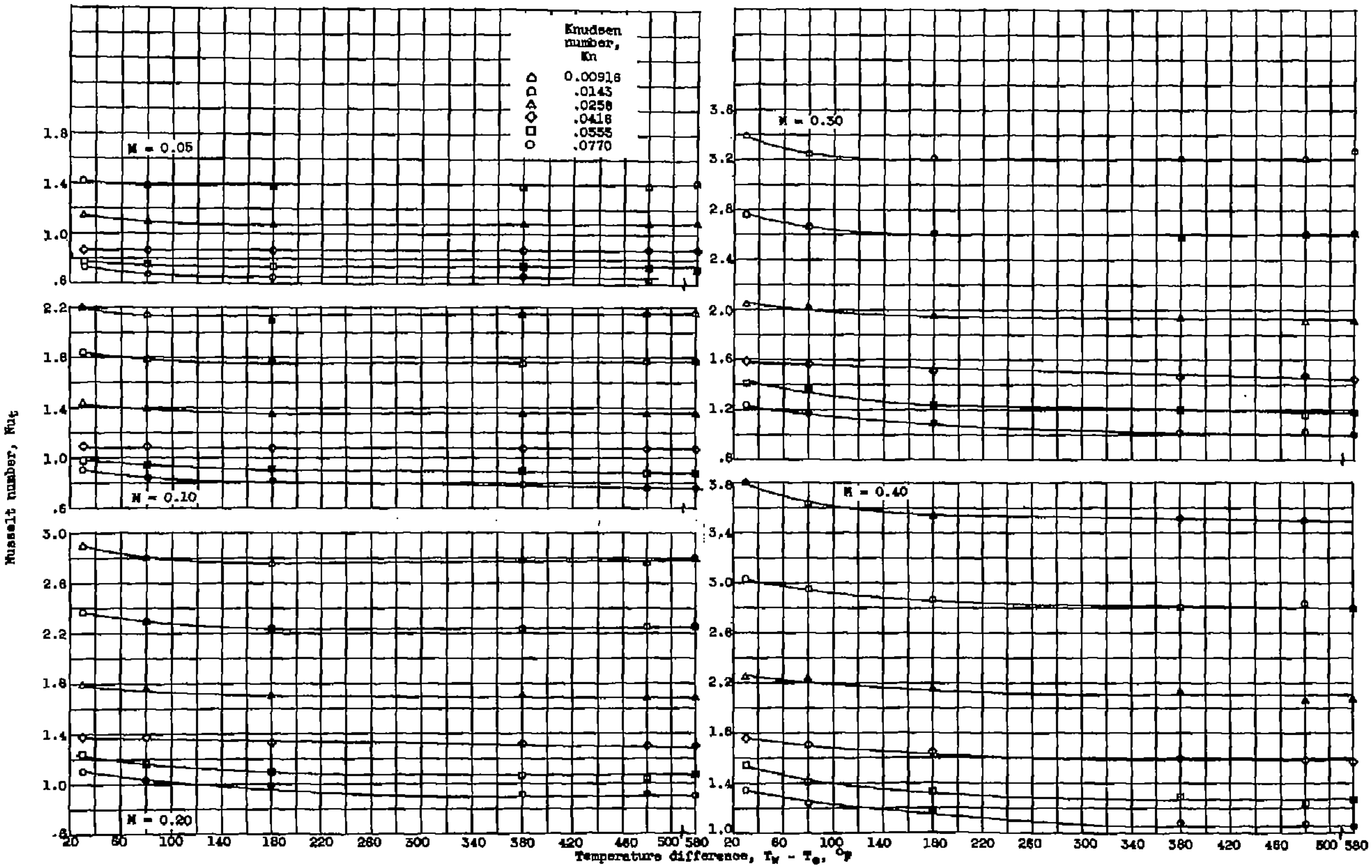

(a) Total air temperature, 0° F (fig. 9(a)).

Figure 10. - Crossplots of figure 9 showing Nusselt number variation with cylinder temperature.

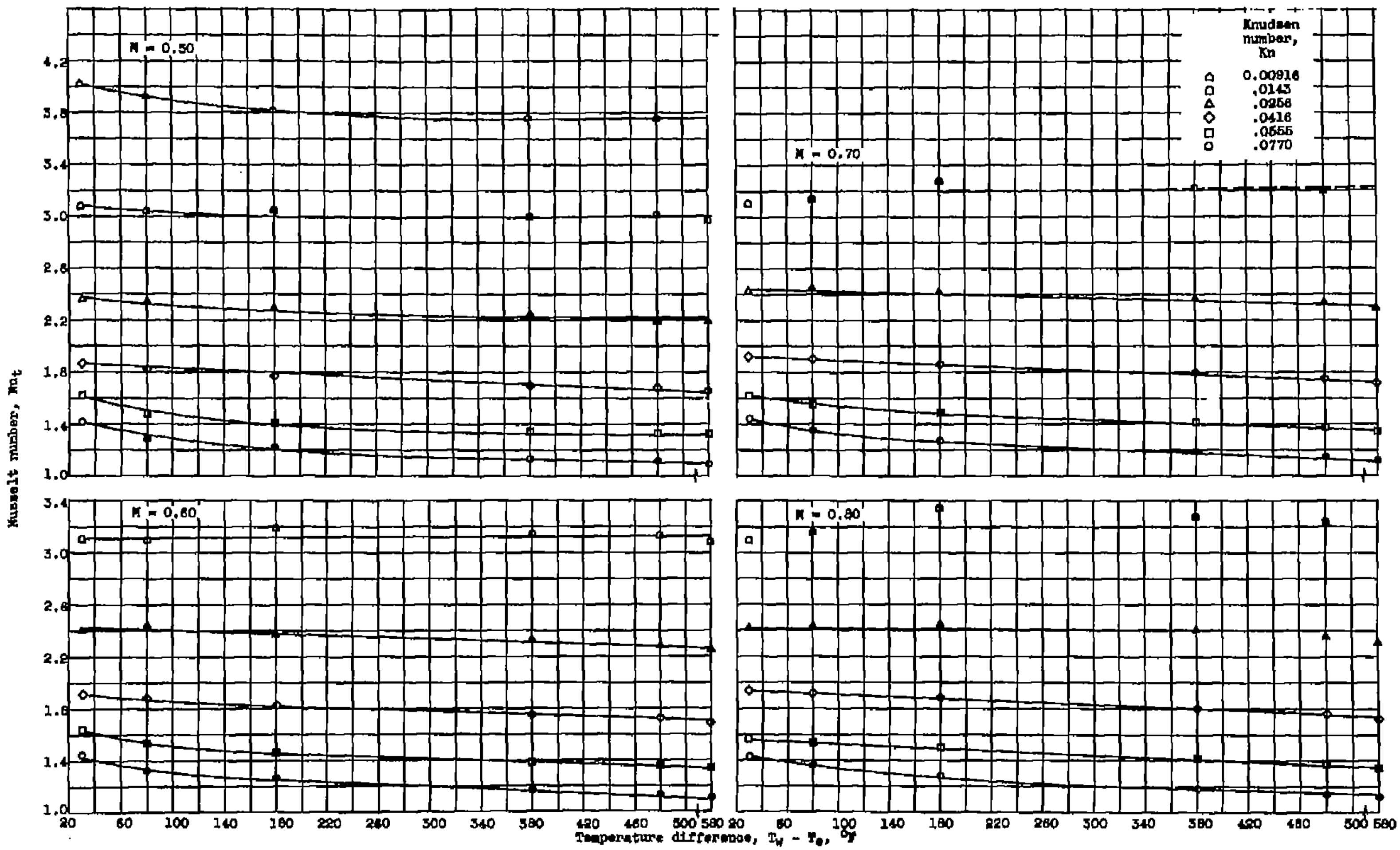

(a) Concluded. Total air temperature, 0° F (fig. 9(a)).

Figure 10. - Continued. Crossplots of figure 9 showing Nusselt number variation with cylinder temperature.

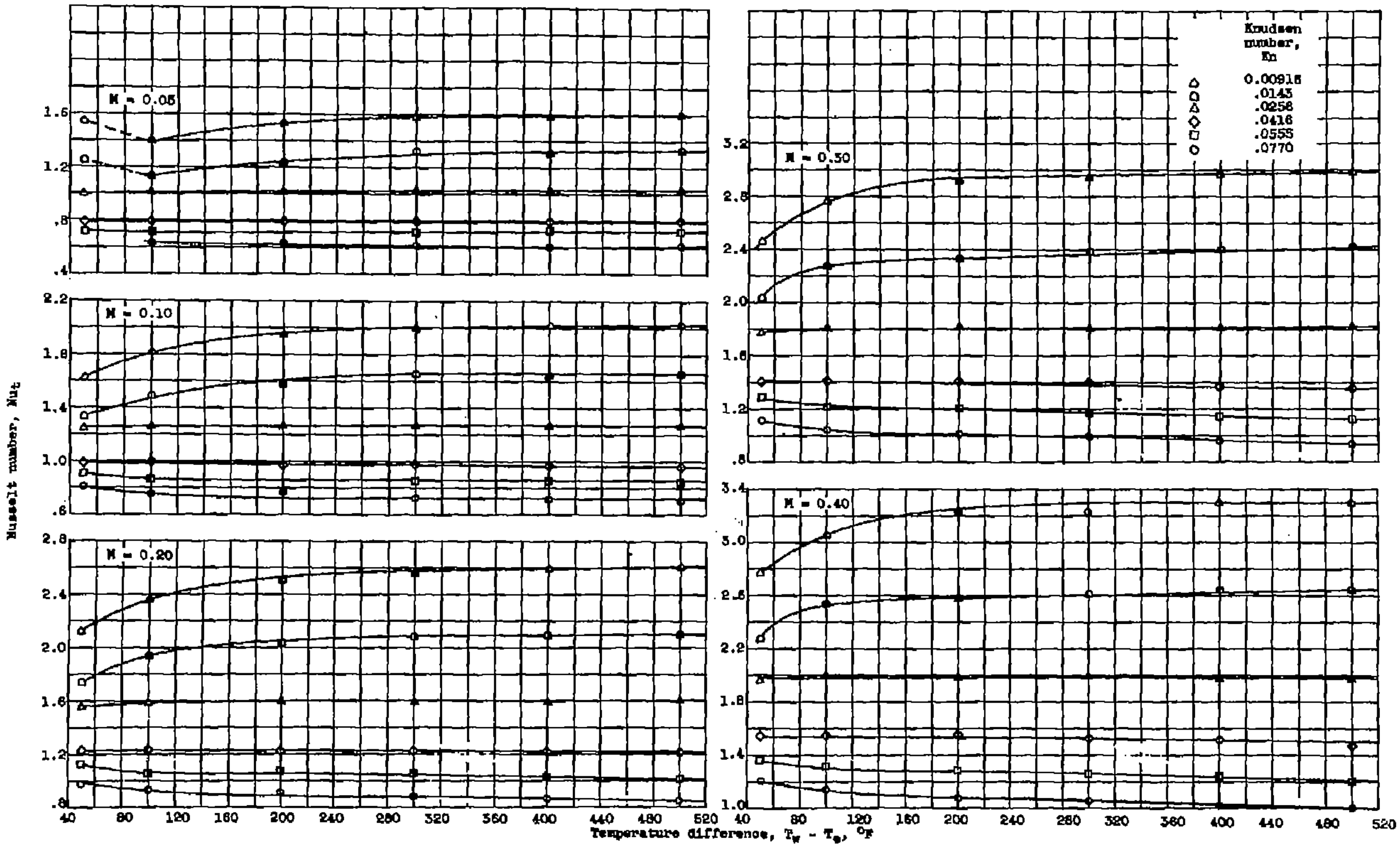

(b) Total air temperature, 80° F (fig. 9(b)).

Figure 10. - Continued. Crossplots of figure 9 showing Nusselt number variation with cylinder temperature.

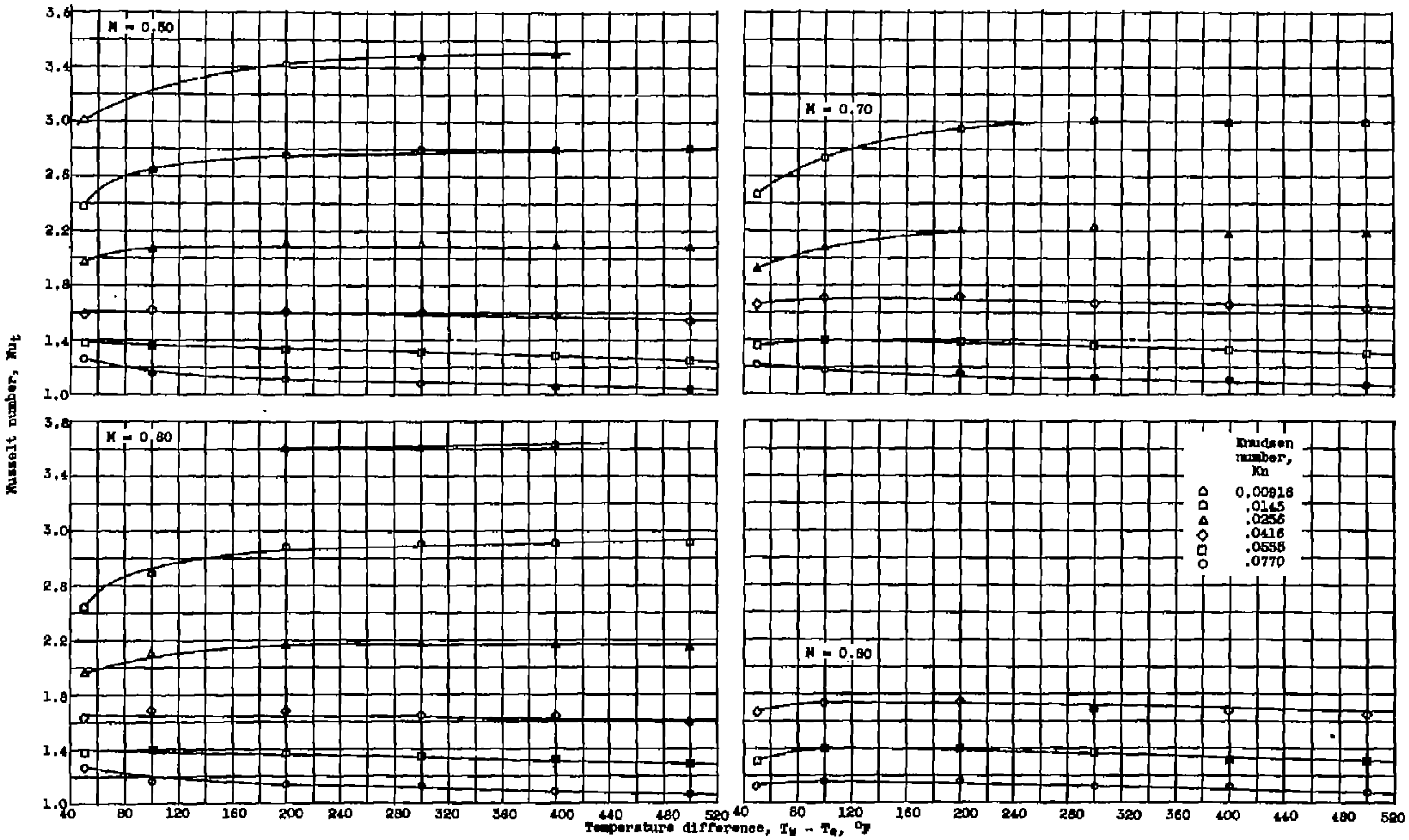

(b) Concluded. Total air temperature, 80° F (fig. 9(b)).

Figure 10. - Continued. Crossplots of figure 9 showing Nusselt number variation with cylinder temperature.

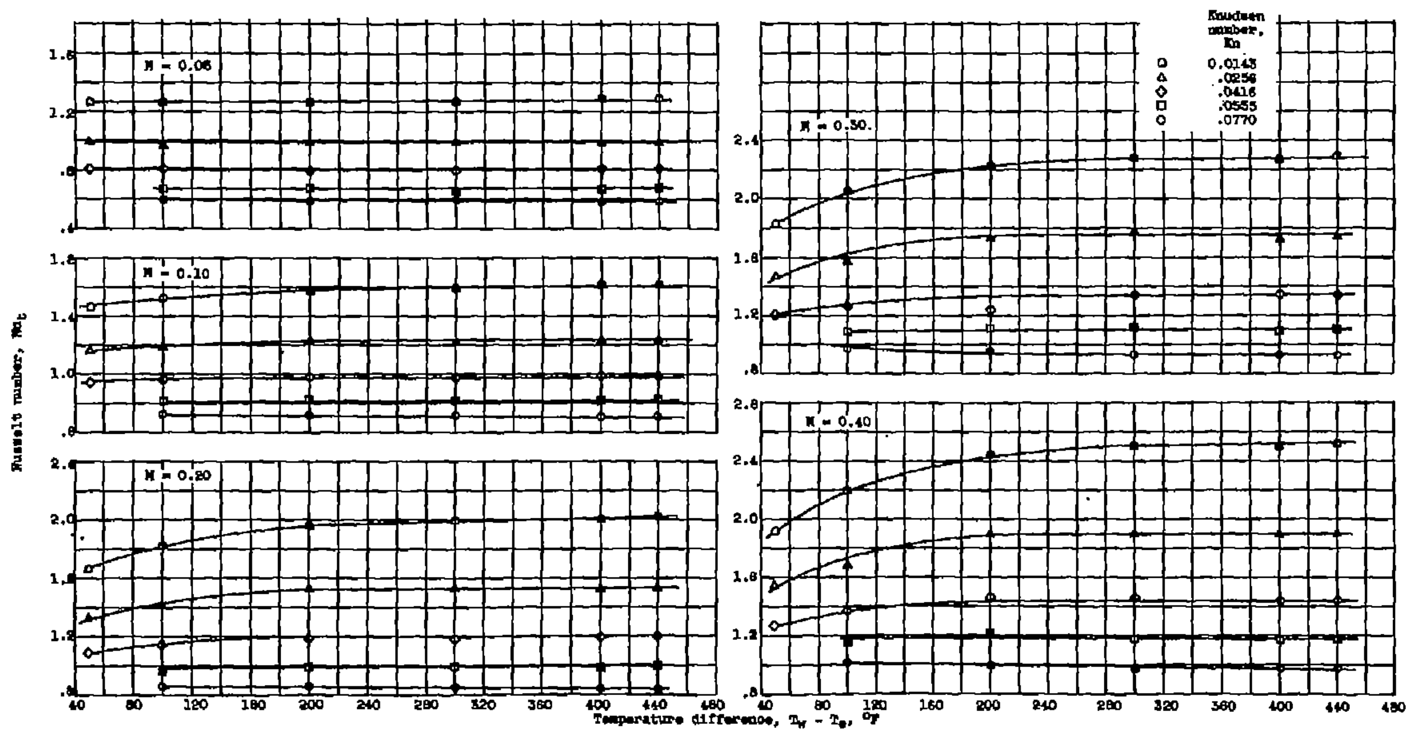

(c) Total air temperature, 180° F (fig. 9(c)).

Figure 10. - Continued. Crossplots of figure 9 showing Nusselt number variation with cylinder temperature.

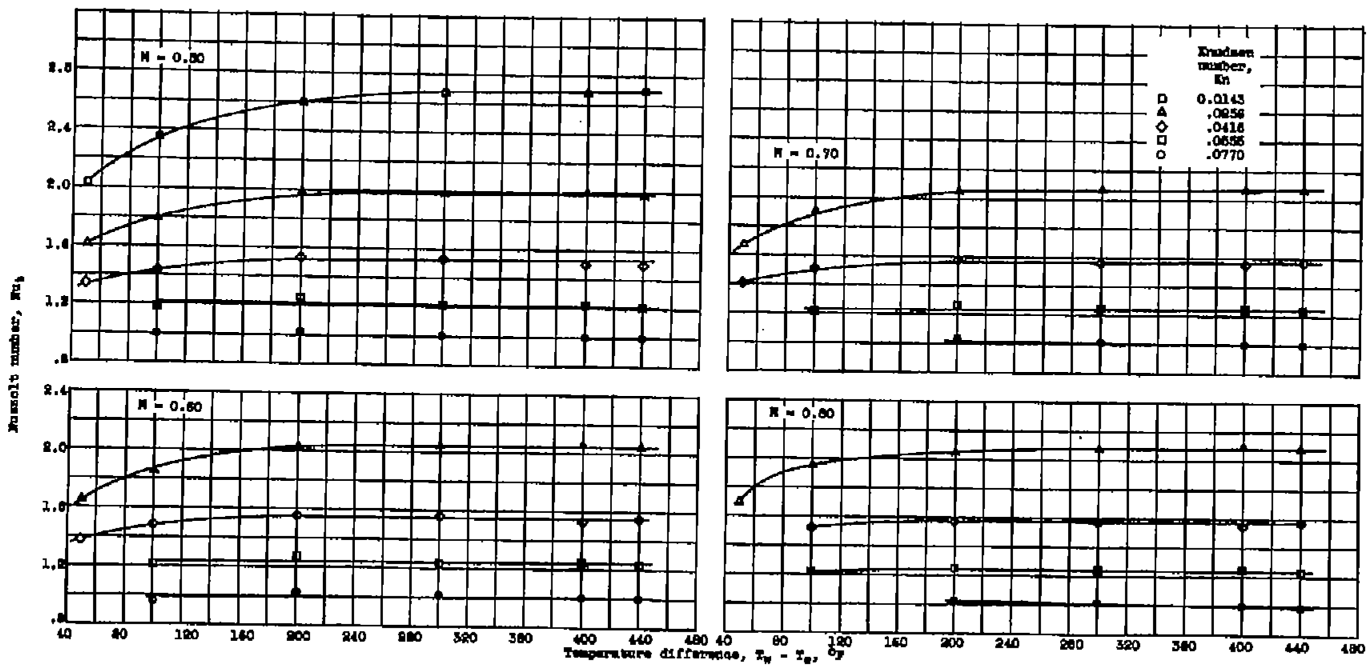

(a) Concluded. Total air temperature, 180° F (fig. 9(c)).

Figure 10. - Continued. Crossplots of figure 9 showing Nusselt number variation with cylinder temperature.

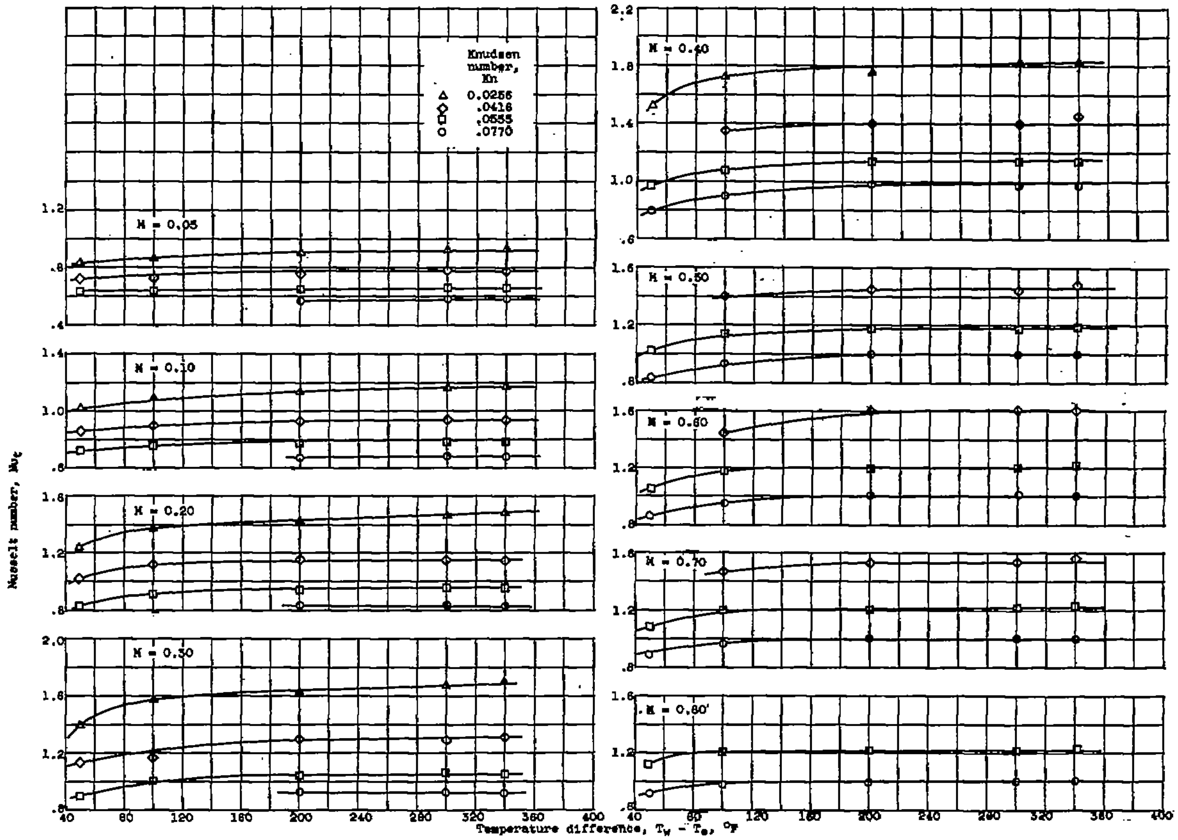

(d) Total air temperature, 260° F (fig. 9(d)).

Figure 10. - Concluded. Crossplots of figure 9 showing Nusselt number variation with cylinder temperature.

5111

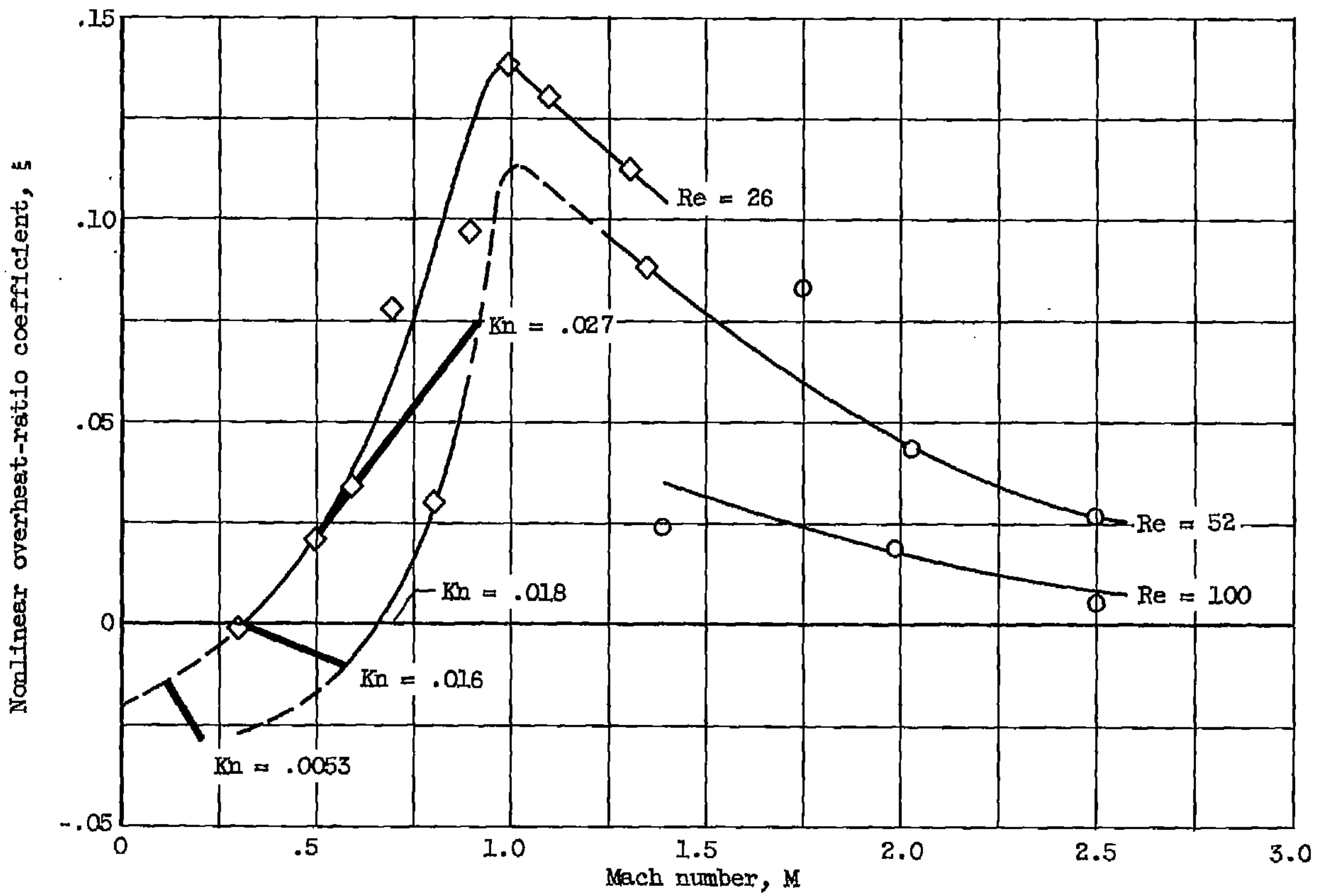

Figure 11. - Nonlinear overheat-ratio coefficient of reference 16 as function of Reynolds and Mach numbers with constant Knudsen number lines superimposed; $h = h_0(1 - \xi \bar{a}_w)$. Data points of reference 16.

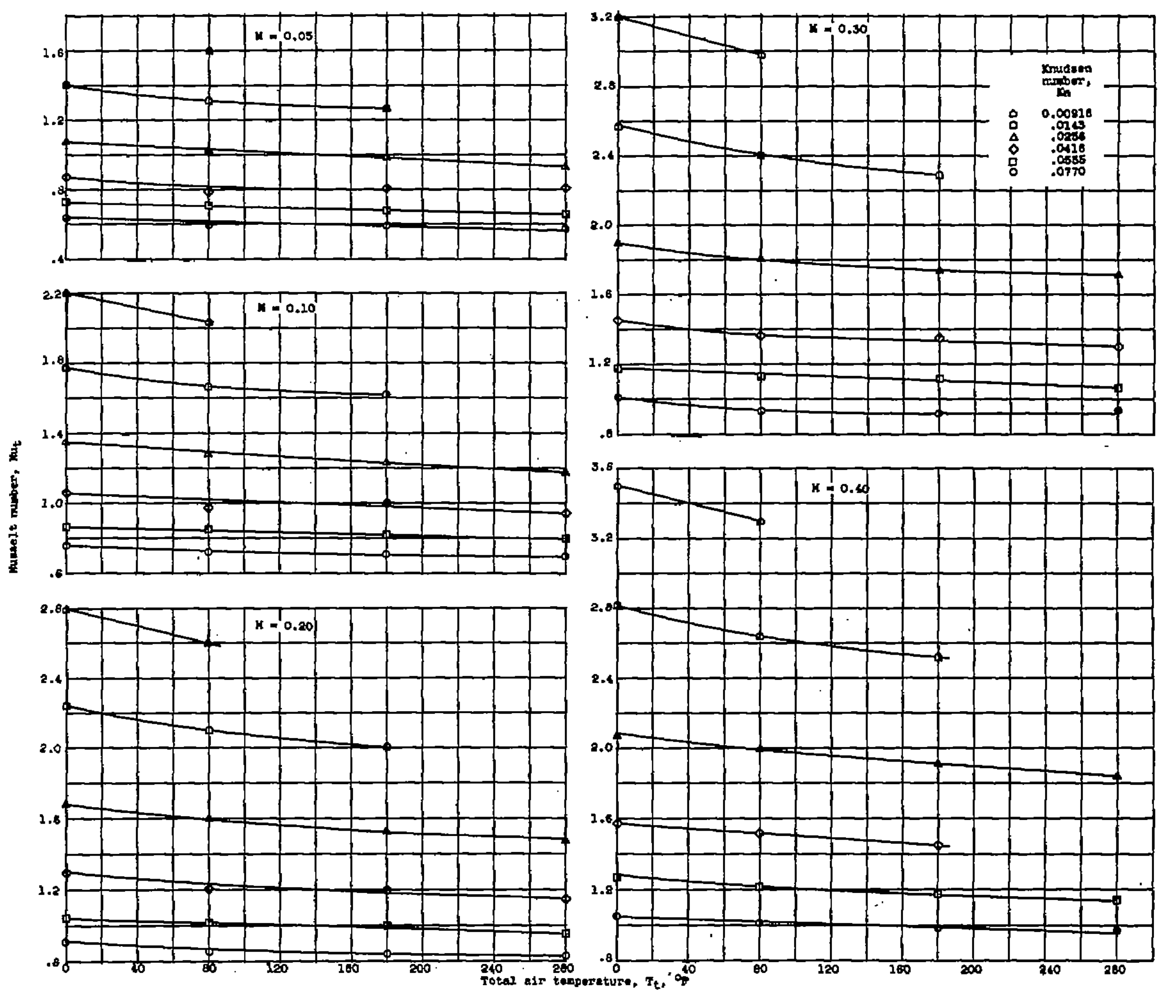

(a) Mach number, 0.05 to 0.40.

Figure 12. - Variation of Nusselt number with total air temperature. Crossplots of figure 10 showing asymptotic Nusselt number at $\Delta T > 200^\circ$ F.

5111

5111

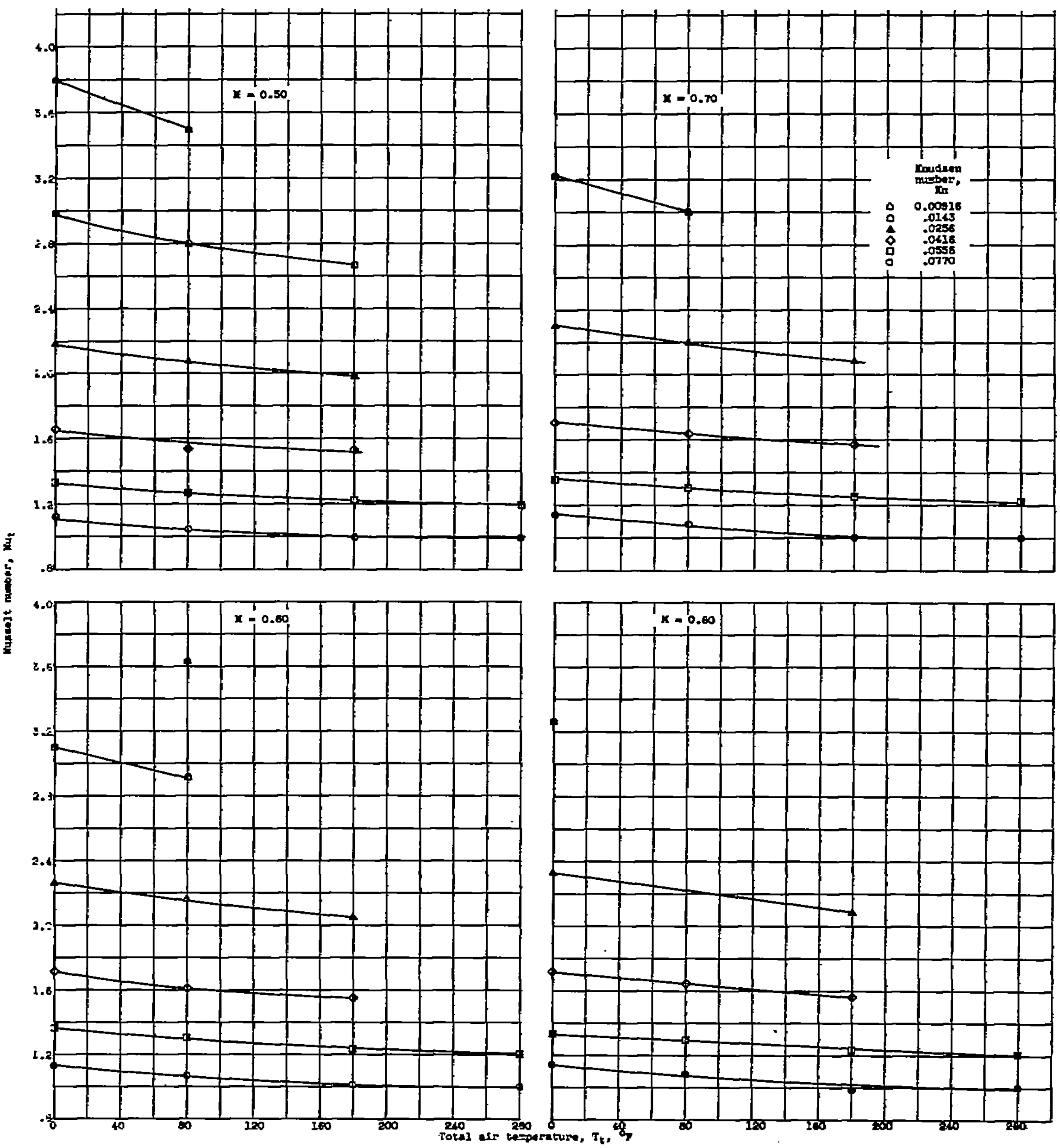

(b) Mach number, 0.50 to 0.80.

Figure 12. - Concluded. Variation of Nusselt number with total air temperature. Crossplots of figure 10 showing asymptotic Nusselt number at $\Delta T > 200^{\circ}$ F.

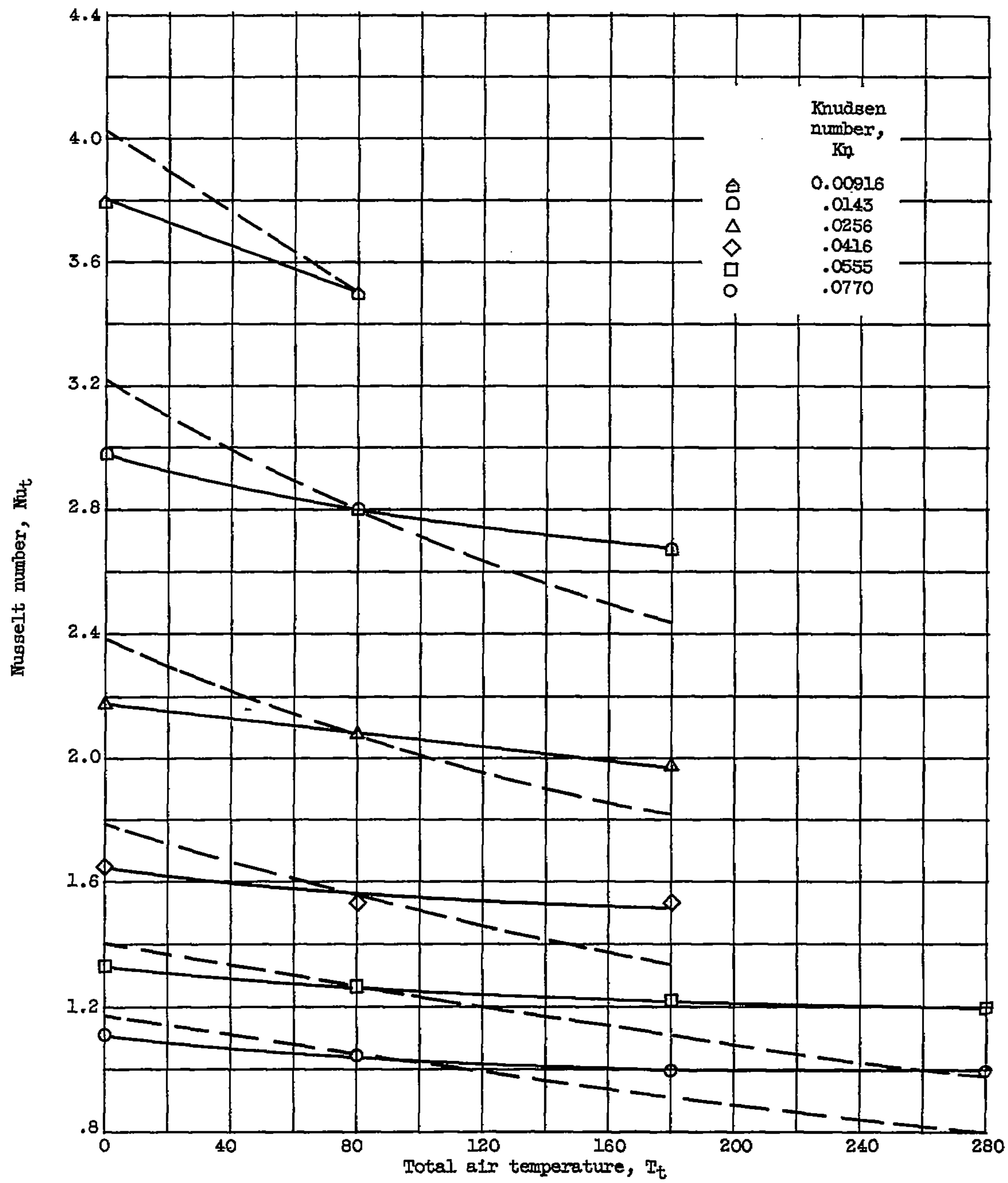

Figure 13. - Variation of Nusselt number with total air temperature. Curves of constant heat-transfer coefficient h_{80^oF} superimposed on figure 12(b) for M = 0.50.

5111

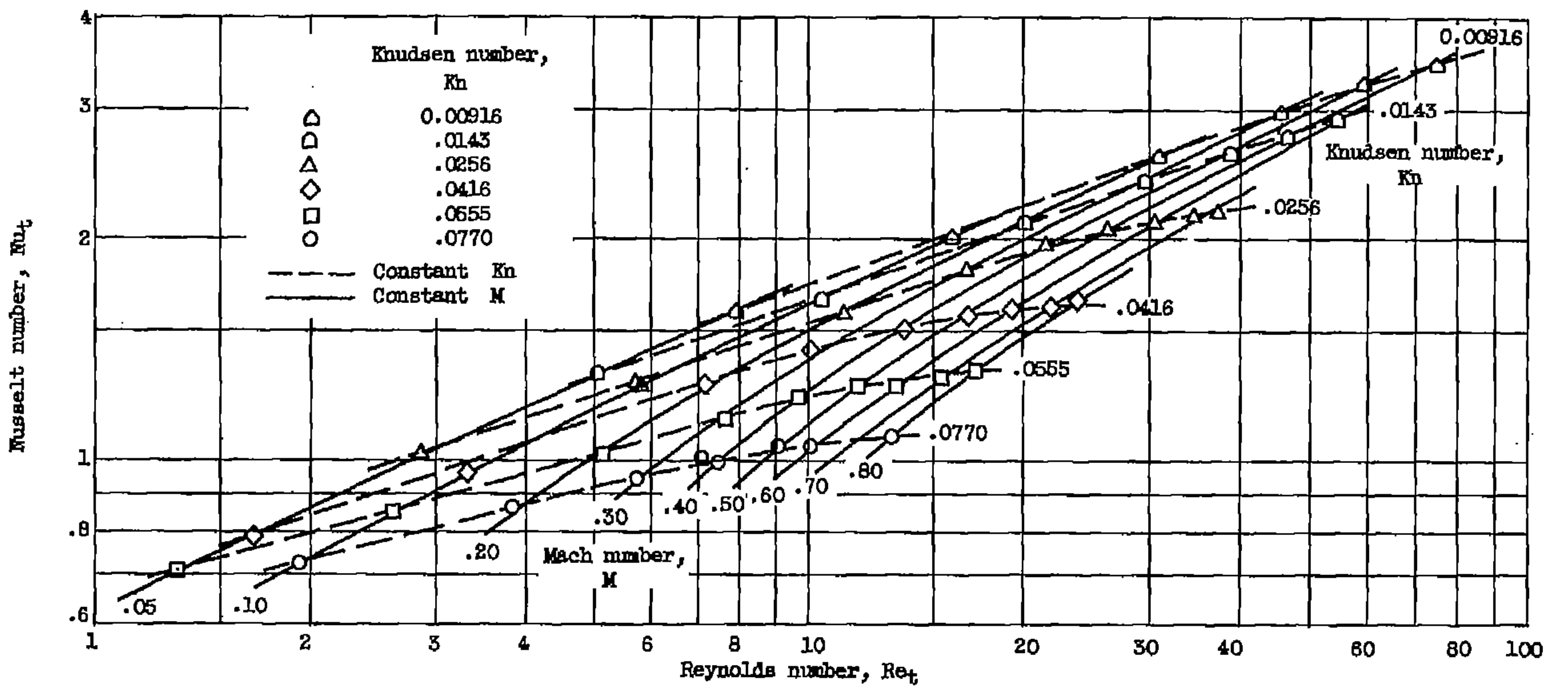

Figure 14. - Nusselt number correlation for cylinders in subsonic slip flow. Total air temperature, 80° F; length-average wire temperature, 584° F.

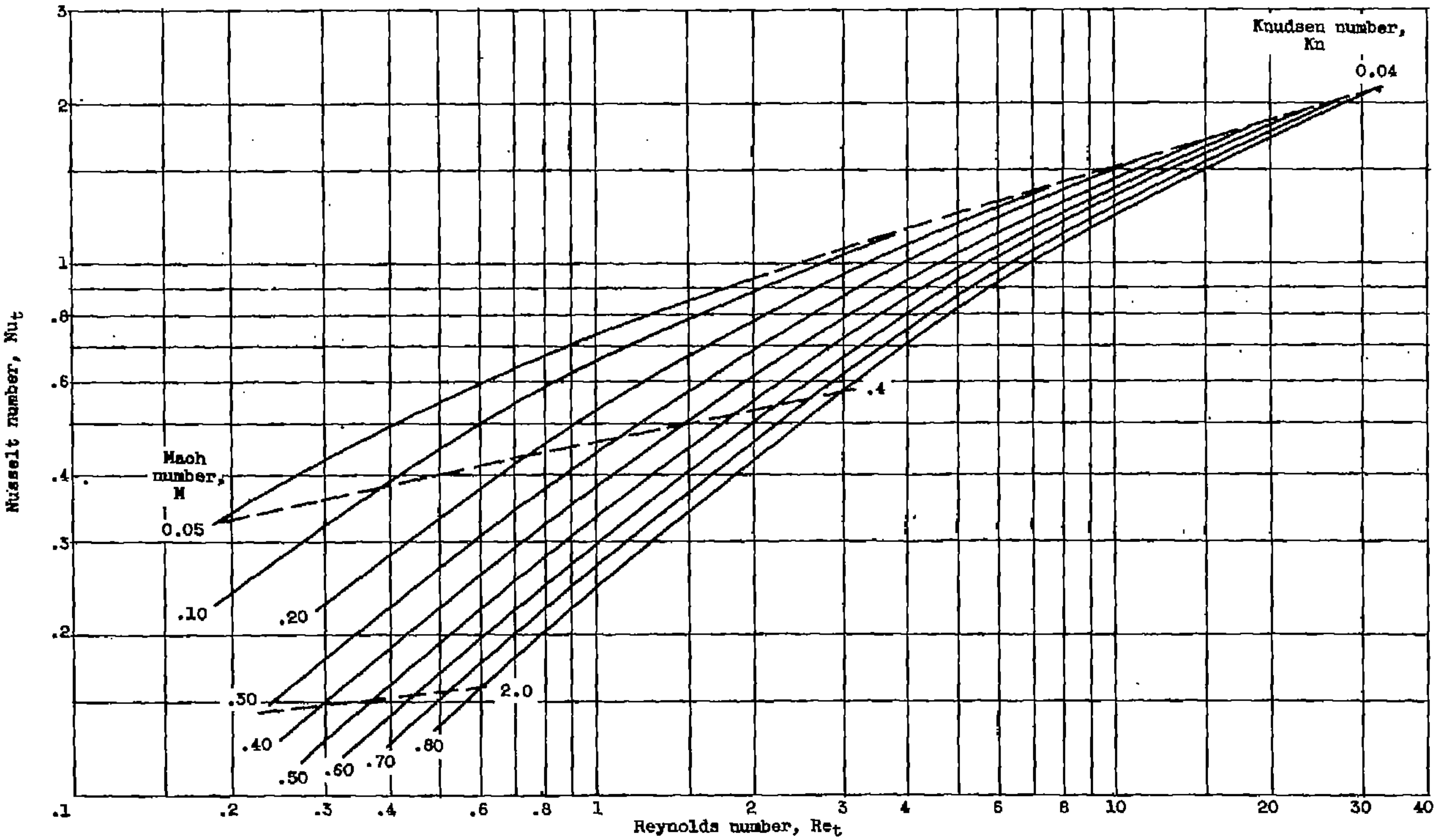

Figure 15. - Predicted Nusselt number correlation from approximate slip-flow theory (after ref. 23).

5111

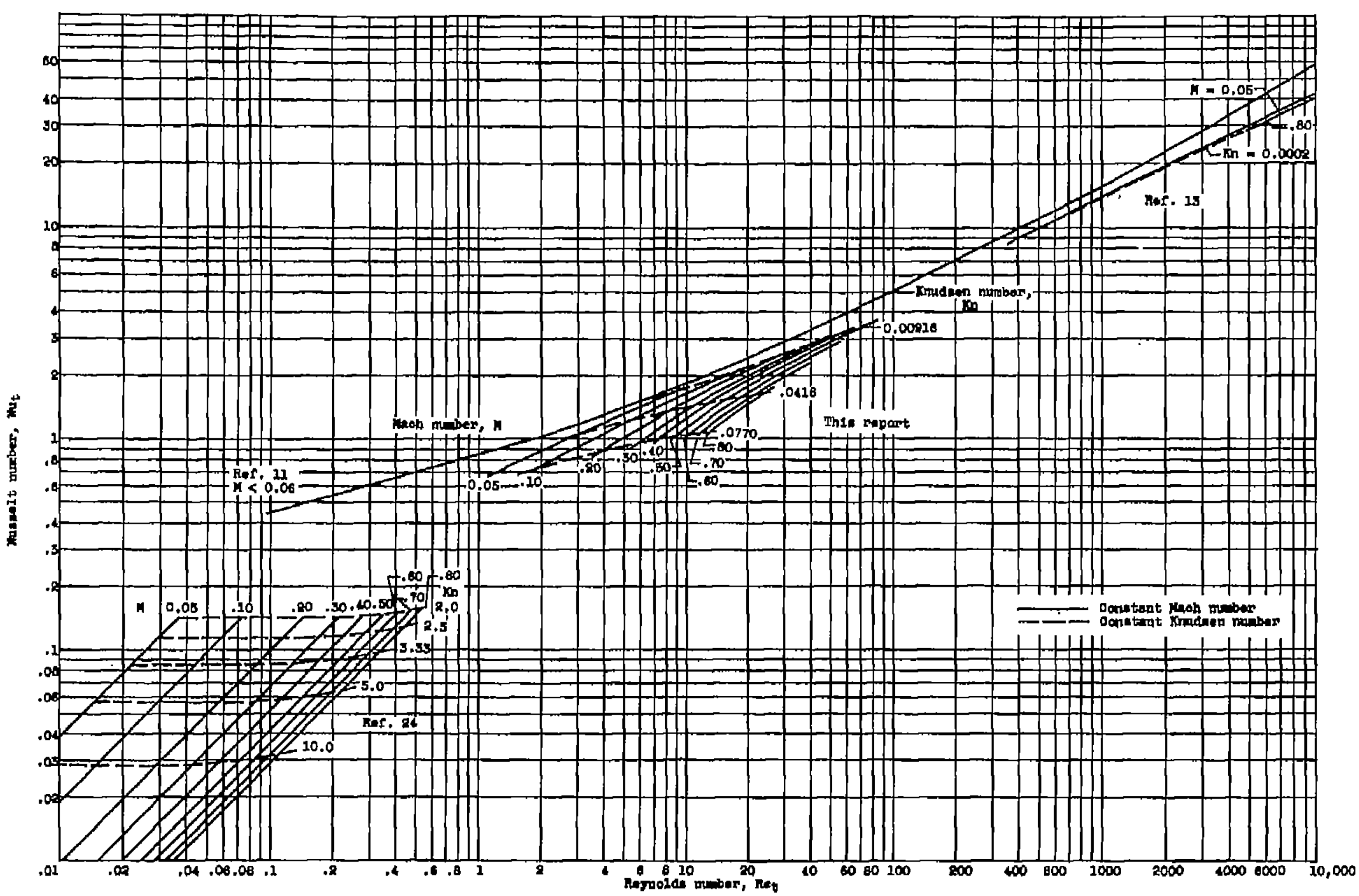

Figure 15. - Attempted Nusselt number correlation for cylinders in subsonic continuum, slip, and free-molecule flows.

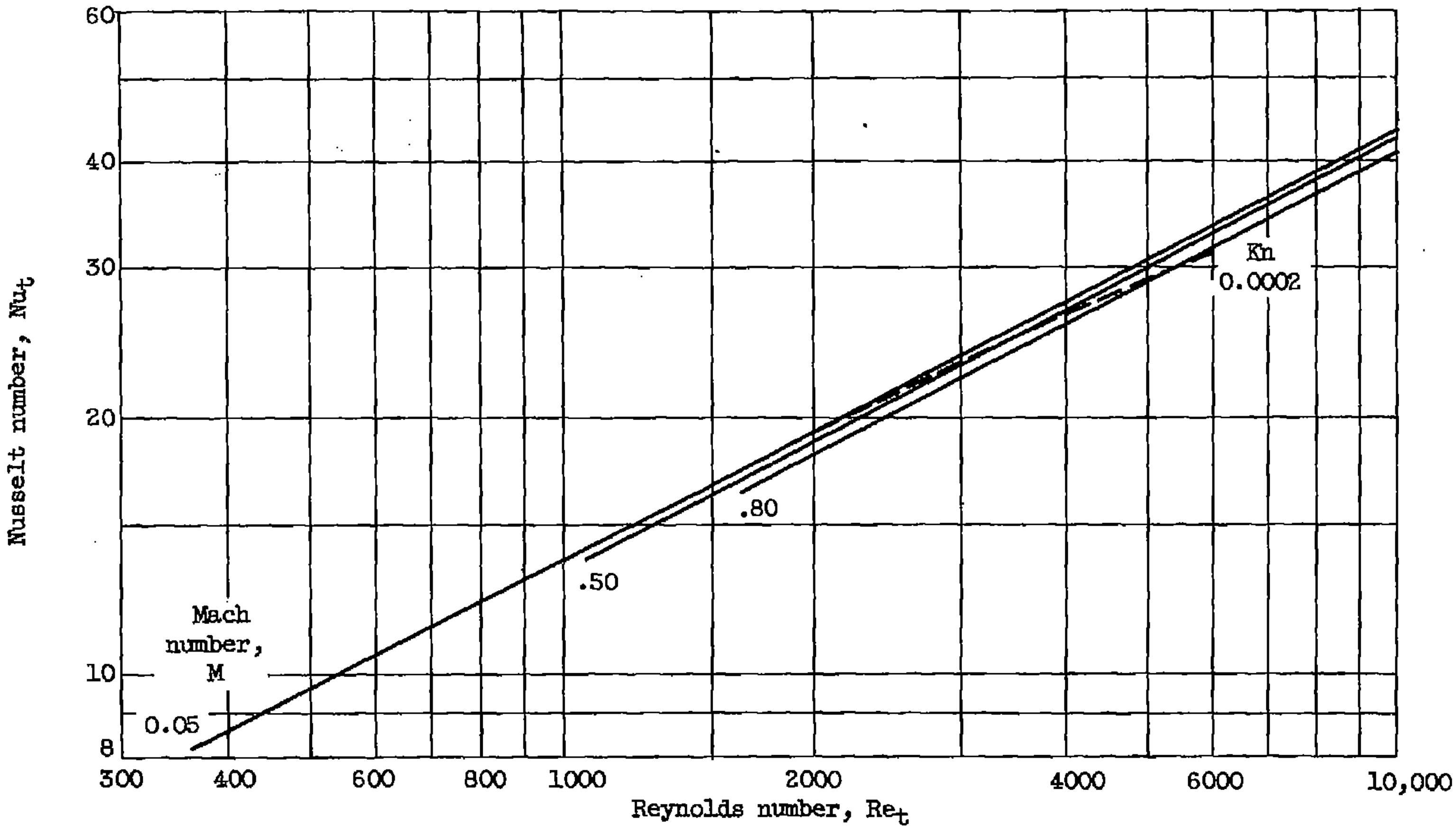

Figure 17. - Continuum-flow experimental Nusselt number correlation (after ref. 13).

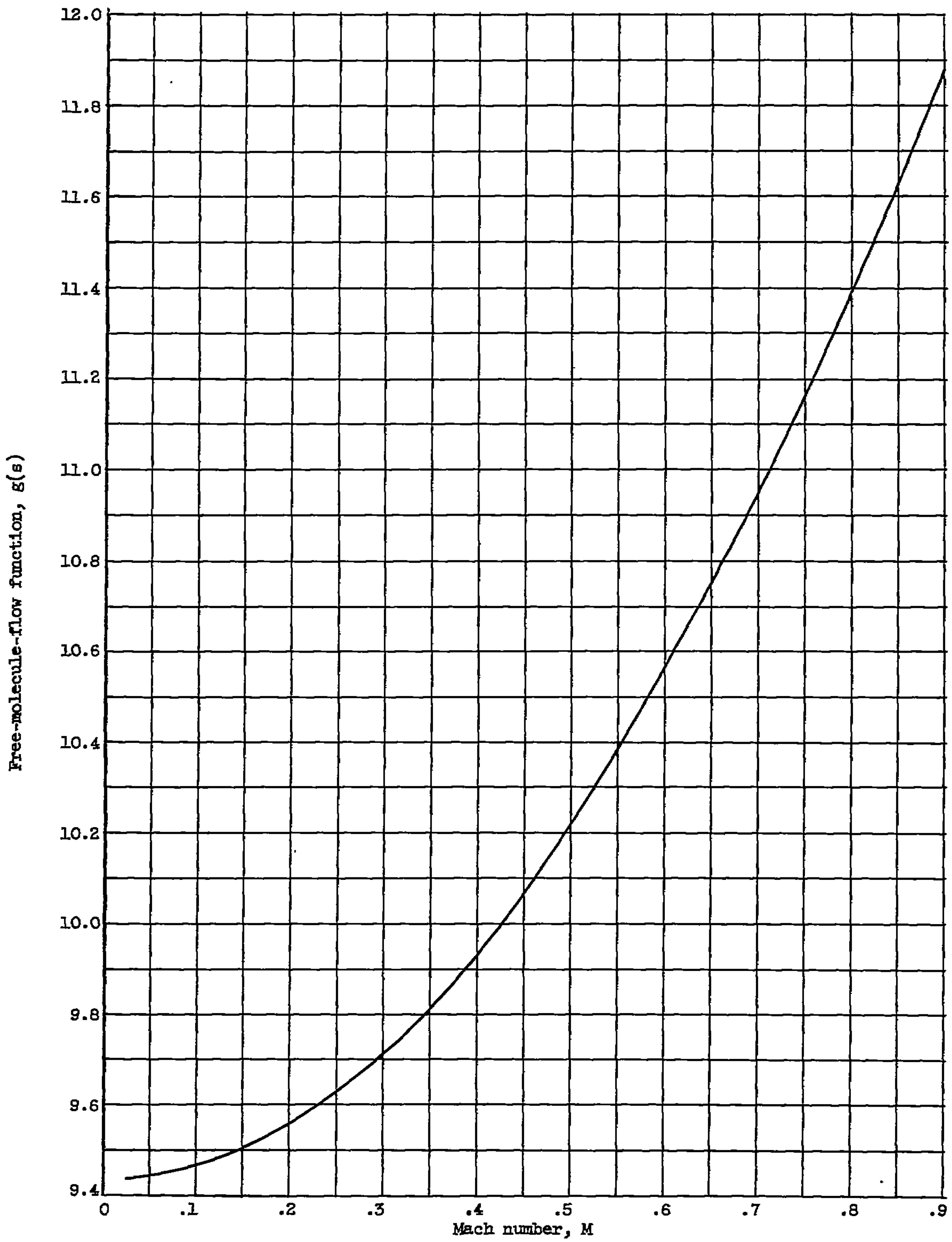

Figure 18. - Free-molecule-flow function $g(s)$ as function of Mach number.

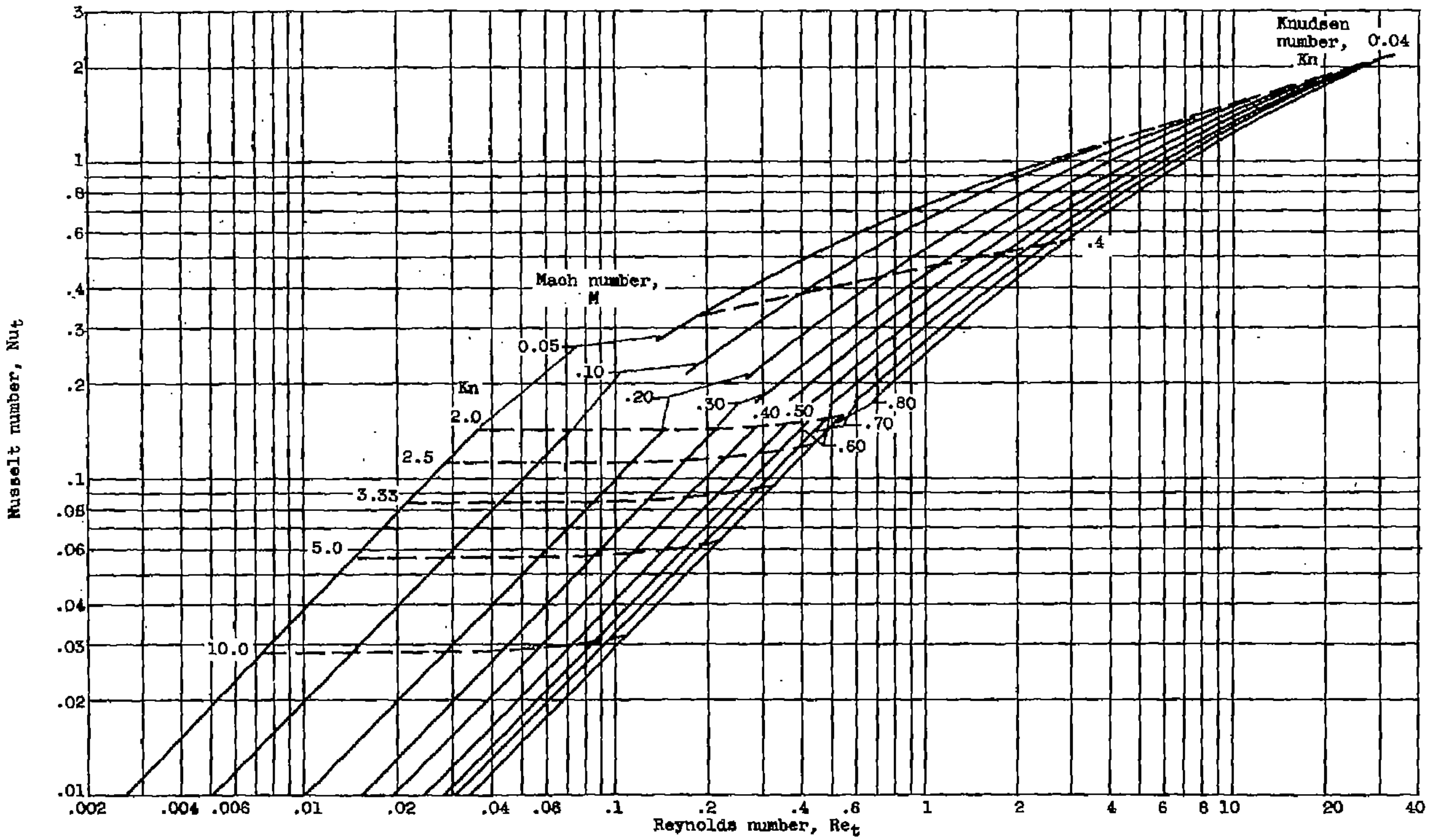

Figure 19. - Comparison of approximate slip-flow theory with free-molecule-flow prediction.

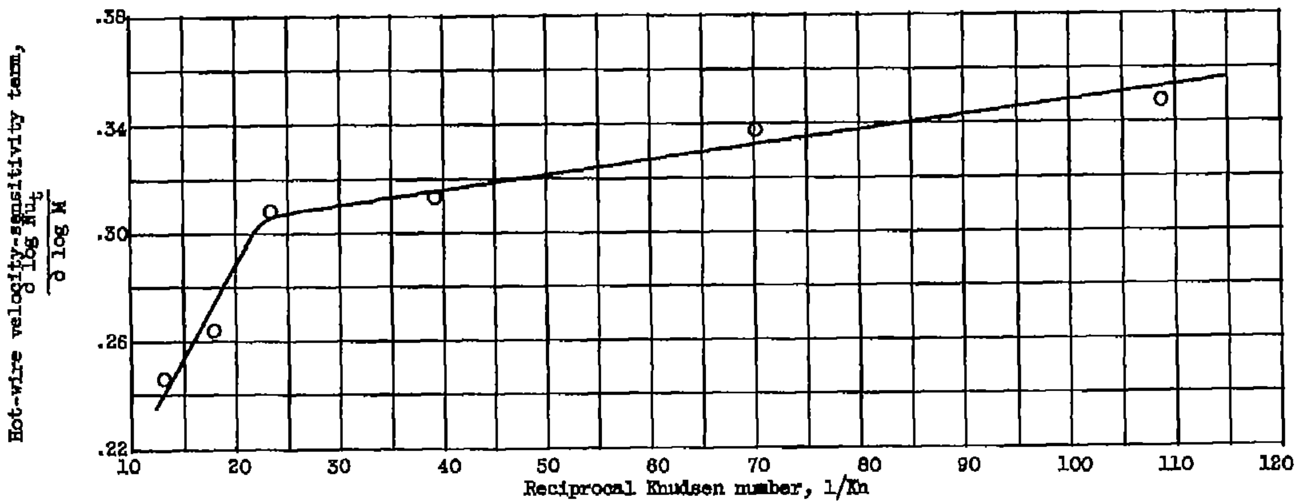

(a) Velocity sensitivity: $0.05 < M < 0.40$.

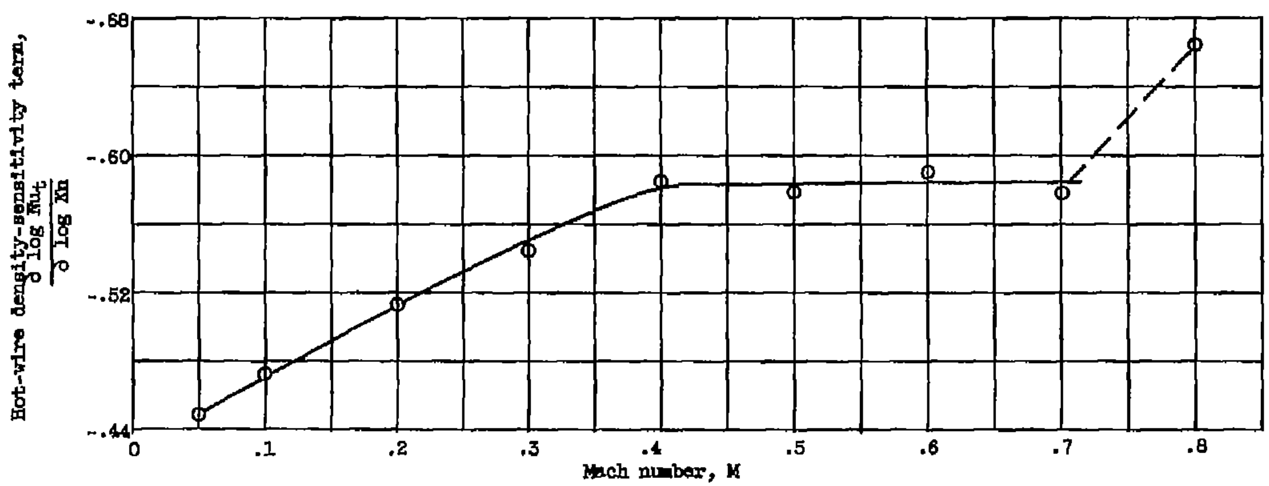

(b) Density sensitivity: $0.009 < Kn < 0.077$.

Figure 20. - Hot-wire sensitivity terms. Restrictions: $T_t \approx 80^{\circ}$ F; $T_w - T_e > 200^{\circ}$ F.